P.PORTO

ESCOLA SUPERIOR DE SAÚDE

M MESTRADO
BIOQUÍMICA EM SAÚDE

Characterisation of volatilomics in fungal samples extracted from the homes of patients with hypersensitivity pneumonitis

Ana Sofia Taveira Relvas

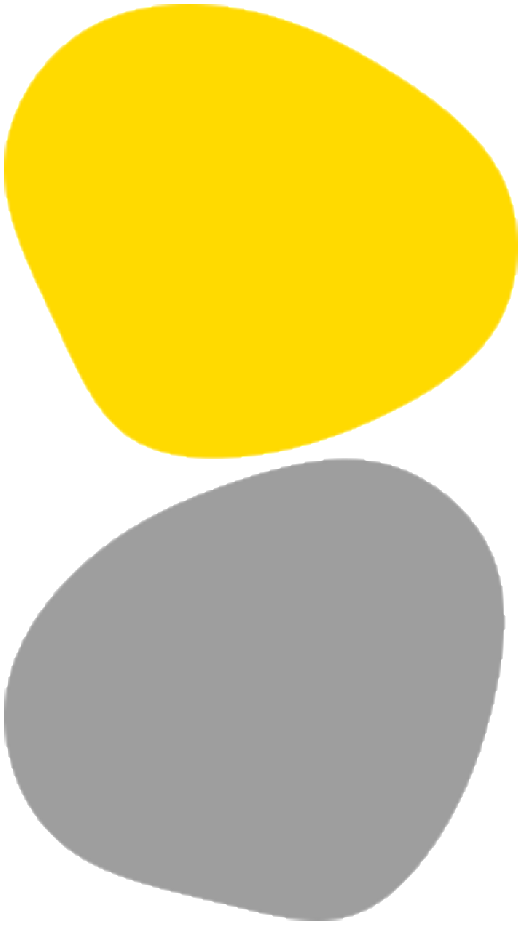

09/**2025**

Characterisation of volatilomics in fungal samples extracted from the homes of patients with hypersensitivity pneumonitis

Author

Ana Sofia Taveira Relvas

Supervisor

PhD/João Rufo/ Professor

School of Health, Polytechnic Institute of Porto, E2S IPP

Epidemiology Research Unit, Public Health Institute of University of Porto, ISPUP

Institutional supervisor

PhD/Mónica Vieira/Professor

School of Health, Polytechnic Institute of Porto, E2S IPP

RISE-Health, Center for Translational Health and Medical Biotechnology Research, TBIO

*Dissertation presented to fulfil the necessary requirements to obtain the Master's Degree in **Biochemistry in Health** – Branch in **Applied Biochemistry** by School of Health of Polytechnic Institute of Porto.*

Financial Support

This project was partially funded by FCT through the research grant 2024.15890.PEX.

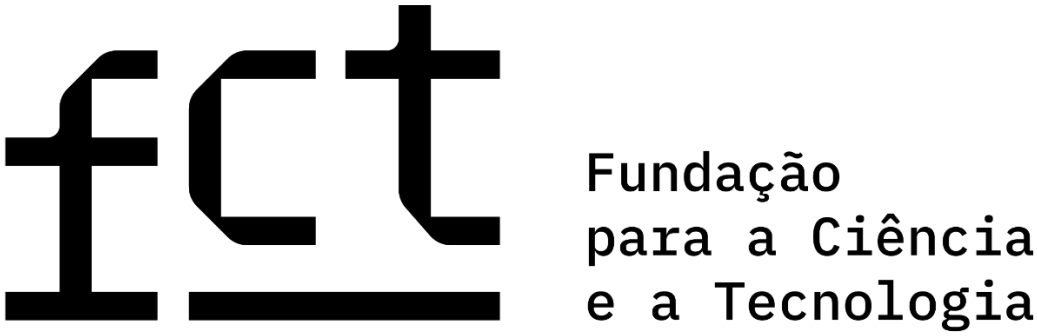

Agradecimentos

Ao chegar ao fim deste percurso académico, não posso deixar de olhar para trás e reconhecer todas as pessoas que, de alguma forma, me acompanharam, apoiaram e motivaram ao longo deste caminho. Este trabalho não é apenas o culminar do meu esforço individual, mas também o reflexo do contributo, carinho e presença de muitos que estiveram ao meu lado.

Em primeiro lugar, quero expressar a minha gratidão ao meu orientador, Dr. João Rufo, por toda a dedicação, paciência e orientação constante ao longo deste ano. Agradeço não só os ensinamentos científicos e académicos que permitiram alargar os meus conhecimentos em novas áreas, mas também a motivação e a confiança depositada em mim ao longo de todas as fases do projeto.

À minha coorientadora e orientadora institucional, Dra. Mónica Vieira, agradeço também pela envolvência e ajuda ao longo do ano, reconhecendo o meu trabalho e demonstrando sempre disponibilidade e apoio para qualquer dúvida que surgisse.

Gostaria também de agradecer à E2S por me acolher ao longo destes 5 anos, e fazer menção aos professores com quem me cruzei ao longo deste mestrado, alguns já conhecidos da licenciatura em Biotecnologia Medicinal, pelo conhecimento transmitido e pelas oportunidades de aprendizagem que me proporcionaram.

Não posso deixar de mencionar quem se cruzou comigo neste projeto. Obrigada Maria, por me teres dado a oportunidade de te ajudar no projeto de licenciatura e de poder trabalhar contigo. Sempre demonstraste vontade e iniciativa em fazer os passos dos protocolos e a trabalhar em conjunto em prol da parte interligada entre os projetos.

Aos meus amigos e colegas do mestrado, quero agradecer pela amizade criada e pela partilha de tantas experiências durante este tempo. Obrigada, em especial a ti, João, que me acompanhas há 5 anos neste caminho académico, começando na licenciatura onde mal nos conhecíamos porque só nos víamos de máscara, percorrendo até ao final deste mestrado, no qual entramos também juntos. Levo comigo tudo o que vivemos e "sofremos" juntos. Agradeço também a ti padrinho Gonçalo, por teres sido um bom mentor no começo da faculdade e um apoio constante ao longo deste tempo.

Tenho também de agradecer à minha família escutista nomeadamente aos meus amigos caminheiros e chefes. Convosco, aprendi valores de companheirismo, resiliência e entreajuda que foram essenciais, não só na minha vida pessoal, mas também na forma como tracei este caminho académico. Além disso, tenho de mencionar várias pessoas também marcantes pertencentes a este grupo. A ti Rita, agradeço-te por teres sido sempre um exemplo a seguir e pela amizade de longa data, contando sempre

com o teu apoio. Às minhas meninas do clã, obrigada por tudo e por acreditarem sempre em mim. Faço uma menção especial à Catarina, agradecendo o seu companheirismo e por me também permitir acompanhar o seu percurso académico sendo sua madrinha e, à Matilde, agradeço também pela força que transmite. Vocês estão sempre prontas para tudo o que preciso e sempre foram um apoio nesta etapa.

Quero também recordar e agradecer aos meus amigos de sempre, aqueles que me acompanham desde o básico pela amizade que resiste ao tempo. Apesar dos diferentes caminhos tomados na faculdade, continuam a fazer parte do meu percurso até hoje e permitiram me vivê-lo da melhor forma possível. Às minhas amigas do secundário, faço também um agradecimento especial por continuarem a ser presentes na minha vida e a apoiar as minhas vitórias.

Devo agradecer também a outro grupo que foi importante na minha vida académica. À minha TeSuna da E2S, obrigada por tudo o que me permitiram viver ao longo destes 5 anos. Tornaram o meu trajeto na faculdade ainda mais enriquecedor e as memórias vividas nunca serão esquecidas. Obrigada, em especial às minhas meninas que entraram comigo e com quem partilhei caminho, a ti minha madrinha Picasso por tudo o que fizeste por mim e, a ti afilhada Ana Marta "Voluntária", que me permitiste acompanhar o teu percurso mais de perto e ser um exemplo.

Por último, o agradecimento mais especial dirige-se à minha família, especialmente aos meus pais, à minha irmã, à minha avó "Lena", à minha afilhada Clarinha e à minha prima Beatriz, e aos meus gatinhos, Simba e Nala e, em memória, ao meu gatinho Quico. Obrigada por terem sido o meu alicerce em todos os momentos, celebrando as minhas conquistas e ajudando-me a superar as dificuldades que senti ao longo deste percurso. Mãe e Pai, agradeço não só o vosso apoio incondicional, mas também por nunca terem deixado de acreditar em mim mesmo quando eu tinha medos e inseguranças. Obrigada por me ensinarem o valor do trabalho, da humildade e da perseverança, valores que levaram este percurso a ser possível e que levarei comigo para toda a vida. Rita, obrigada por estares sempre pronta a ouvir, a apoiar e compreender e, muitas vezes, a dar aquela palavra que servia de incentivo e exemplo e me fazia seguir em frente. Sem vocês, nada disto teria sido possível, e por isso este trabalho é também vosso.

Finalizando esta etapa, olho para o futuro com entusiasmo e confiança, certa de que tudo o que aprendi e todas as pessoas que caminharam comigo me prepararam para os desafios que virão. Este trabalho simboliza o fechar de um ciclo, mas também o início de novos caminhos e oportunidades, que espero abraçar com a mesma dedicação e vontade de aprender que me trouxeram até aqui.

"Prepara-te para o pior, espera o melhor e aceita o que vier"

Resumo

Uma resposta hipersensível, mediada por células, a antígenos ambientais inalados resulta em pneumonite por hipersensibilidade (PH), uma doença pulmonar intersticial. É a terceira DPI mais frequente e é mais comum em trabalhadores expostos ao bolor e poluentes microbiológicos. Avaliações clínicas e imunológicas são utilizadas no processo de diagnóstico. A identificação fenotípica das espécies de fungos é crucial para diferenciar esses microrganismos, envolvendo a observação das características morfológicas coloniais. No entanto, esse método tem limitações, como o tempo necessário para o cultivo e a necessidade de profissionais altamente qualificados para esse fim. Produzidos por bactérias, fungos e outros microrganismos, os compostos orgânicos voláteis (COV) fazem parte do metabolismo desses micróbios e têm um papel importante em muitos campos. Esses compostos incluem alguns grupos funcionais, como álcoois, cetonas, benzenóides, ácidos carboxílicos e aldeídos.

Neste projeto, o objetivo consistiu em identificar perfis distintos de COV a partir de amostras de fungos coletadas nas casas de pacientes com PH.

Os perfis de compostos orgânicos voláteis de cinco fungos coletados nas casas de pacientes com pneumonite por hipersensibilidade (*Penicillium sp., Alternaria sp., Gliocladium virens, Aspergillus flavus e Aspergillus niger*) foram avaliados usando um nariz eletrónico e os resultados foram comparados com a identificação fenotípica baseada em métodos micológicos. A análise de componentes principais (PCA) foi utilizada para redução da dimensionalidade e o agrupamento hierárquico foi utilizado para agrupar perfis relacionados em estruturas aninhadas. Testes qui-quadrado foram usados para comprar proporções entre os clusters, e curvas ROC foram criadas usando os dados para avaliar a sensibilidade e a especificidade do perfil.

Os resultados da análise do nariz eletrónico mostraram uma diferenciação significativa nos perfis dos compostos orgânicos voláteis após 48 horas de inoculação. Os perfis de COV consistiram essencialmente em alcanos, cetonas, álcoois, hidrocarbonetos aromáticos e aldeídos. Além disso, a metodologia foi eficaz na diferenciação clara do *Penicillium sp.* relativamente às outras amostras. Todos os fungos, exceto *Alternaria sp.,* foram claramente diferenciados do grupo de controlo. As descobertas também permitiram a criação de um modelo possível para prever a exposição a fungos em casa, verificado pela alta área sob a curva ROC.

O presente estudo mostrou que o nariz eletrónico é muito promissor como método rápido e eficiente para distinguir várias espécies de fungos.

Palavras-chave: pneumonite de hipersensibilidade; compostos orgânicos voláteis; nariz eletrónico; fungos

Abstract

A cell-mediated hypersensitive response to inhaled environmental antigens results in hypersensitivity pneumonitis (HP), an interstitial lung disease. It is the third most frequent ILD and is more common in workers exposed to mold and microbiological pollutants. Clinical and immunological evaluations are used in the diagnosis process. The phenotypical identification of fungi species is crucial for differentiating these microorganisms, involving the observation of colonial morphological characteristics. However, this method has limitations such as the time required for cultivation and the need for highly qualified professionals for this purpose. Produced by bacteria, fungus, and other microorganisms, volatile organic compounds (VOCs) are part of the metabolism of these microbes and have an important role in many fields. Those compounds include some functional groups such as alcohols, ketones, benzenoids, carboxylic acids and aldehydes.

In this project, the goal consisted of identifying distinct VOC profiles from samples of fungi collected in homes of patients with HP.

The volatile organic compound profiles from five fungi collected in the houses of patients with hypersensitivity pneumonitis (*Penicillium sp., Alternaria sp., Gliocladium virens, Aspergillus flavus* and *Aspergillus niger*) were evaluated using e-nose and the findings were compared with phenotypic identification based on mycological methods. Principal component analysis (PCA) was used for dimensionality reduction and hierarchical clustering was used to group related profiles into nested structures. Chi-square tests were used to compare proportions between clusters, and ROC curves were created using the data to assess the profile's sensitivity and specificity.

Results of the e-nose analysis showed a significant differentiation in the profiles of volatile organic compounds after 48 hours of inoculation. The VOC profiles consisted essentially in alkanes, ketones, alcohols, aromatic hydrocarbons and aldehydes. Also, the methodology was effective in clearly differentiating the *Penicillium sp.* from other samples. All fungi apart from *Alternaria sp.* were clearly differentiated from the control group. The findings also enabled the creation of a possible model to predict fungi exposure at home, verified by the high area under the ROC curve.

The current study has shown that the electronic nose has a lot of promise as a quick and efficient method for distinguishing various fungi species.

Keywords: hypersensitivity pneumonitis; volatile organic compounds; electronic nose; fungi

Index

List of Abbreviations

PH	Pneumonite por hipersensibilidade
DPI	Doença pulmonar intersticial
COV	Compostos orgânicos voláteis
HP	Hypersensitivity pneumonitis
ILD	Interstitial lung disease
IPF	Idiopathic pulmonary fibrosis
NKT	Natural killer T
BAL	Bronchoalveolar lavage
VOCs	Volatile organic compounds
VVOCs	Very volatile organic compounds
SVOCs	Semi volatile organic compounds
MOS	Metal oxide semiconductor
QCM	Quartz crystal microbalance
E-nose	Electronic nose
COPD	Chronic obstructive pulmonary disease
DNA	Deoxyribonucleic acid
ROC curve	Receiver Operating Characteristic curve
PDA	Potato Dextrose Agar
YEPD	Yeast Extract Peptone Dextrose
OD	Optical Density
CFUs	Colony forming units
PCA	Principal component analysis
OR	Odds ratio
CI	Confidence intervals
2D	Two dimensions
AUC	Area under the curve
MEA	Malt Extract Agar
GC-MS	Gas chromatography- mass spectrometry

List of Tables

List of Figures

1. Introduction

1.1. Hypersensitivity Pneumonitis

Hypersensitivity pneumonitis (HP), also known as Extrinsic Allergic Alveolitis, is a complex interstitial lung disease (ILD) (1) marked by a hypersensitization reaction to inhalable antigenic particles that are frequently found in the environment (2) being this exposure the main cause of this disease.

HP is the third most common ILD, being behind idiopathic pulmonary fibrosis (IPF) and interstitial lung disease associated with connective tissue illness (3).

Cross-sectional studies estimate the frequency of HP in farmers, bird breeders and mushroom workers, and the prevalence is higher in at-risk communities (4). Although it is a relatively uncommon diagnosis in children, hypersensitivity pneumonitis makes up about 50% of all interstitial lung diseases in this age range. The majority of HP diagnoses in the paediatric population occur in youngsters under the age of ten (5).

Relatively to the exposure, birds (up to 30% of HP groups) are the most often implicated exposures, primarily from feather dust, droppings, and serum, which are primarily sourced from pigeons, budgerigars (parakeets), cockatiels, parrots, and canaries, as well as duck and goose down products. Water-related mold growth and bacterial and microbiological contamination of air conditioners and ventilation systems are the second risk factors for this disease, and the first for those not exposed to birds (4).

Furthermore, typically, HP-inducing antigens are divided into five major groups, each of which is represented by a disease prototype: mycobacteria, bacteria, fungi, proteins, and chemical compounds (6). Molds, protozoa, animal (mainly bird) proteins, and even low-molecular-weight chemical compounds are among included in those most prevalent antigens (7). More than 300 antigens have been related to this disease, in which along the others mentioned before, plants and metals antigens seem to have a connection to HP as well (2). Moreover, HP can also result from some drugs in a non-inhalational form (7).

Depending on the pattern of exposure and length of sickness, HP was traditionally classified as acute, subacute, or chronic. However, individuals had varied clinical histories regardless of this classification. Recent classification of the disease into fibrotic and non-fibrotic categories based on clinical, pathological, and/or imaging characteristics was necessitated by the need to add prognostic value (8). A few studies show that compared to the acute, subacute, and chronic classifications, the nonfibrotic and fibrotic classifications provide a more accurate picture of disease development and

prognosis. Combining the two classifications, makes it clear that whereas chronic HP can be either nonfibrotic or fibrotic and acute HP cases are always nonfibrotic (9).

The primary symptom of both fibrotic and non-fibrotic HP is dyspnea (10). Coughing and mid-expiratory screeching are the other unspecific clinical manifestations of HP, aside from a history or proof of antigen exposure. There are occasions when constitutional symptoms like chills, a low-grade fever and malaise appear (11). Acute influenza-like symptoms can occasionally appear in patients with non-fibrotic illness a few hours after a (typically) significant exposure. In these situations, symptoms may reappear with re-exposure but may progressively worsen over hours or days (10). Patients with nonfibrotic HP are more likely than fibrotic HP patients to have a relatively acute onset and to have a detectable antigen (11). Those typically experience progressive dyspnea over the course of a few weeks or months, along with some of the constitutional symptoms referred and others such as chills, fever, tightness in the chest, wheezing and weight loss. In the case of patients with fibrotic HP they experience a persistent cough that lasts for months or years as well as they can develop (often subtle) exertional dyspnea (10).

In HP, a shift from a Th1 to Th2 inflammatory response, the suppression of regulatory T cells, and the overexpression of NKT cells all play a role in the transition from an acute, inflammatory phase to a chronic, fibrotic process (4).

The diagnosis of the disease currently requires a comprehensive search in history, clinical and imaging data, bronchoalveolar lavage (BAL) pattern, serum immunological and histological findings (1). There are different types of diagnosis depending on the type of hypersensitivity pneumonitis, in which, three main differential diagnoses for nonfibrotic HP are primary bronchiolitis, microaspiration, and sarcoid and, for fibrotic HP, the pattern of fibrosis determines the differential diagnosis (12).

Finding and addressing the implicated exposure is part of the first care for people with HP diagnoses (4). The key components of HP treatment are corticosteroids and immunosuppressive medication combined with antigen avoidance (10). Simultaneously, antifibrotic medications exhibit encouraging outcomes in the HP progressive fibrotic phenotype. Lung transplantation is another therapy option reserved for patients with advanced illness (1).

The mortality rate linked to HP appears to be rising, which emphasizes the need for increased precision, speed and identification of exposure in order to improve the course of the disease (8).

1.2. Hypersensitivity Pneumonitis and Fungal Exposure

Fungi exposure is linked to several different conditions, such as hypersensitivity pneumonitis, allergic fungal sinusitis and allergic bronchopulmonary mycoses, in addition to rhinitis and asthma (13).

Exposure to a single component antigen is extremely uncommon, and environmental exposure is typically complicated. Farmers have been inhaling dust that contains a variety of bacteria and fungus, as well as mycotoxins, volatile organic compounds, endotoxins and peptidoglycans, all of which may be involved in the disease's biopathology (14).

The complex ecology that includes bacteria like *Klebsiella* species and molds like *Pullularia, Aureobasidium, Curvularia, Chaetomium, Penicillium* and *Cephalosporium* genus and that may be found in a contaminated humidifier system are examples of fungal antigens (15), as well such as those from *Alternaria alternata* and *Aspergillus sp.* have also been linked to different types of occupational HP. It is thought that fungi's mycelial components and airborne spores have a major role in HP (2).

The identification of environmental fungi related to this disease usually follows the normative EN 13098:2003 (16). Analytical processes might intensify the challenges and uncertainties, that is, the technique employed might make it difficult to identify the biological entities present or might unintentionally interfere with one another. Considering this, the method can be complicated, and new ways of identification should be implemented.

1.3. Volatile organic compounds (VOCs)

Volatile organic compounds (VOCs) are organic chemical compounds which are released as gases and can be found in various products and organisms (17). These chemicals containing carbon are easy to evaporate at room temperature (18).

These compounds can be classified into three categories such as very volatile organic compounds (VVOCs), volatile organic compounds (VOCs) and semi volatile organic compounds (SVOCs). The first classification represents the most dangerous pollutants, and they are characterised to be toxic at very low concentrations. VOCs are found in ordinary products and can be observed in environment. Lastly, SVOCs are compounds with higher values of molecular weight and boiling points comparing to the previous class, however, they can be dangerous as well (17).

VOCs are exposed through different sources such as air, water, food, landfills and soil (18) and can be found in the environment. Talking about that last context, their composition in both indoor and outdoor environments can be very complex. Indoor VOCs can have a major effect on children's or vulnerable people's respiratory health being associated with irritative symptoms, including those with asthma, bronchitis, or reduced lung function (19). Also, certain human activities, air exchange rate, conditions like temperature and humidity, types of the structure of buildings and lifestyle habits can have a substantially influence on indoor VOCs levels. Furthermore, in the case of outdoor VOCs, the chemical composition is linked to its source across different regions (20).

The detection and monitoring of volatile organic compounds hold a great applicability in a variety of industries, including public health safety, agriculture, food production, health management and monitoring of environment (21).

However, VOCs can also be originated from the metabolism of living organisms. The volatilome of an organism englobe the entire spectrum of volatile metabolites within the metabolome (22). Certain volatiles are specific to a given species, even though a wide variety of VOCs can be found in many distinct organisms (23). These substances, which include many kinds of organic compounds, are the end products of the metabolism of various microorganisms, including fungus, molds, and bacteria. Therefore, there is a close correlation between the VOC profile and microbial species and strains (24).

Among the VOCs released by microorganisms' metabolism, it is frequent to find alkenes and other compounds such alcohols, ketones and hydrocarbon compounds with C6–C16 chains, which come from the intermediates of fatty acids metabolism, such as β-oxidation (25).

Through primary and secondary metabolic processes, fungi produce combinations of volatile organic compounds which permeate soil and enter the atmosphere. The peak of fungal VOCs generated by secondary metabolism appears to coincide with sporulation and mycotoxin formation. Numerous variables related to the fungal strain and its growing environment, such as physiological status, temperature, pH, oxygen, nutrition and incubation period affect the profile of the released mixture (23).

During the metabolism of these microorganisms, carbohydrates, lipids, amino acids and other molecules containing sulfur and nitrogen are released (26). Fungi, in particular, may also release alcohols, ketones, benzenoids, carboxylic acids, aldehydes, and isoprenoids (27).

1.4. Volatilomics and Fungal VOCs

Volatilomics is a type of category belonging to the group of metabolomics that is interested in the detection of volatile organic compounds (28).

The topic of endogenous volatile organic compounds produced by molds growing inside, particularly in relation to moist conditions and potential health risks for people has been addressed in several studies.

Aspergillus and *Penicillium* are the most investigated fungal genera in volatilomics studies due to its widespread use in interior settings (29).

The understanding of why and when distinct volatile organic compounds (VOCs) are released by fungi is still in its early stages, in contrast to the more frequent morphological, physiological, and biochemical features. A growing body of research indicates that fungal VOCs have important roles in both direct and indirect fungal interactions (30).

Compared to conventional molecular methods, VOC-based diagnosis offers a significant advantage because it can use VOC sampling to distinguish between different fungus-infected samples (27).

Furthermore, a few studies have demonstrated the effectiveness of fungal VOCs in a variety of biomedical applications, including as nematocidal agents, fungicides, insecticides, bactericides, and inducers of resistance to abiotic and biotic stressors (31).

1.5. Electronic nose

Another method relies on the detection of volatile organic compounds using sensor-based devices, such as polymer sensors that react to changes in electrical conductivity caused by VOC adsorption or electronic noses, which enable the quick identification of a predetermined range of volatile compounds (29).

An electronic nose (e-nose) is a technology that mimics human olfactory perception in order to identify scents, usually known as the artificial olfactory system. This device includes different features and components such as a sampling system, a variety of heterogeneous electrochemical gas sensors, a signal gathering unit and a software for pattern identification (32).

In an e-nose system, the hardware that is the sensor array and the algorithm corresponding to the software are two fundamental parts of the equipment. There are distinct sensor types that can be from a metal oxide semiconductor (MOS) and quartz crystal microbalance (QCM), which are suitable for constructing a sensor array (20).

The electronic nose has a variety of particular sensors and a sophisticated pattern recognition algorithm that can distinguish between both basic and complicated smells contributing to the study of volatilomics (33). For that, this instrument presents an encoding that can preserve the important information that is necessary for the identification of samples of interest (34).

Essentially, each sensor of the device displays different selectivity and sensitivity related to certain components of the sample, besides the fact that, a characteristic chemical representation of the gas mixture is generated, being called a "fingerprint" that characterises the volatilome of the species (35).

The detection of VOCs has led to the development of portable, quick, and inexpensive sensor-based equipment thanks to recent advancements in biosensor engineering (12). Over the past years, there has been a significant acceleration in the development of electronic nose technology and devices for use in applications related to disease diagnostic.

E-noses were first employed in medicine focusing on bacterial infections or non-infectious conditions such asthma, lung cancer and chronic obstructive pulmonary disease (36).

The significant developments in e-nose diagnostic methods have led to a wide range of new e-nose applications that are helpful for the identification and detection of diseases with a wide range of etiologies (biotic, abiotic, and genetic). Detecting microbial infections on or within diseased organisms is the main use of e-nose devices for biotic cause identification.

There are numerous specialized applications of the electronic nose in different fields being used for biosecurity, forensics, military operations, transportation safety, aerospace, agricultural environmental protection and scientific research (37). It can be used as well in other industries such as food, biomedical, cosmetic, pharmaceutical and analytical chemistry ones (38).

Applications of e-nose devices have grown significantly in the last ten years in the biomedical and allied pharmaceutical industries because of the demand for new, more user-friendly technologies that can quickly and inexpensively provide reliable non-invasive diagnosis (37).

Lung cancer, breast cancer, colorectal cancer, ovarian cancer, gastric cancer, head-and-neck cancer, chronic obstructive pulmonary disease (COPD), interstitial lung disease, liver cirrhosis, ventilator-associated pneumonia and COVID-19 are among the diseases for which the e-nose is currently being used in research (39).

1.6. Phenotypical identification of fungi

The phenotypical identification of fungi species is an important method used to differentiate types of these microorganisms. This study has some elements among the visualization of colonial morphological characteristics, growth rate and microscopic observations (40). These consist in the diverse observations of colony features considering the colour, size and the aspect visible by the naked eye corresponding to the macro morphology. The observation of shapes formed from the arrangement of spores produced by the fungus analysed with a microscope correlate to a micro morphological study (41).

This classical method presents some advantages and disadvantages comparing to advanced techniques used in the identification of fungi. This method using morphology is more economical and requires less specialized equipment (40). In the case of when there is an absence of sequence data or a limited quantity of a fungus species is accessible, this method is advantageous comparing to novel techniques such as DNA identification. For this reason, morphology continues to be the most conventional and reliable procedure to study fungi (42).

However, the time for cultivation of these microorganisms can be extensive, usually requiring a minimum of seven days of incubation, prolonging to more days in some species (43). This technique is inadequate in the case of fungi species that are incapable of growing or form reproductive structures in culture, becoming a restriction for detecting, categorising and characterising fungus. Also, there has been a decreasing interest by young researchers in becoming classical taxonomists as the career in classical mycology takes a long duration of training and specializing (40). Morphology of a single species of fungus can present some variations under different circumstances such as environmental conditions, geographical source and specific hosts.

The findings of taxonomic investigations based on morphology are also significant and utilised in other fields of study, including physiology, plant pathology, biotechnology, bioremediation and fungal biochemistry (42).

1.7. Objectives

The main objective of this study was to identify distinct VOC profiles from samples of fungi collected in homes of patients with HP, measuring their classification efficacy.

More specifically, the objectives of the project consisted in:

i. Optimisation of the colony counting method by optical density measurements and the creation of concentration curves;
ii. Development of cultures of fungi associated with patients with hypersensitivity pneumonitis;
iii. Volatilomic analysis of fungal cultures by electronic nose;
iv. Identification of volatile biomarkers associated with different species of pathogenic and toxinogenic fungi;
v. Calculate efficacy measurements for the test, including the estimation of sensitivity and specificity, and area under the ROC curve.

2. Methods

In this project, different fungal species were analysed using e-nose (indexing method) and the results were compared with the reference method (phenotypic identification following mycological procedures based on micro- and macro-morphological characterisation of the samples). The results were used to construct a ROC curve to determine the sensitivity and specificity of the method.

2.1. Medium preparation

The culture media used in this project were Potato Dextrose Agar (PDA) for the Petri plate and Yeast Extract Peptone Dextrose (YEPD) broth for the fungi of interest.

The preparation of these mediums consisted, initially, in the weighing of the components of the culture medium (powders and extracts) accurately, following the proportions indicated by the manufacturer. Then, the ingredients were dissolved in distilled water and homogenized. The next step was the sterilization of the cultures, using an autoclave at 121°C for 15 minutes, to eliminate contaminating microorganisms. Finally, the mediums were distributed while still hot into sterile Petri plates in the case of PDA medium or bottles (YEPD), using an aseptic environment to avoid contamination (Figure 1).

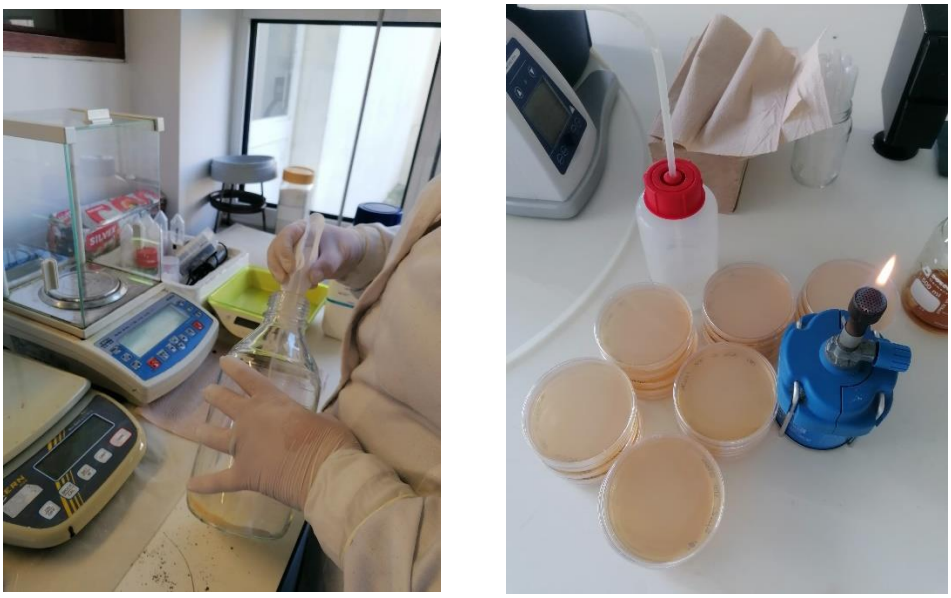

Figure 1: Preparation of culture media into Petri plates.

2.2. Processing of the fungi samples

Fungi isolates were collected from the homes of patients with HP, in the framework of a different project, carried out in the Institute of Public Health of the University of Porto ("*Avaliação dos fatores de exposição ambiental na habitação que possam estar associados ao desenvolvimento de pneumonite de hipersensibilidade*").

A specialized team, led by an investigator with prior expertise in this methodology, conducted comprehensive household inspections and microbiologic air sampling. Shortly, indoor fungal air samples were gathered employing a single-stage microbiologic air impactor, specifically the Merck Air Sampler MAS-100. This collection procedure adhered to the guidelines stipulated in the NIOSH method 0800 and EN 13098. The selection of participants' bedrooms for air sampling was based on the rationale that these spaces typically represent areas of prolonged indoor air exposure. In each bedroom, a total of two malt extract agar plates were cultured by impaction, with a total air volume of 250 L for each plate.

Subsequently, the collected samples were transported to the laboratory for quantification of colony forming units (CFU) and species identification, following standardized protocols. The fungal samples were incubated at a temperature of 25°C for a duration of 72 hours. Specific fungal identification was conducted seven days after incubation, either directly on the original sampling media or after implementing subculturing procedures, as necessary, for colony isolation and growth observation. The conidia in the isolates were swabbed, transported to a glycerol-rich media in a cryotube, and stored under -80°C for use in the present project.

2.3. Optimisation of the construction of concentration curve for environmental fungi

2.3.1. Initial optimisation method

Firstly, 100 mL of YEPD broth was inoculated with the desired fungus in an Erlenmeyer named flask A and covered with a cotton stopper and let to incubate overnight at 25ºC on an orbital shaker (120 rpm). When incubation was complete, the next day, 1 mL was transferred to a spectrophotometry cell and the optical density was read at 600nm, using the sterile broth as a blank, considering diluting the solution if OD > 1,2.

Since the growth was lower than expected, Erlenmeyer A was allowed to incubate for up to 72 hours, measuring the optical density in three additional time points (18h, 24h and 72h).

Using the formula Ci x Vi = Cf x Vf and considering a final concentration of OD = 0.1 in 100 mL, the initial concentration volume was calculated, 28 mL, which was a high number of inoculum to transfer to an Erlenmeyer B.

Because of inconsistency in fungal growth, this process was repeated for the same fungus, so 100 mL of broth was inoculated with the fungus in an Erlenmeyer A and it incubated overnight at 25ºC on an orbital shaker (120 rpm) (Figure 2A). Also, a PDA plate was inoculated with the fungus to see if there was any growth. When incubation was completed, after approximately 62 hours, 1 mL was transferred to a spectrophotometry cell (Figure 2B) and the optical density was read at 600 nm, using the sterile broth as a blank.

Using again the formula Ci x Vi = Cf x Vf and considering a final concentration of OD = 0,01 in 100 mL, the initial concentration volume was calculated. Then the calculated volume (33 mL) was transferred to an Erlenmeyer flask B, using the remaining broth (67 mL) to make 100 mL. The Erlenmeyer was incubated for 72 hours at 25ºC on orbital shaker (120 rpm), having growth times points: 0h, 1h, 2h, 3h, 4h, 5h, 6h, 7h, 8h, 24h, 48h and 72h to measure the optical density for each growth time. For each growth time, 6 Eppendorf tubes were prepared with 450 µL of saline solution in each and serial dilutions were performed with 50 µL of Erlenmeyer B. Vortex between each dilution was necessary to guarantee it was well mixed. For each of the last 4 dilutions, 50 µL of solution was pipetted onto a plate with culture medium (PDA) and spread evenly with a microbiology loop (Figure 2C). The plates were incubated at room temperature for at least 72 hours and after incubation, the number of colonies were counted and CFUs calculated using the equation:

$$\frac{CFU}{ml} = n \times \frac{1}{d} \times \frac{1}{v}$$

After that, the concentration curve was drawn.

Although this optimisation was only done for one fungus of interest (*Gliocladium virens*), results can be extrapolated to the other fungi.

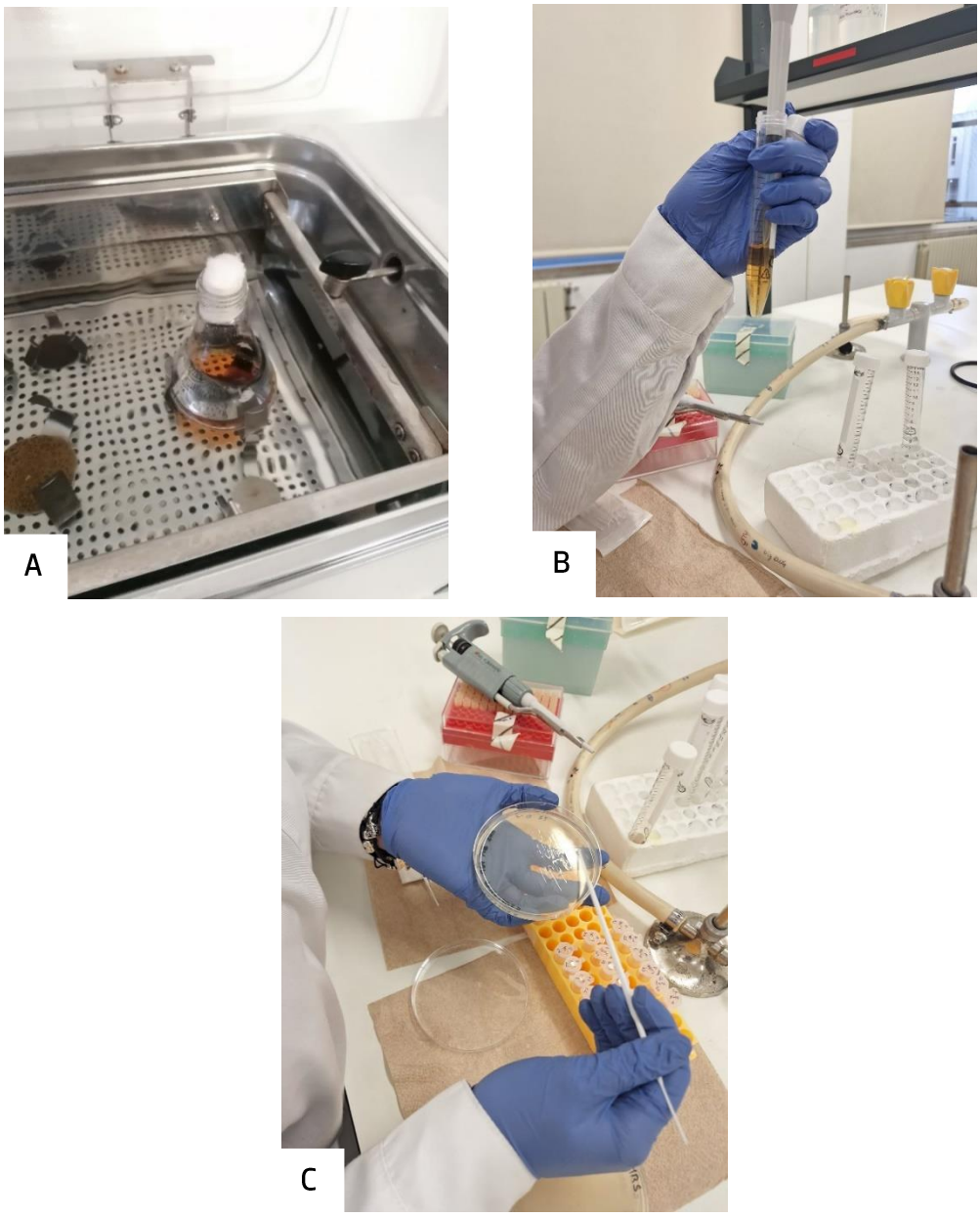

Figure 2: A – Incubation of Gliocladium virens in agitation (120 rpm); B – Transfer of 1 mL from the fungus culture to a spectrophotometry cell for optical density read at 600 nm; C – Inoculation of fungi to plates for colony forming units' count.

2.3.2. Concentration curve method

This method was adapted from the A. Aberkane *et al.* study (44), consisted of the "*Comparative evaluation of two different methods of inoculum preparation for antifungal susceptibility testing of filamentous fungi*". The fungus used in this assay was also the *Gliocladium virens*.

An inoculum of the desired fungus was placed on a plate with PDA medium to grow at room temperature until it reached maturity. Then 3 plates of inoculum were prepared from this mature culture and were left to grow for 4 days at room temperature.

The next step was to prepare the Tween 20 solution with the tween reagent and sterile distilled water and then pass 20 mL of the Tween 20 solution with a sterile syringe attached to a sterile filter with a pore diameter of 0,45 µm to a new Falcon tube. Then, the colonies were covered with 5 mL of the 1% Tween 20 solution (Figure 3A), and the conidia of the fungus were extracted carefully with the swab (Figure 3B) and transferred to a sterile Falcon tube (one for each plate) containing 25 mL of sterile distilled water. The suspensions were homogenized for 15 seconds on a vortex at 2000 rpm. The remaining solution of the plate containing the Tween 20 solution were transferred to another sterile Falcon tube (one for each plate).

If a significant number of hyphae were detected (>5% of fungal structures), the solution would be transferred to a sterile syringe attached to a sterile filter with a pore diameter of 0,45 µm into a sterile tube. This step removes the hyphae and results in a suspension composed of spores. If agglomerates were still detected, it would be needed to vortex again at 2000 rpm for a further 15 s and repeat this step as many times as necessary.

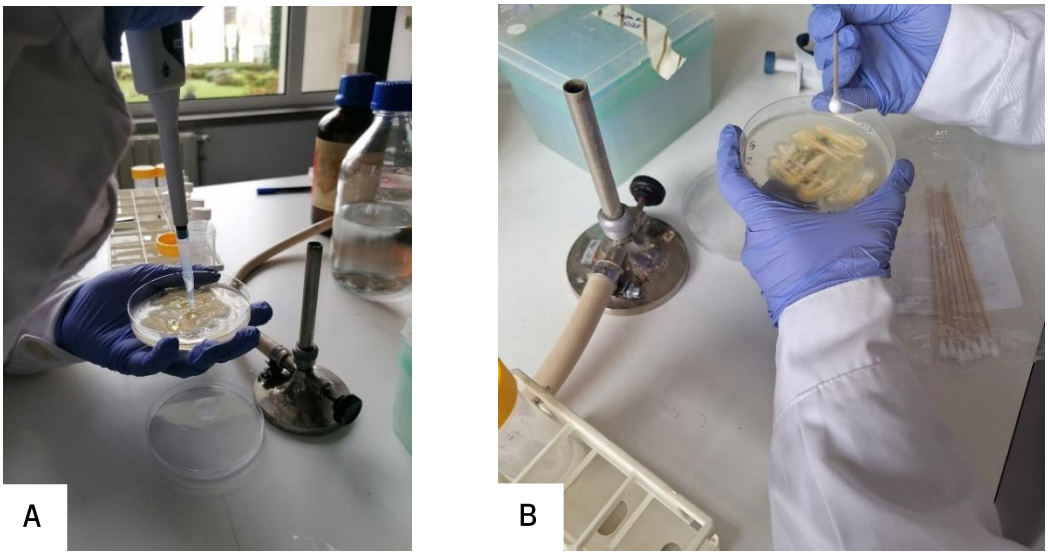

Figure 3: A –Tween 20 solution covering the fungus. B– Swabbing the conidia from the fungus.

To read the optical density at 530, 600 and 670 nm, 1 mL was transferred to a spectrophotometry cell using sterile distilled water and sterile Tween 20 solution as blanks.

After that, 6 Eppendorf tubes were prepared with 450 µL of sterile distilled water in each, for each of the plates and serial dilutions were performed with 50 µL of the Falcon tubes' solutions (sterile distilled water and Tween 20 solution) and between each dilution, the Eppendorf tube was vortexed.

For each of the last 4 dilutions and the concentrated solution (without dilution), 50 µL of solution was pipetted onto a plate with culture medium (PDA) and spread evenly with a microbiology loop. The plates were incubated at room temperature for at least 72 hours and after incubation, the number of colonies were counted and CFUs calculated using the equation:

$$\frac{CFU}{ml} = n \times \frac{1}{d} \times \frac{1}{v}$$

For the repetition of this method, the protocol was adapted according to the results obtained and four more species of fungi were now used and had a correspondent identification number: *Gliocladium virens* –10 (already used) and *Penicillium sp.* – 5, *Alternaria sp.* – 3, *Aspergillus niger* – 39 and *Aspergillus flavus* – 19. The previous method was done for each fungus.

2.3.3. Final optimisation strategy

The first part of the method was the same, changing the next procedure to only prepare 1 plate of inoculum from the mature culture. Also, it changed to only transfer the swab of conidia to a sterile Falcon tube (one for each plate) containing 25 mL of sterile distilled water.

To read the optical density at 530, 600 and 670 nm, 1 mL was transferred to a spectrophotometry cell using only sterile distilled water as blank.

After that, 6 sterile Falcons tubes of 50 mL were used and were prepared with 4,5 mL of sterile distilled water in each, for each of the plates and the serial dilutions were performed with 500 µL of the Falcon tubes' solutions (sterile distilled water) and between each dilution, the tubes were gently vortexed.

It is shown in several studies that the process of CFUs count from a diluted sample brings the number of colonies within a countable range on a plate, allowing for accurate calculation of the original concentration (45, 46).

After counting the CFUs, the concentration curve was drawn.

2.4. Measurement of volatile organic compounds of fungi using the electronic nose

For this part of the method (Figure 4), inoculum of the desired fungus was placed on a plate with PDA medium to grow at room temperature until it reached maturity.

Subsequently, the conidia were carefully scanned with the swab (doing a line) and transferred to a glass test tube (three for each fungus) containing 3 mL of YEPD broth, in which, each tube was covered with a cotton stopper. Also, three glass tubes containing only YEPD broth were also prepared, consisting in the control solutions. The suspensions were then homogenized and incubated for 72 hours on an orbital shaker (120 rpm) at 25ºC after the first measurement.

Measurement times were set: 0h, 1h, 2h, 3h, 6h, 24h, 48h and 72h and for each these timepoints, the volatile compounds in each test tube were measured, in the hotte, using the electronic nose, noting the corresponding values indicated on the device (Figure 5A and 5B). The electronic nose used was the MIDAS Breathprinter (Figure 5C) that was previous developed and is currently waiting for a patent approval (requirement number: 2025007123262). This device had metal oxide sensors (MOS) and it connected throughout bluetooth with an electronic device such as a mobile phone through a "serial bluetooth terminal".

Within 72 hours, 3 Eppendorf tubes were prepared with 450 µL of saline solution for each of the test tubes (9 for each fungus plus 9 for the control, a total of 54 Eppendorf tubes). After that, serial dilutions were performed up to 10^{-3} with 50 µL of the solution from the tube with the fungus and the broth. The Eppendorf tubes were vortexed between each dilution.

For the 10^{0} (without dilution) and the 10^{-3} dilution, 50 µL of the solution was pipetted onto a plate with culture medium (PDA) by the drop method (Figure 6) and also, for the 10^{-3} dilution, a spread method was involved, doing it evenly with a microbiology loop. The plates were incubated at room temperature for at least 72 hours.

After incubation, the number of colonies were counted and CFUs calculated.

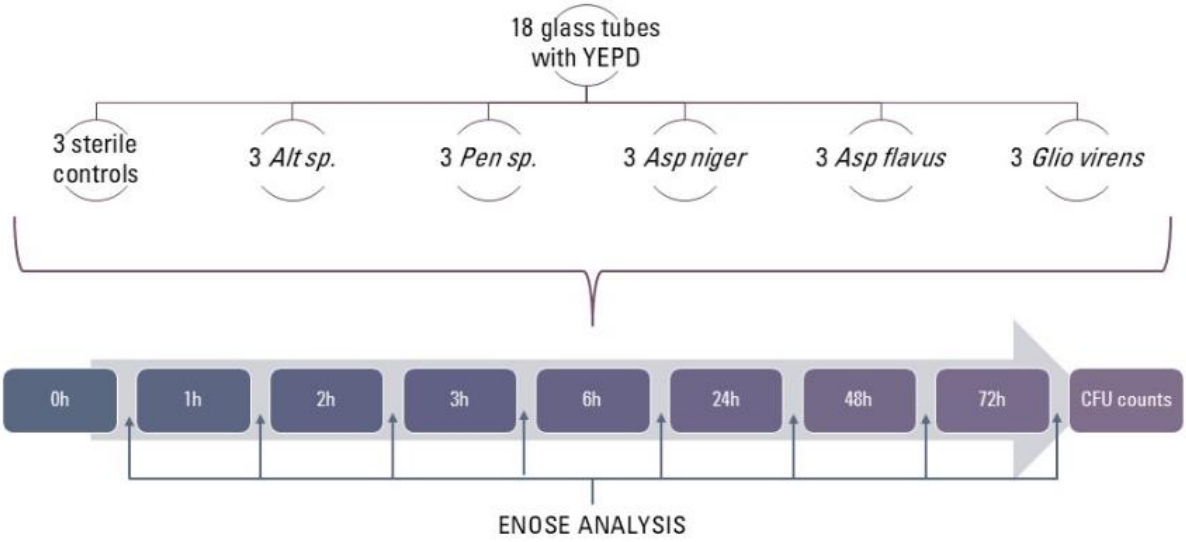

Figure 4: Schematic image of the methodology adopted in this part of the protocol.

Figure 5: A and B – Function of the electronic nose used to detect the volatilome of fungi. C – Electronic nose MIDAS Breathprinter.

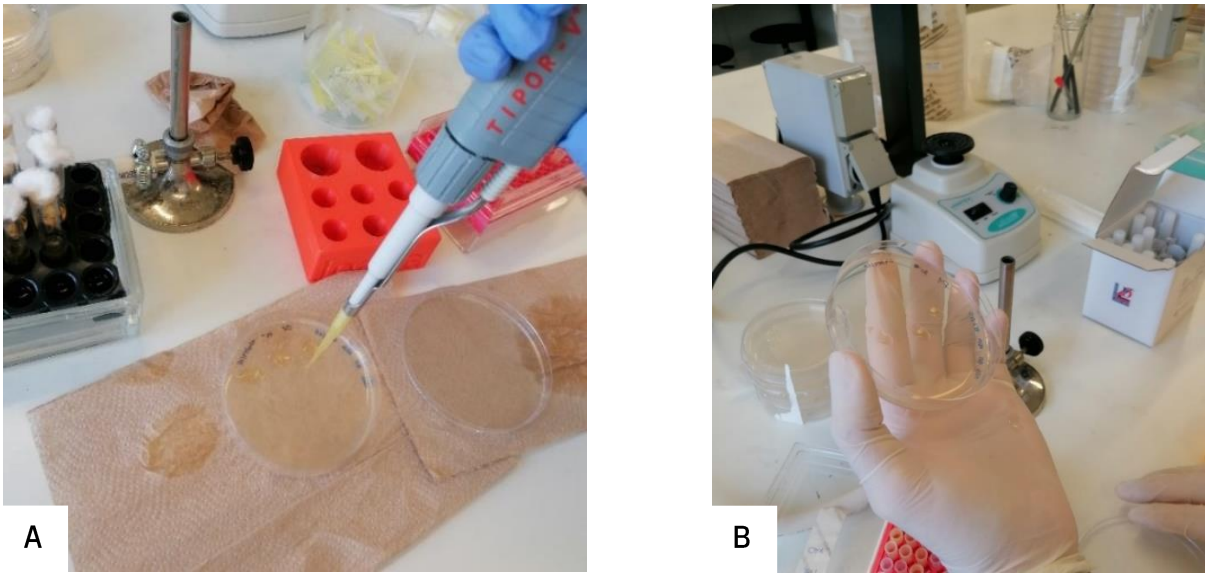

Figure 6: A and B – Drop method used for the following process of CFUs count.

2.5. Phenotypical identification of fungi

To confirm the different types of fungi used in this project, phenotypical identification was carried out.

Plates of PDA were prepared, and the five fungi were inoculated in those plates and incubated at room temperature for 7 days, to reach the right level of maturation.

The observation of the macroscopic characteristics of the cultivated fungus was determined by different aspects such as surface and opposite colors, as well as the texture of the colony and macroscopic structures visible to the naked eye.

Microscopic observation was based on preparing a laminate with a sample of the colony of the fungi of interest (Figure 7). A drop of fixing agent, in this case, ethanol 70%, was placed on the laminate with a Pasteur pipette. In a sterile environment, the culture plate was opened and, carefully, a small amount of sample was removed with the microscopy needle and distributed over the fixing agent. Then, a drop of lactophenol blue was placed on the preparation with a Pasteur pipette and left to act for at least 1 minute.

In the end, the coverslip was placed above, and the preparation was sealed.

These phenotypic observations were accompanied by a manual for identifying fungi. For this purpose, "Larone's Medically Important Fungi: A Guide to Identification" (47), was chosen because it is one of the most comprehensive identification guides. The guide comprises a set of tables with various

colour combinations (surface and opposite colours) and the possible fungal structures associated with each combination.

Figure 7: Laminates of each fungus for microscopic observation.

2.6. Statistical analysis

Following the reunification of all sample data, a database was produced. Results from the identification and quantification of fungi species through the reference method were used as inputs during algorithm development.

To compile and display the sensor data, a principal component analysis (PCA) was used to dimensionally condense the data and investigate its spatial distribution using Euclidean. After that, hierarchical clustering models and clustering stability tests were conducted. The chi-square test was used to examine statistical differences between clusters and the fungi. Statistical significance was defined as a *p* value less than 0,05.

A bootstrapping method was used to create bootstrap distribution plots and q-q plots in order to see if the model is according to expected. This method is a verified statistical technique for variance reduction (48) as is normally used in several studies.

Pearson's correlation was used to measure the correlation between sensor affinity and the two main components explaining the variance of data.

Based on the determinant sensors identified through PCA, logistic regression models were fitted for fungi classification. Results were reported as OR with respective 95% confidence intervals (CI).

Accuracy measures included sensitivity, specificity, overall accuracy, positive and negative likelihood ratios, and diagnostic odds ratio, calculated from confusion matrices. Finally, ROC curves were constructed for each approach to assess algorithm performance, aiming to achieve a threshold of at least 75% sensitivity.

All statistical analysis were performed in R environment (version 4.4.1).

3. Results

3.1. Optimisation of the construction of concentration curve for environmental fungi

3.1.1. Initial optimisation method

As in the beginning, the culture in Erlenmeyer A was prepared and set to measure the optical density at 600 nm right at 0h. The result demonstrated a negative number, which is not so normal, but it could had mean it was a wrong measurement. Therefore, that culture was maintained until 72h, to measure the OD as well at other different timepoints, being those 0h, 18h, 24h, 48h and 72h. Those results as it can be seen in Table 1, didn't present regularity because at 18h, the OD was 0, which isn't the normality as fungus usually grow fast so it should had grown. After the first time point, positive values were shown being the highest one at t72 (0,356), having a big gap with the previous time point (t48). Also, the 24h and 48h results demonstrated that it was possible that the spectrophotometer was measuring in a not so correct way, although the optical density at 72h showed that the culture of the fungi had been growing as correlating to what's seen in the Figure 8B.

Table 1: Time of incubation and the optical density of Gliocladium virens measured at 600 nm.

Time (h)	OD (600 nm)
0	-0,020
18	0
24	0,006
48	0,001
72	0,356

The Erlenmeyer flask with the culture of *Gliocladium virens* was incubated in agitation until 72h. The inoculum grew during that time and formed little agglomerations in the YEPD medium as it shows in Figure 8.

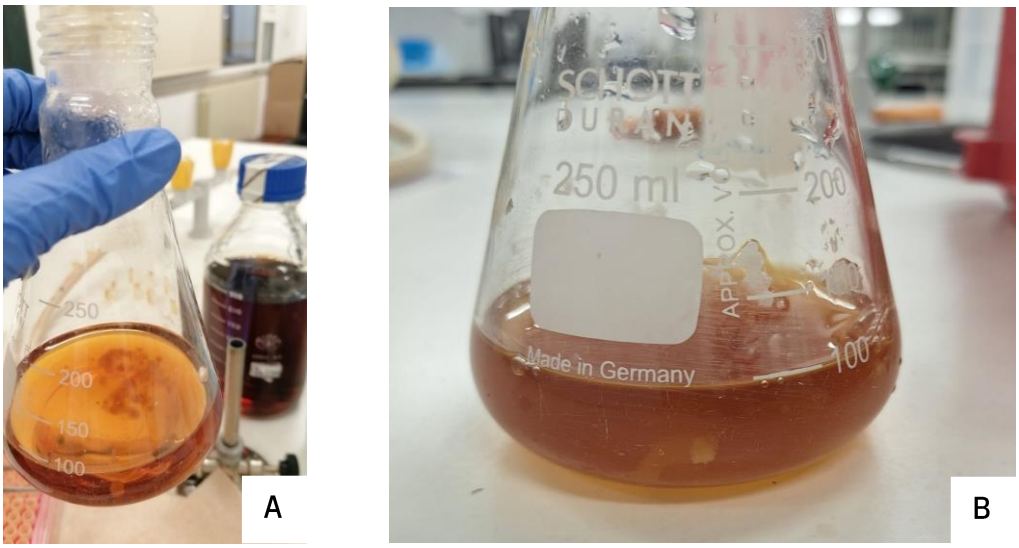

Figure 8: A and B- Growth of Gliocladium virens in Erlenmeyer A – 24h (A) and 72h (B).

Repetition of the protocol

To confirm the previous results, the protocol was repeated and the new Erlenmeyer A with the fungus culture was again measured for OD at 0h and there were two different numbers with the same sample, which indicated inconsistency as seen in Table 2. Then, the procedure was continued to the culture in Erlenmeyer B and optical density was measured at distinct timepoints from 0 until 72h. The repetition, as it can be seen in Table 3, showed a negative value of optical density at the first measure (t0) and at t72. The next hours showed positive values being the highest one at t24 (0,810), having a big difference relating to the other values. The numbers were varying from time to time but despite that, they showed increase of OD in some hours, which can tell that the culture is growing, as seen in Figure 9.

Table 2: Time of incubation and the optical density of Gliocladium virens in the first measurement at 600 nm.

Time (h)	OD (600 nm)
0	0,030
	0,100

Table 3: Time of incubation and the optical density of Gliocladium virens measured at 600 nm.

Time (h)	OD (600 nm)
0	-0,020
1	0,020
2	0,015
3	0,047
4	0,143
5	0,030
6	0,020
7	0,031
8	0,075
24	0,810
48	0,055
72	-0,039

The inoculum of *Gliocladium virens* was incubated in Erlenmeyer A in agitation for 72h. The growth showed agglomeration of the inoculum, and it can be observed below in Figure 9.

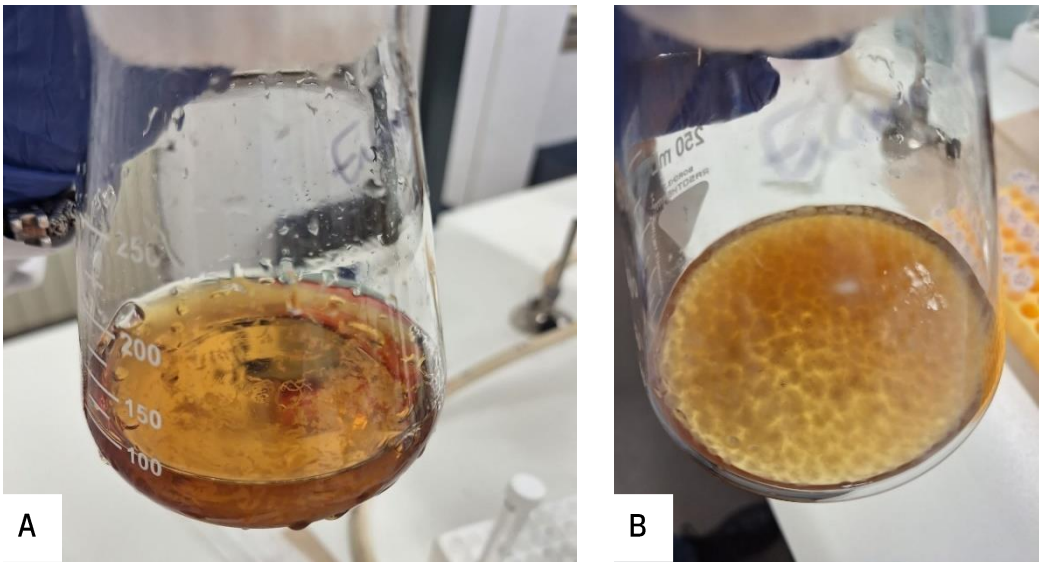

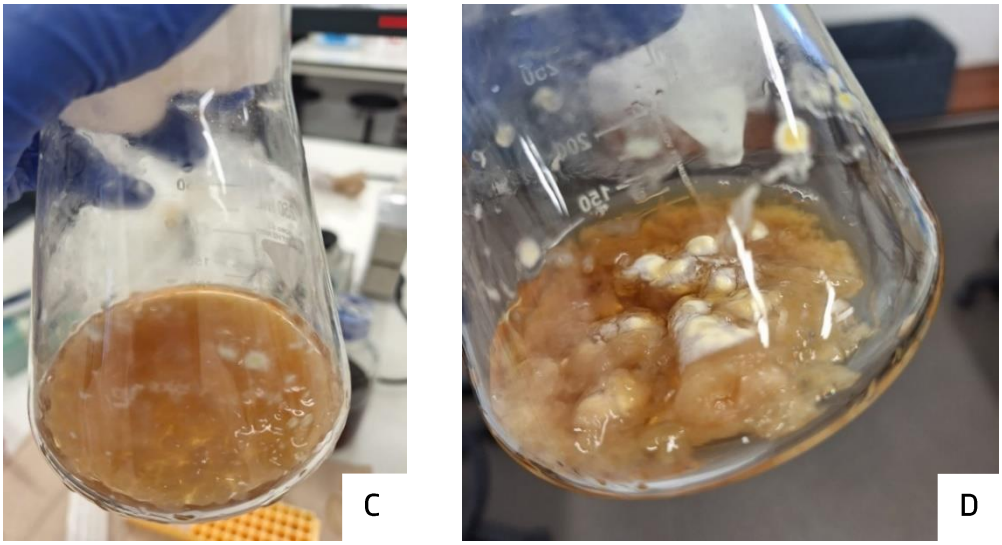

Figure 9: Gliocladium virens growth on broth medium (A - 8h, B- 24h, C- 48h, D- 72h).

The colonies from the growth of *Gliocladium virens* were counted for each time point and the respective dilution. Only 7 plates showed some growth, being four from the 10^{-3} dilution and three from the 10^{-6} dilution. As seen in the Table 4, the colonies count was low, being 3 the highest number of colonies in one plate being from 8h of incubation (Figure 11). Meanwhile there were only some colonies counted on the early hours of incubation for example from 2h to 8h, the plates from 24h time to 72h only showed one colony forming unit at 24 and 48h at the 10^{-6} dilution. Those results were not as planned because the number of colonies were supposed to increase as the incubation time passed, as usually it happens, and even more, from seeing that one colony formed being from a high dilution instead of the low dilutions. Figure 12 showed the growth of the *G. virens* and its morphological characteristics.

Table 4: Time points, associated with CFUs counts of Gliocladium virens at different dilution factors.

Time (h)	CFUs				CFUs/mL				
	10^{-3}	10^{-4}	10^{-5}	10^{-6}	10^{-3}	10^{-4}	10^{-5}	10^{-6}	Total
0	0	0	0	0	0	0	0	0	0
1	0	0	0	0	0	0	0	0	0
2	0	0	0	1	0	0	0	2000000	2000000
3	2	0	0	0	4000	0	0	0	4000
4	0	0	0	0	0	0	0	0	0
5	1	0	0	0	2000	0	0	0	2000
6	1	0	0	0	2000	0	0	0	2000
7	0	0	0	0	0	0	0	0	0
8	3	0	0	0	6000	0	0	0	6000
24	0	0	0	1	0	0	0	2000000	2000000
48	0	0	0	1	0	0	0	2000000	2000000
72	0	0	0	0	0	0	0	0	0

The relation of the optical density and CFUs/mL of this fungus allowed the creation of the growth curve, having a positive slope and a R^2 of 0,26 as seen in Figure 10. As it showed a linear regression, the protocol was continued to the second part of the method proposed.

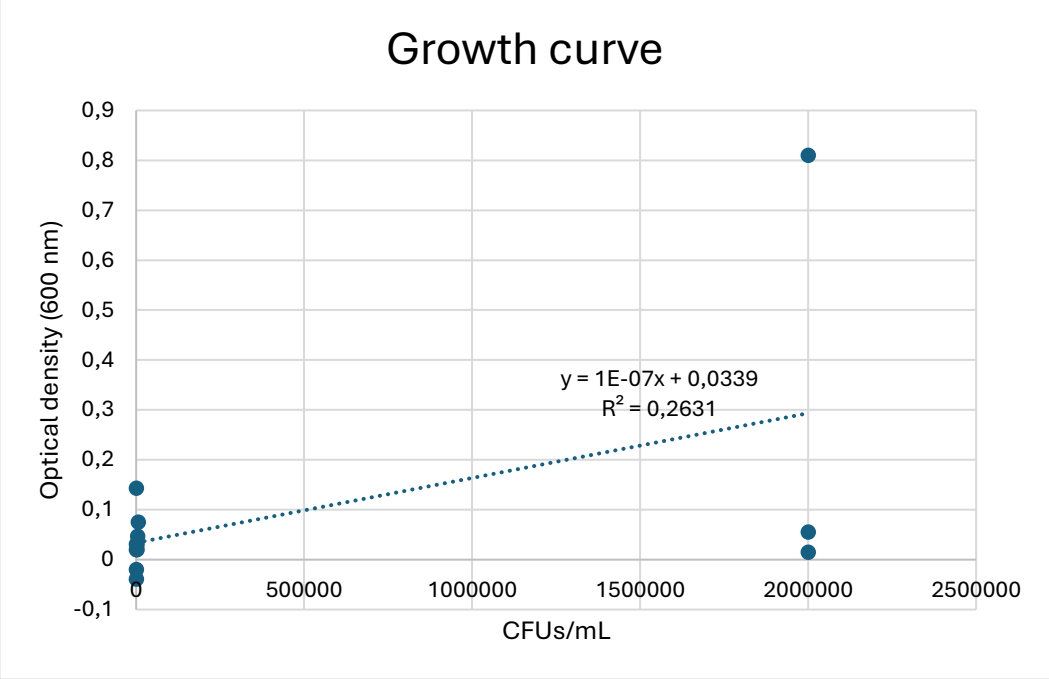

Figure 10: Growth curve of Gliocladium virens.

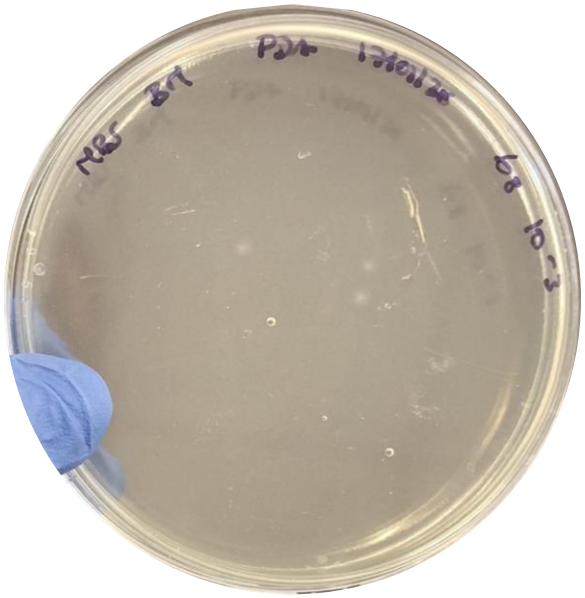

Figure 11: CFU count of Gliocladium virens at t8 in a 10^{-3} dilution.

Figure 12: Colonies growth of Gliocladium virens at seven days of incubation at room temperature.

3.1.2. Final optimisation strategy

In this protocol, the optical density of *Gliocladium virens* was measured in three different wavelengths (530, 600 and 670 nm) also relating to two different types of samples, one with sterile distilled water and the other with Tween 20 solution.

The results shown in Table 5 demonstrated variation in some measurements, due to the possible difficulty of stabilizing the spectrophotometer. Furthermore, the values from the triplets weren't precise in the two types of samples, noticing it more in the Tween 20 solution samples, as the samples tubes contained more or less content of the fungus, which determinate the optical density. It also revealed that the highest value of optical density was 0,141 for the sample 10(1) at 670 nm and the lowest value was for 10(3) at 670 nm as well.

Table 5: Optical density of Gliocladium virens measured at three different wavelengths (530, 600, 670 nm).

Sample	OD		
	530 nm	600 nm	670 nm
10(1)	0,043	0,047	0,141
10(2)	0,043	0,043	0,039
10(3)	0,019	0,020	0,016
10(1) Tween 20	0,085	0,123	0,067
10(2) Tween 20	0,064	0,064	0,051
10(3) Tween 20	0,047	0,063	0,059

The CFUs were also counted in those samples as it can be seen in Table 6. The plates from the sterile distilled water samples had, in general, less growth observed than the samples with Tween 20 solution. Tween 20 solution may have played a role in the dispersion of the conidia, so it can lead to the growth of more colonies in the plate, which was noticed. It can also be observed the dilution correlation with the quantity of the colonies formed, because the no dilution (10^0) showed more colonies formed than the highest dilution (10^{-6}), in which, only 1 colony was formed in only two samples. It was also revealed that the highest number of CFUs counted was more than 400 colonies for the sample 10(2) with no dilution (10^0) and the lowest quantity, in this case, 0 colonies, was for some samples at the highest dilutions (10^{-5} and 10^{-6}). The CFUs/mL are also revealed in Table 7.

Table 6: CFUs count of Gliocladium virens for two different types of samples and their distinct dilution factor.

Samples	CFUs						
	10^0	10^{-1}	10^{-2}	10^{-3}	10^{-4}	10^{-5}	10^{-6}
10(1)	>300	152	24	5	0	0	1
10(2)	>400	188	29	9	3	0	1
10(3)	300	73	5	2	0	0	0
10(1) Tween 20	>200	>200	77	24	6	2	0
10(2) Tween 20	>400	>200	136	28	10	5	0
10(3) Tween 20	>300	159	20	5	0	0	0

Table 7: CFUs/mL count of Gliocladium virens for two different types of samples and their distinct dilution factor.

Samples	CFUs/mL						
	10^0	10^{-1}	10^{-2}	10^{-3}	10^{-4}	10^{-5}	10^{-6}
10(1)	-	3040	4800	10000	0	0	2000000
10(2)	-	3760	5800	18000	60000	0	2000000
10(3)	600	1460	1000	4000	0	0	0
10(1) Tween 20	-	-	15400	48000	120000	400000	0
10(2) Tween 20	-	-	27200	56000	200000	1000000	0
10(3) Tween 20	-	3180	4000	10000	0	0	0

Protocol repetition with the other fungi

After analysing those results, it was evident that the ideal type of sample to use in the further steps was the fungi sample from the sterile distilled water solution. All of 5 fungi of interest were tested, and, additionally, the optical density was measured again in the three different wavelengths (530, 600 and 670 nm) in each dilution made. The CFUs were also counted and the concentration curve for each fungus and each wavelength was performed. The results are shown in the tables and figures below.

Alternaria sp.

Table 8 showed some negative values of optical density in the three wavelengths tested and the highest positive value was 0,020 for the sample with no dilution at 530 nm. These results were inconsistent. The highest number of CFUs counted was 53 colonies for the sample with no dilution (10^0) and the lowest quantity was 0 colonies for some samples at the 10^{-2} and 10^{-3} and the highest dilutions (10^{-5} and 10^{-6}).

Table 8: Optical density of Alternaria sp. measured at three different wavelengths (530, 600, 670 nm) and CFUs count for the different dilutions.

Dilution	OD			CFUs	CFUs/mL
	530 nm	600 nm	670 nm		
10^0	0,020	0,019	0,018	53	10,60
10^{-1}	0,004	0,003	0,003	7	14,00
10^{-2}	-0,002	-0,003	-0,002	0	0,00
10^{-3}	-0,002	-0,004	0,000	0	0,00
10^{-4}	-0,005	-0,005	-0,003	2	4000,00
10^{-5}	0,000	-0,001	0,001	0	0,00
10^{-6}	-0,003	-0,004	-0,004	0	0,00

The concentration curve for *Alternaria sp.* for the wavelength 530 nm, showed a negative slope and a R^2 of 0,11, as it can be seen in Figure 13.

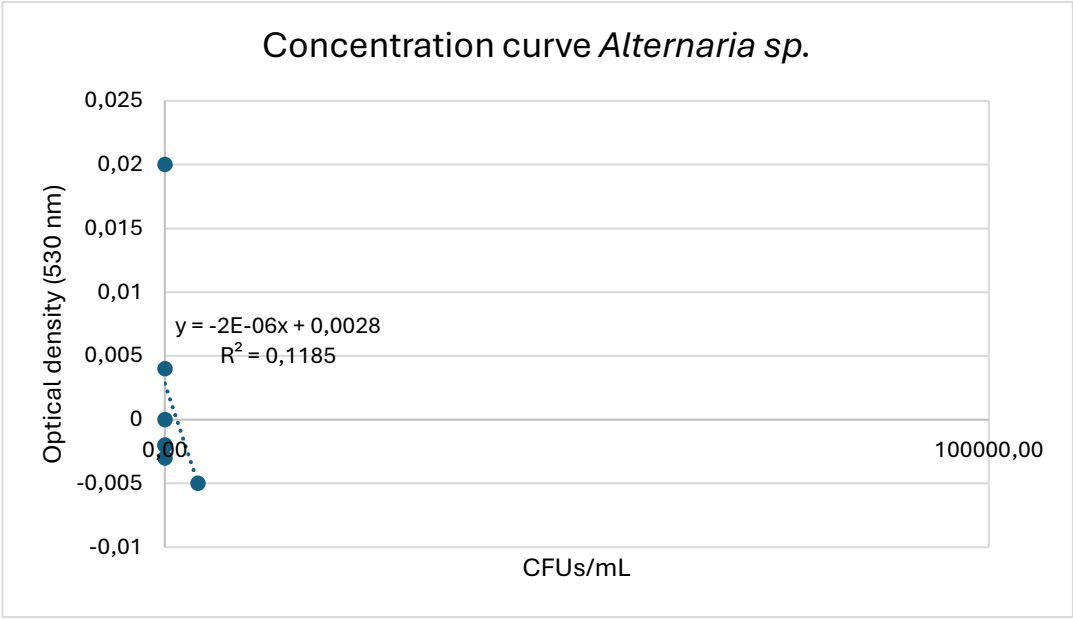

Figure 13: Concentration curve of Alternaria sp. with optical density at 530 nm.

The concentration curve for *Alternaria sp.* for the wavelength 600 nm, showed a negative slope and a R^2 of 0,086, as it can be seen in Figure 14.

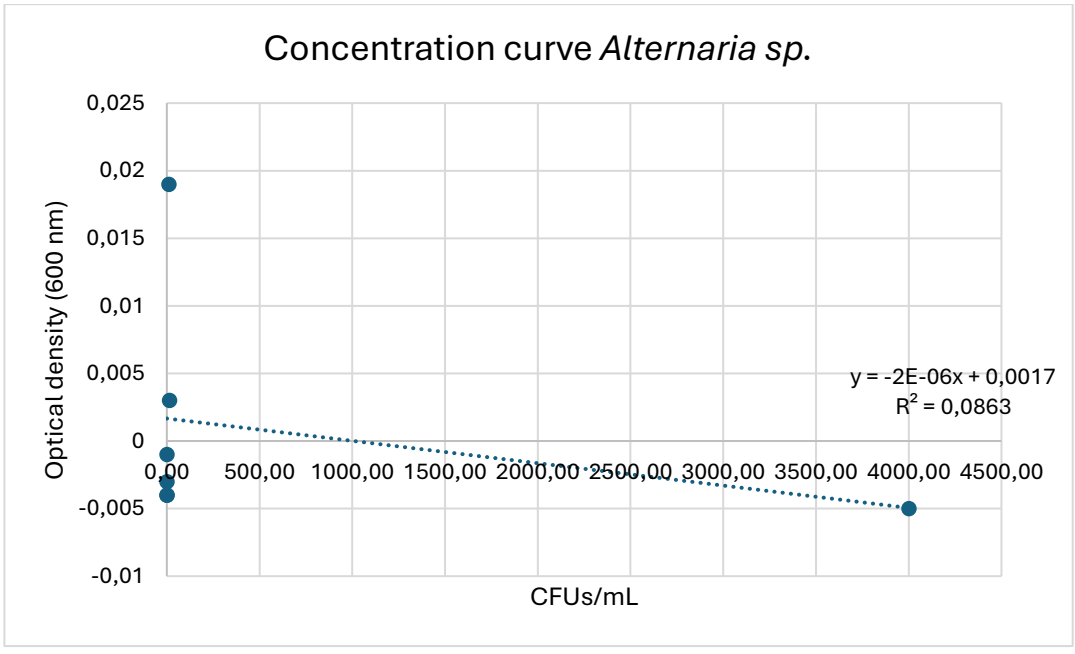

Figure 14: Concentration curve of Alternaria sp. with optical density at 600 nm.

The concentration curve for *Alternaria sp.* for the wavelength 670 nm, showed a negative slope and a R^2 of approximately 0,08 as it can be seen in Figure 15.

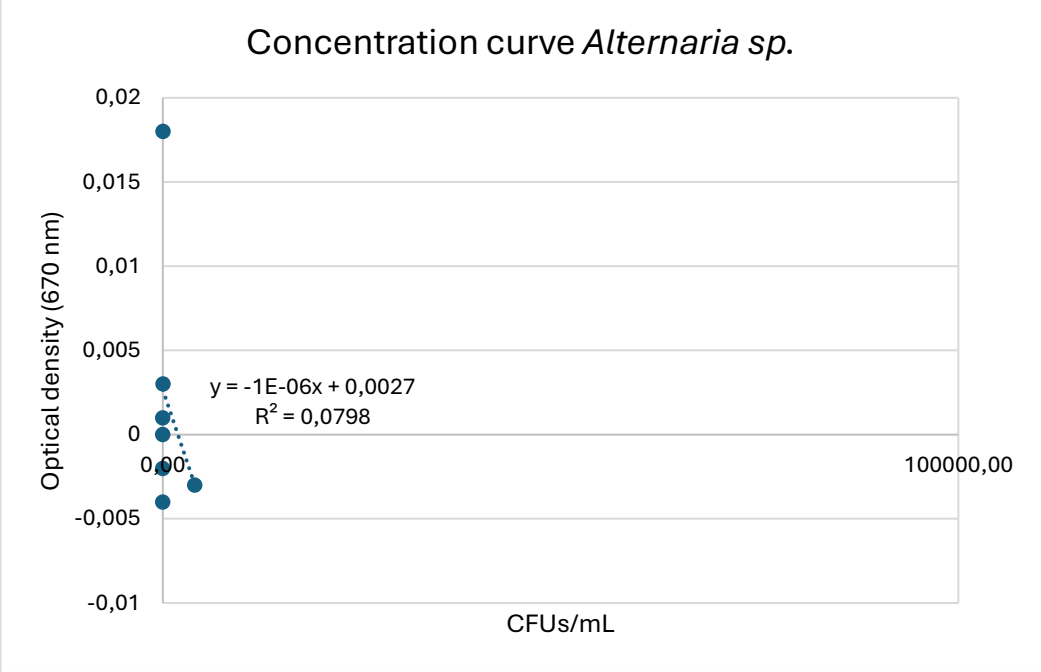

Figure 15: Concentration curve of Alternaria sp. with optical density at 670 nm.

Aspergillus flavus

Table 9 showed negative values of optical density in the three wavelengths tested and the highest positive value was 0,001 for the sample with no dilution at 530 nm. These results were inconsistent. The highest number of CFUs counted was 1 colony for the sample with no dilution (10^0) and the lowest quantity was, in this case, 0 colonies for all other samples.

Table 9: Optical density of A. flavus measured at three different wavelengths (530, 600, 670 nm) and CFUs count for the different dilutions.

Dilution	OD			CFUs	CFUs/mL
	530 nm	600 nm	670 nm		
10^0	0,001	0,000	-0,001	1	0,20
10^{-1}	-0,002	-0,003	-0,003	0	0,00
10^{-2}	-0,001	-0,003	-0,003	0	0,00
10^{-3}	0,000	-0,002	-0,002	0	0,00
10^{-4}	-0,003	-0,005	-0,004	0	0,00
10^{-5}	-0,001	-0,003	-0,001	0	0,00
10^{-6}	-0,005	-0,004	-0,006	0	0,00

The concentration curve for *Aspergillus flavus* for the wavelength 530 nm, showed a positive slope and a R^2 of 0,32 as it can be seen in Figure 16.

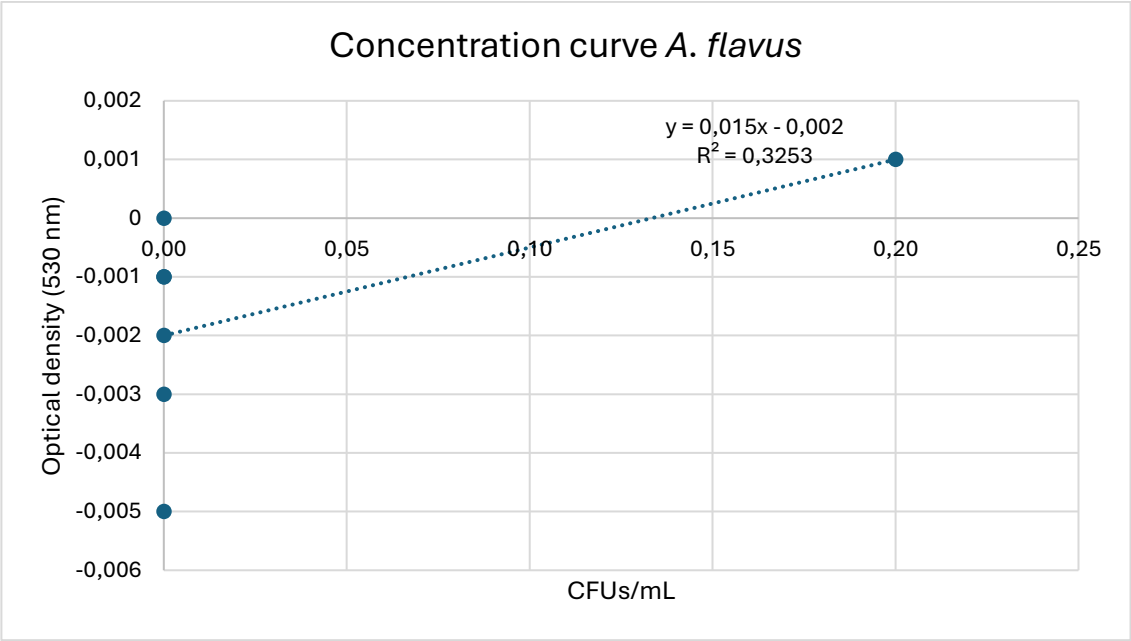

Figure 16: Concentration curve of Aspergillus flavus with optical density at 530 nm.

The concentration curve for *Aspergillus flavus* for the wavelength 600 nm, showed a positive slope and a R^2 of 0,64 as it can be seen in Figure 17.

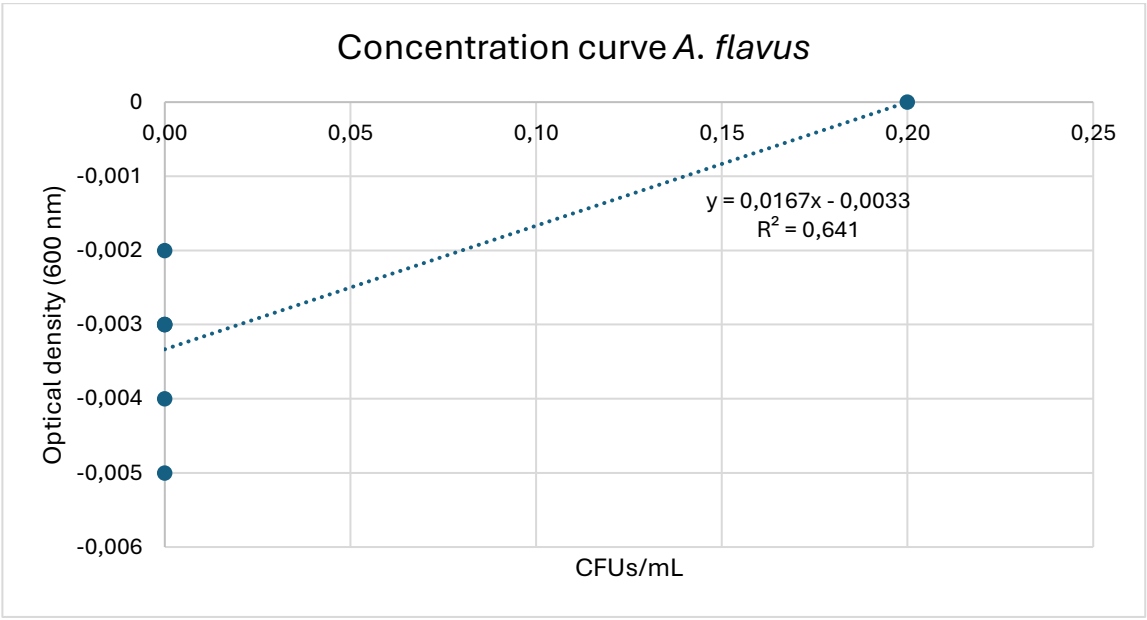

Figure 17: Concentration curve of Aspergillus flavus with optical density at 600 nm.

The concentration curve for *Aspergillus flavus* for the wavelength 670 nm, showed a positive slope and a R^2 of 0,21 as it can be seen in Figure 18.

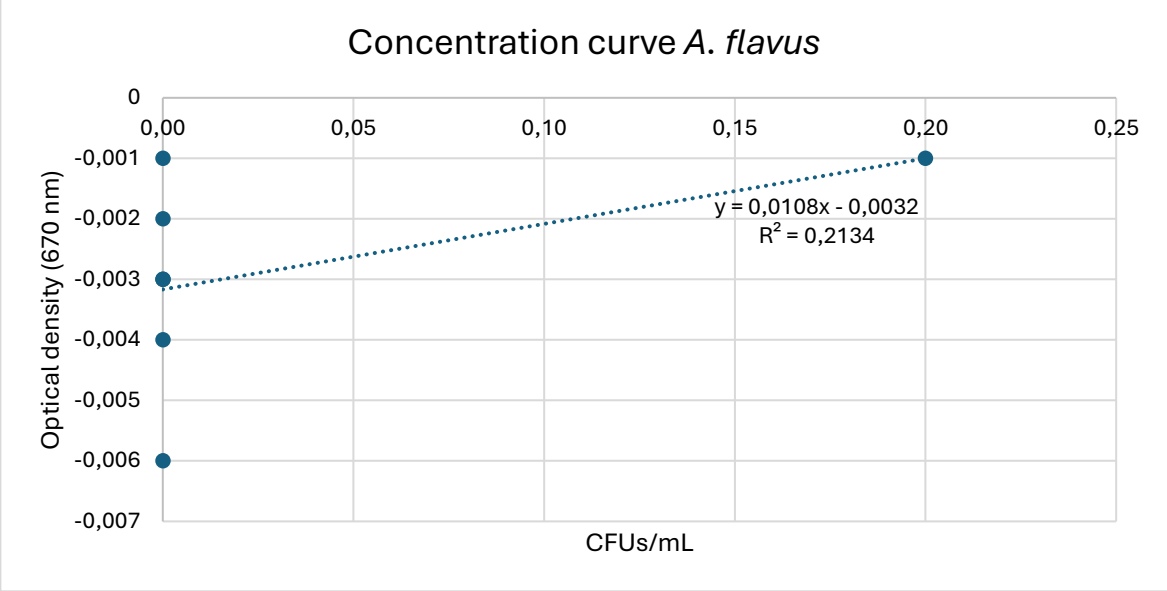

Figure 18: Concentration curve of Aspergillus flavus with optical density at 670 nm.

Aspergillus niger

Table 10 showed as well negative values of optical density in the three wavelengths tested and the highest positive value was 0,007 for the sample with a 10^{-1} dilution at 530 and 600 nm. These results were inconsistent. The highest number of CFUs counted was 23 colonies for the sample with no dilution (10^0) and the lowest quantity was 0 colonies for all other samples except for the 10^{-1} sample.

Table 10: Optical density of A. niger measured at three different wavelengths (530, 600, 670 nm) and CFUs count for the different dilutions.

Dilution	OD			CFUs	CFUs/mL
	530 nm	600 nm	670 nm		
10^0	0,002	0,002	0,000	23	4,60
10^{-1}	0,007	0,007	0,005	2	4,00
10^{-2}	-0,003	-0,004	-0,003	0	0,00
10^{-3}	0,002	-0,002	-0,002	0	0,00
10^{-4}	-0,003	-0,004	-0,004	0	0,00
10^{-5}	-0,002	-0,002	0,000	0	0,00
10^{-6}	-0,004	-0,005	-0,004	0	0,00

The concentration curve for *Aspergillus niger* for the wavelength 530 nm, showed a positive slope and a R^2 of 0,58 as it can be seen in Figure 19.

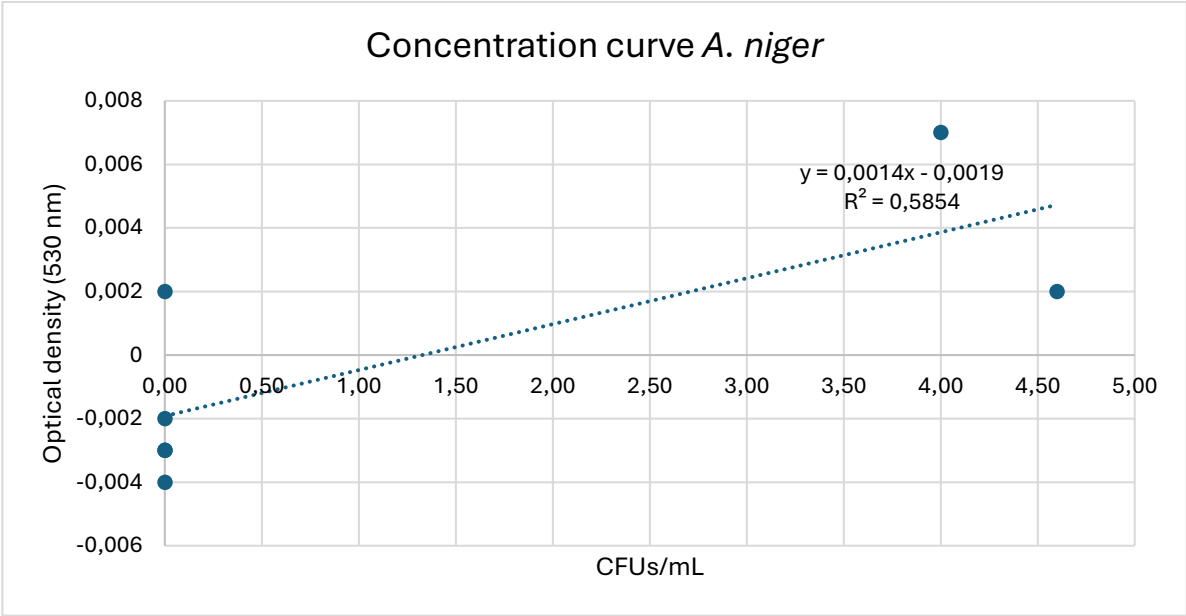

Figure 19: Concentration curve of Aspergillus niger with optical density at 530 nm.

The concentration curve for *Aspergillus niger* for the wavelength 600 nm, showed a positive slope and a R^2 of 0,76 as it can be seen in Figure 20.

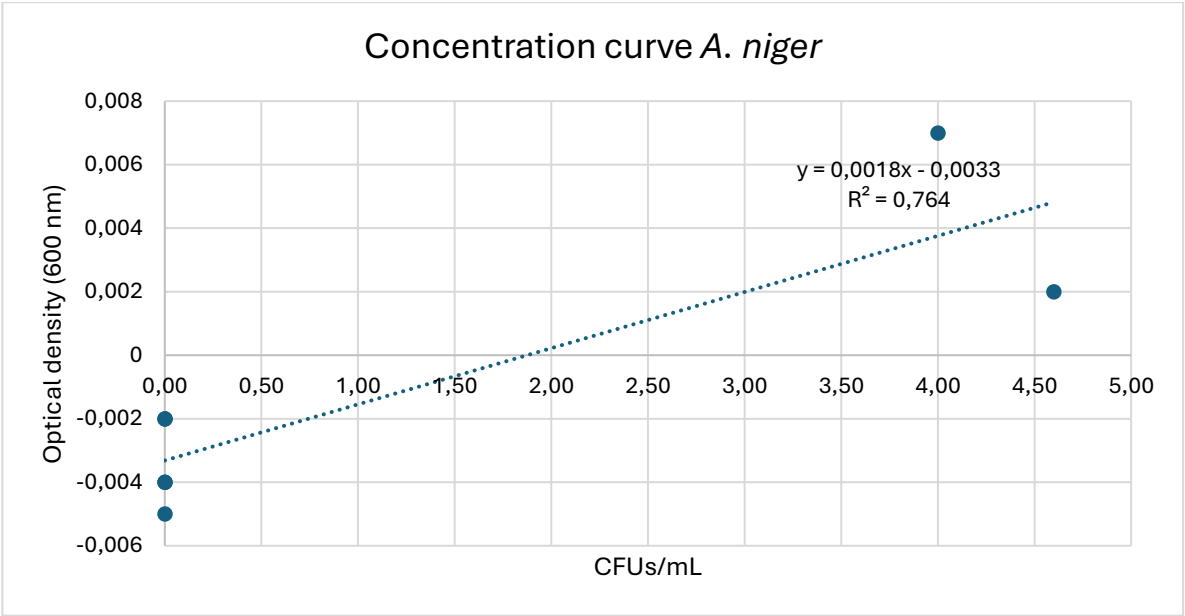

Figure 20: Concentration curve of Aspergillus niger with optical density at 600 nm.

The concentration curve for *Aspergillus niger* for the wavelength 670 nm, showed a positive slope and a R^2 of 0,55 as it can be seen in Figure 21.

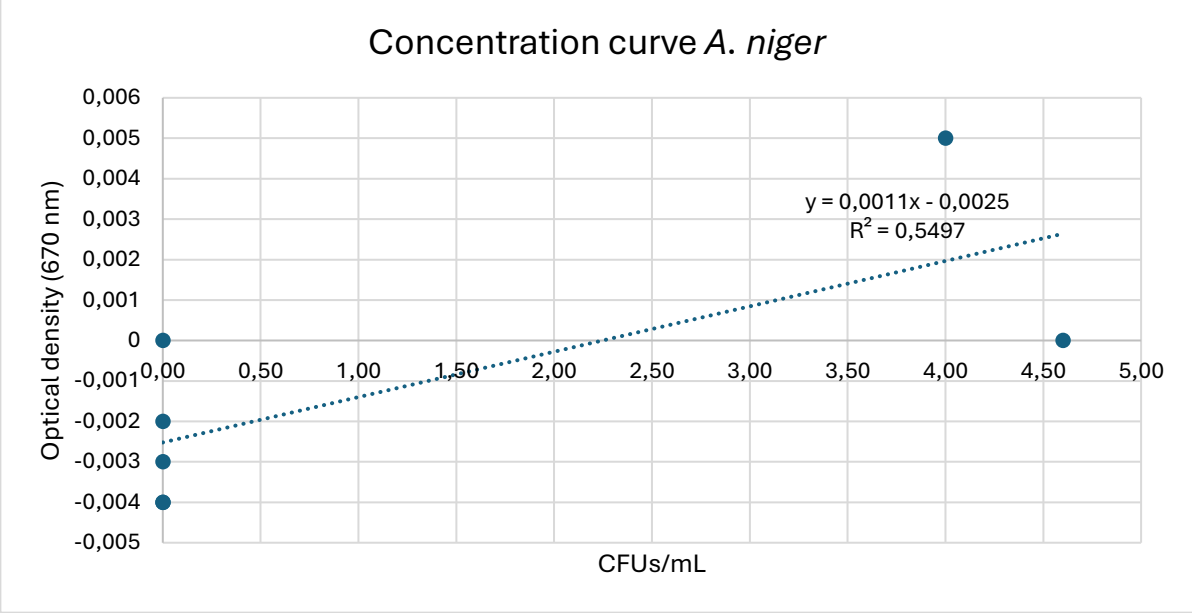

Figure 21: Concentration curve of Aspergillus niger with optical density at 670 nm.

Gliocladium virens

Table 11 showed negative values of optical density in the three wavelengths tested and the highest positive value was 0,034 for the sample with no dilution at 530 nm, being the highest value so far. These results were inconsistent. The highest number of CFUs counted was more than 600 colonies for the sample with no dilution (10^0), followed by the sample 10^{-1} that showed a growth of 535 colonies. The lowest quantity was 1 colony for sample with a 10^{-3} dilution.

Table 11: Optical density of G. virens measured at three different wavelengths (530, 600, 670 nm) and CFUs count for different dilutions.

Dilution	OD			CFUs	CFUs/mL
	530 nm	600 nm	670 nm		
10^0	0,034	0,002	0,004	>600	-
10^{-1}	-0,012	-0,013	-0,01	535	1070,00
10^{-2}	-0,012	-0,012	-0,009	67	1340,00
10^{-3}	-0,015	-0,017	-0,014	17	3400,00
10^{-4}	-0,013	-0,013	-0,01	3	6000,00
10^{-5}	-0,013	-0,013	-0,011	3	60000,00
10^{-6}	-0,013	-0,014	-0,011	1	200000,00

The concentration curve for *Gliocladium virens* for the wavelength 530 nm, showed a negative slope and a very low R^2 of 0,0001 as it can be seen in Figure 22.

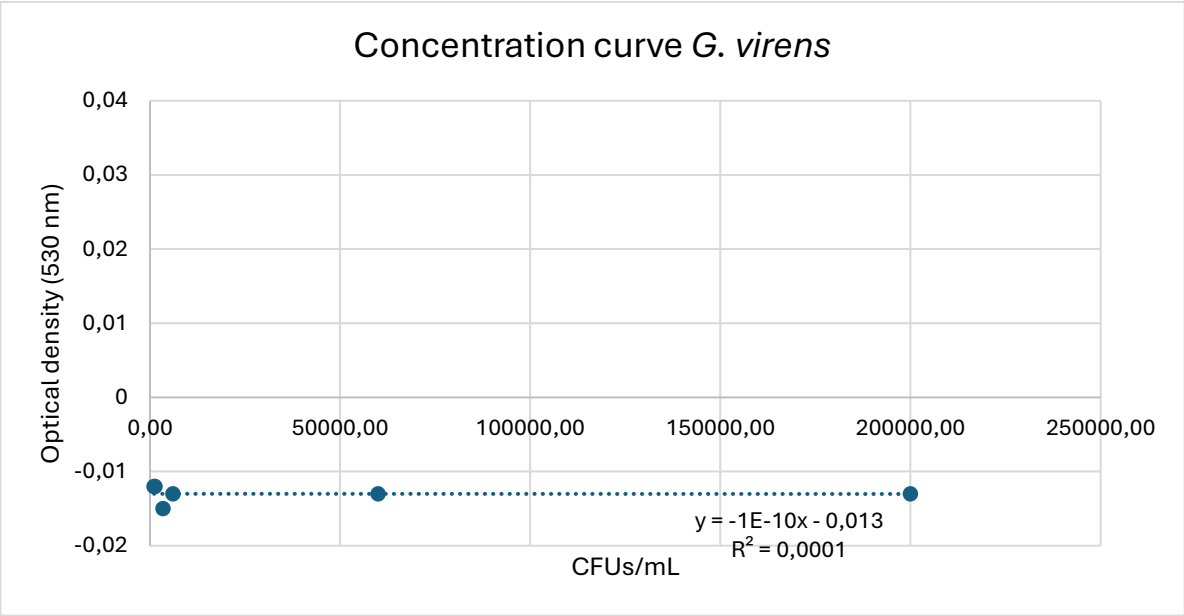

Figure 22: Concentration curve of Gliocladium virens with optical density at 530 nm.

The concentration curve for *Gliocladium virens* for the wavelength 600 nm, showed a negative slope and a very low R^2 of 0,002 as it can be seen in Figure 23.

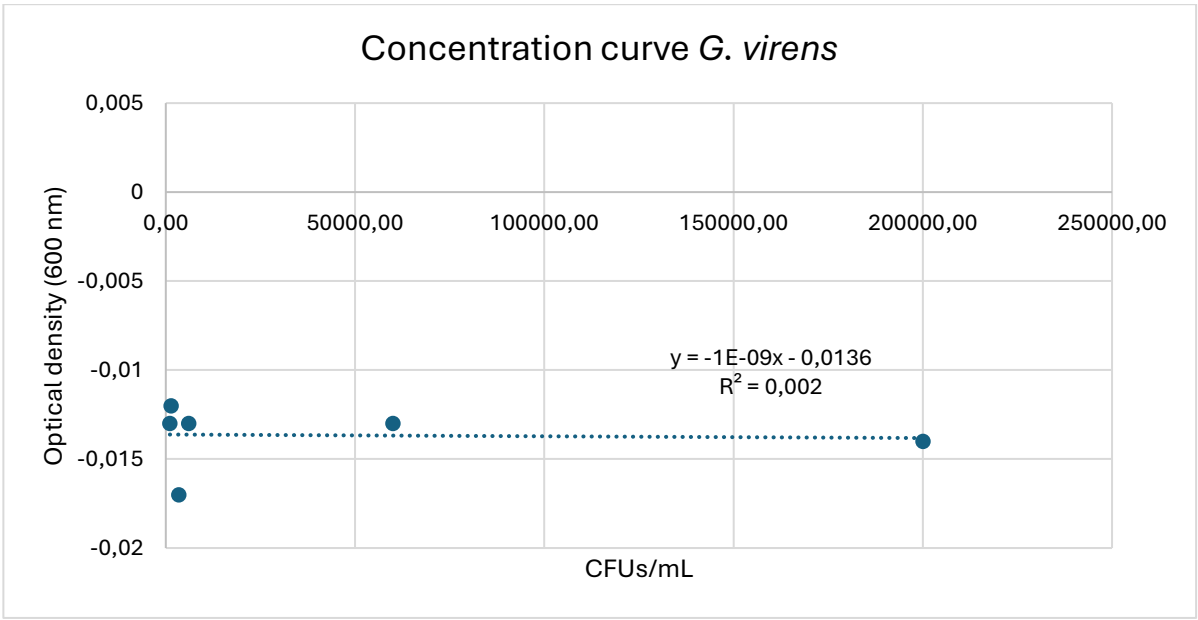

Figure 23: Concentration curve of Gliocladium virens with optical density at 600 nm.

The concentration curve for *Gliocladium virens* for the wavelength 670 nm, showed a negative slope and a very low R^2 of 0,0045 as it can be seen in Figure 24.

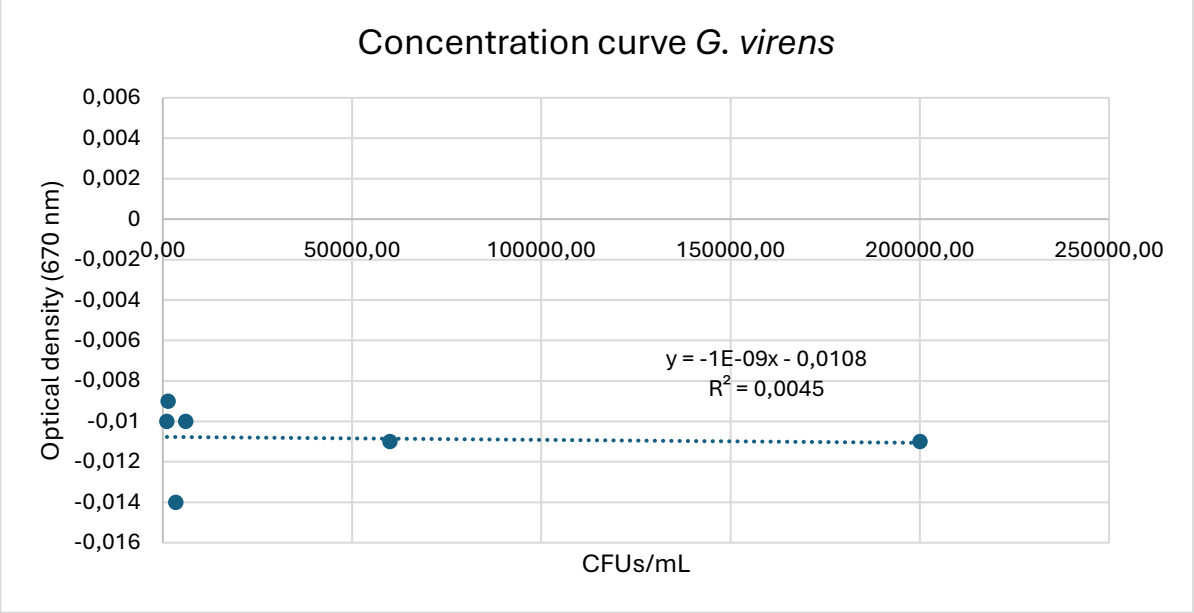

Figure 24: Concentration curve of Gliocladium virens with optical density at 670 nm.

Penicillium sp.

Table 12 showed negative values of optical density in the three wavelengths tested and the highest positive value was 0,016 for the sample with a dilution of 10^{-1} at 670 nm. These results were inconsistent. The plate from the no dilution sample (10^0), revealed to be the one with the more visible growth, having more than 300 colonies formed, followed by 220 colonies observed for the sample with a 10^{-1} dilution. The lowest quantity was, in this case, 0 colonies, for the last two samples with the highest dilution.

Table 12: Optical density of Penicillium sp. measured at three different wavelengths (530, 600, 670 nm) and CFUs count for different dilutions.

Dilution	OD			CFUs	CFUs/mL
	530 nm	600 nm	670 nm		
10^0	0,005	-0,022	-0,002	>300	-
10^{-1}	-0,037	-0,032	0,016	220	440,00
10^{-2}	-0,005	0,014	0,009	60	1200,00
10^{-3}	-0,031	-0,026	-0,02	28	5600,00
10^{-4}	-0,028	-0,023	-0,016	12	24000,00
10^{-5}	-0,04	-0,035	-0,027	0	0,00
10^{-6}	-0,019	-0,016	-0,012	0	0,00

The concentration curve for *Penicillium sp.* for the wavelength 530 nm, showed a negative slope and a R^2 of 0,039 as it can be seen in Figure 25.

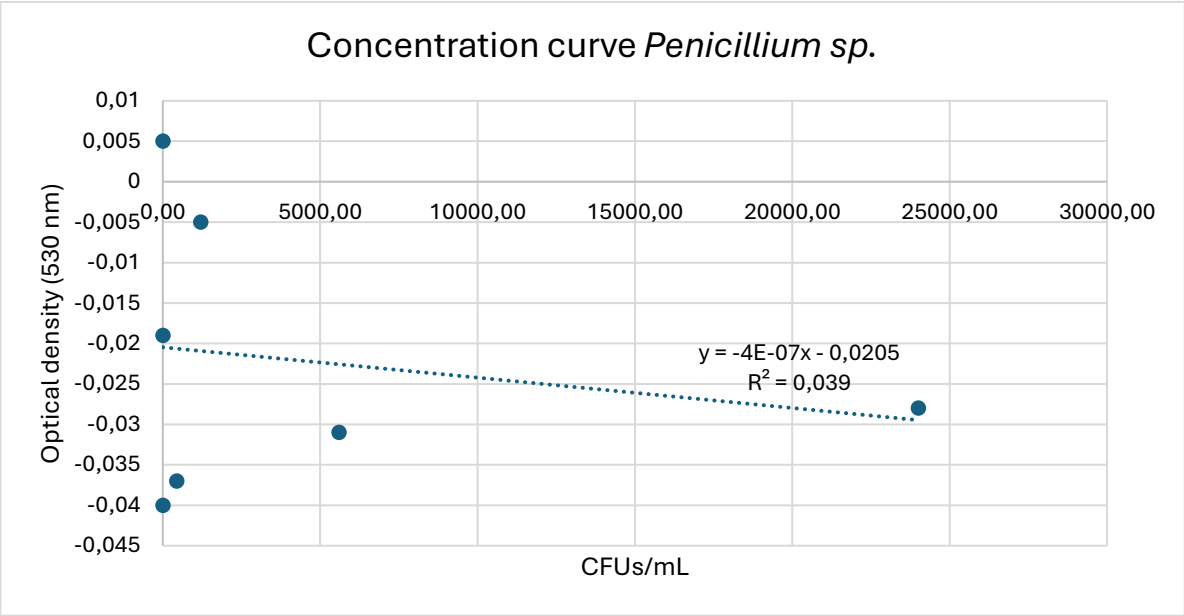

Figure 25: Concentration curve of Penicillium sp. with optical density at 530 nm.

The concentration curve for *Penicillium sp.* for the wavelength 600 nm, showed a negative slope and a R^2 of 0,0066 as it can be seen in Figure 26.

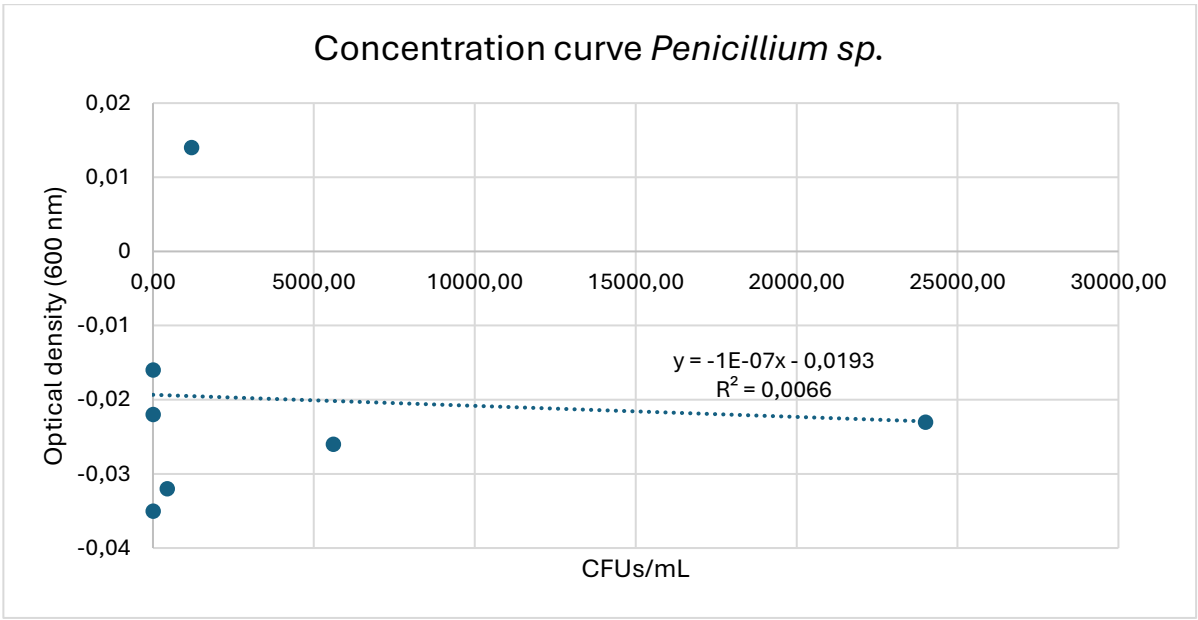

Figure 26: Concentration curve of Penicillium sp. with optical density at 600 nm.

The concentration curve for *Penicillium sp.* for the wavelength 670 nm, showed a negative slope and a R^2 of 0,078 as it can be seen in Figure 27.

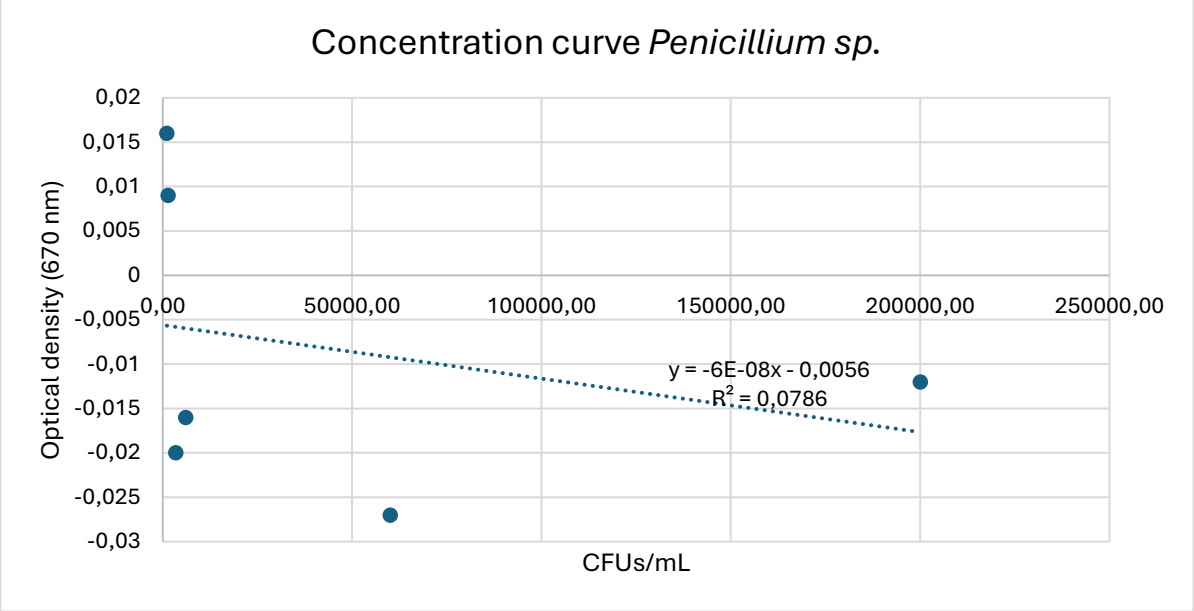

Figure 27: Concentration curve of Penicillium sp. with optical density at 670 nm.

3.2. Measurement of volatile organic compounds of fungi using the electronic nose, CFUs count and statistical analysis

The glass tubes with the fungi of interest were incubated for 72h and the growth of each species was notorious as seen in Figure 28.

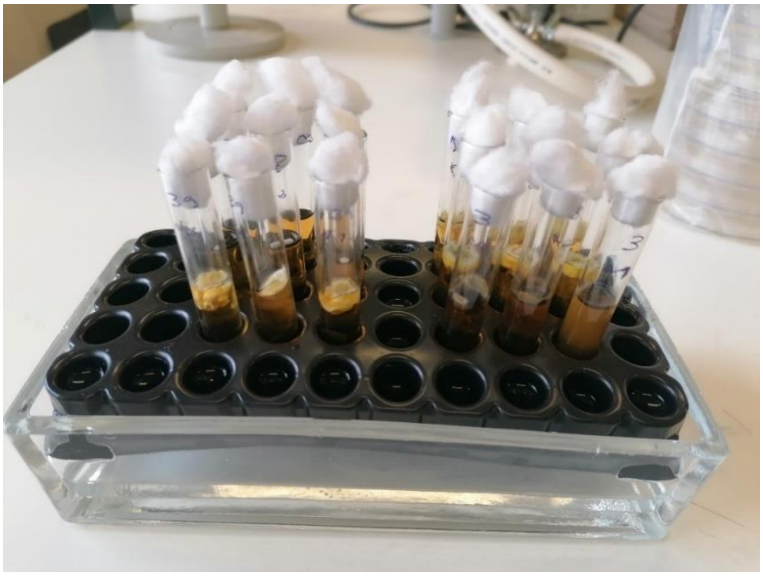

Figure 28: Fungi growth in glass tubes after 72h of incubation.

The values of the measurement of the volatile organic compounds of fungi relating to different parameters, using the electronic nose, are presented in the Annex (Table 23).

3.2.1. Statistical analysis

Initially the data was processed, following the dimension reduction by PCA in order to condense the variables in groups. A scree plot was created (Figure 29) relating the percentage of explained variances to dimensions, resulting in two main components that explain approximately 75% of the sample, meaning that the variance can be correctly represented in a two-dimensional plane.

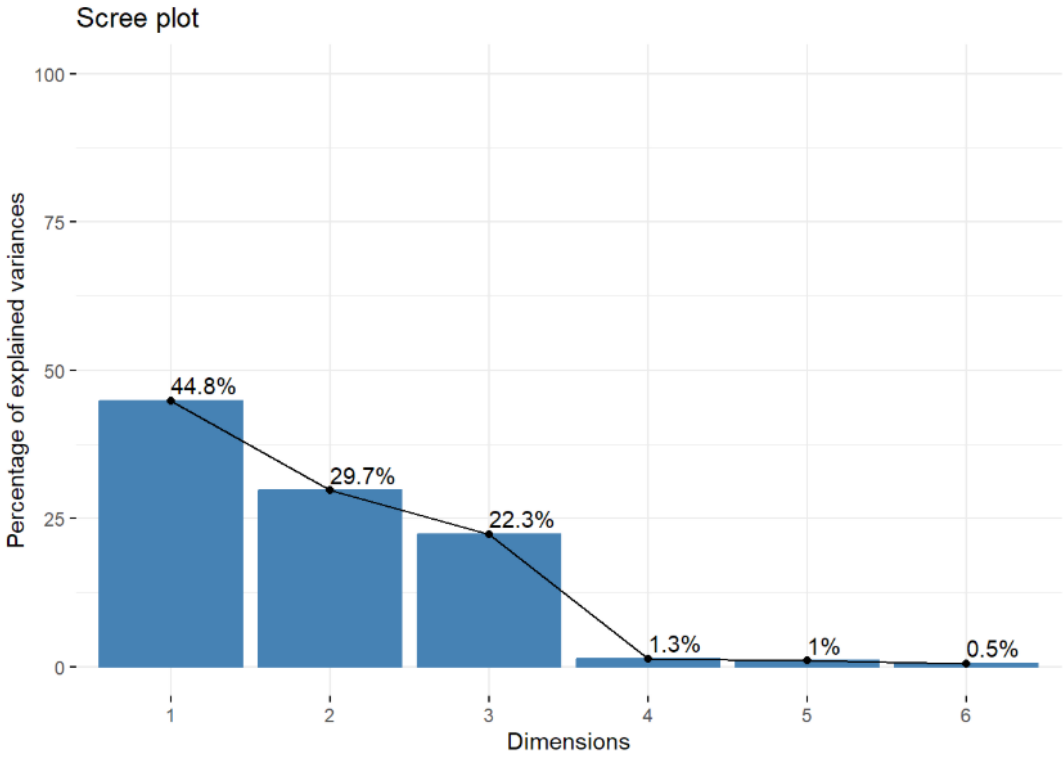

Figure 29: Dimension reduction by principal component analysis (PCA).

Then the results were transposed to a 2D plane, as it can be seen in the Figure 30. The graphic illustrated the differentiation between the species and the control. Nonetheless, the groups appeared to be relatively homogeneous, with considerable overlap among the species, giving an impression of uniformity. Consequently, the observed variation didn't seem to be adequately accounted for by the two components.

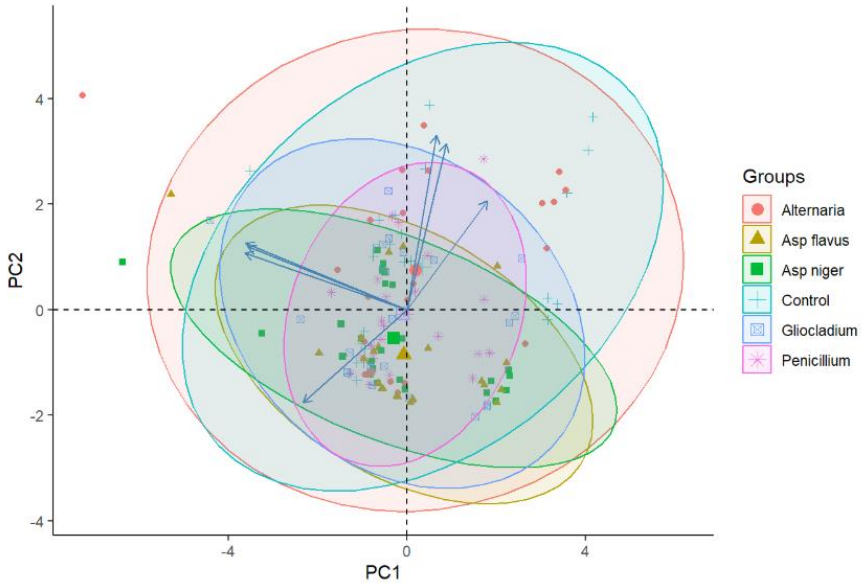

Figure 30: PCA – Differentiation by species.

Because of that, the next step was to perform a PCA to differentiate from time of incubation being divided from group of hours, as seen in Figure 31. The result of that seemed to show 2 different groups of incubation periods from 0, 1, 2, 3, 6 and 24h on the left quadrants and the other two time points (48 and 72h) on the right ones. It also appeared to have a clear distinction between the profiles after 48 hours of incubation shown by a diverse dispersion on the right quadrants.

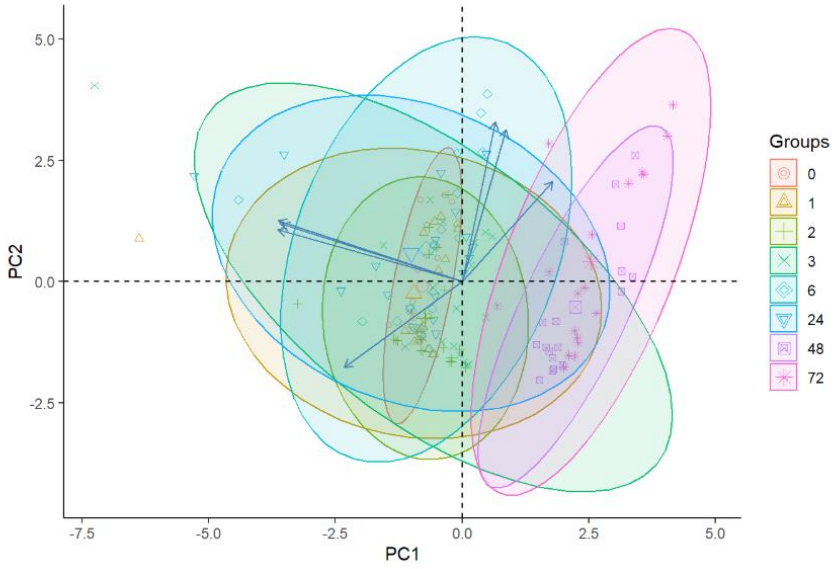

Figure 31: PCA – Differentiation by incubation periods (h).

Data relating the components PC1 and PC2 with the mean and standard division (Table 13) were correlated to two clusters, corresponding to time incubations from 0 to 24h and 48h to 72h. The *p* value showed more significancy in PC1, contrary to PC2 that demonstrated a *p* value (0,845) above the one considered to have significance (0,05).

Table 13: Data used to refer the samples after different times of incubation, relating the components PC1 and PC2 with the mean and standard division. P value was also evaluated.

	0 to 24h (N = 108)	48 and 72h (N = 36)	TOTAL (N = 144)	*p*
PC1	-0,79 ± 1,21	2,38 ± 0,80	-0,00 ± 1,77	< 0,001
PC2	0,014 ± 1,37	-0,041 ± 1,66	-0,00 ± 1,44	0,845

Another scree plot was created (Figure 32), considering only tubes after 48 hours of incubation, relating once again the percentage of explained variances to dimensions, resulting in two main components that explain, in this case, approximately 80% of the sample, and the variance was correctly represented in another two-dimensional plane, showing a more robust result.

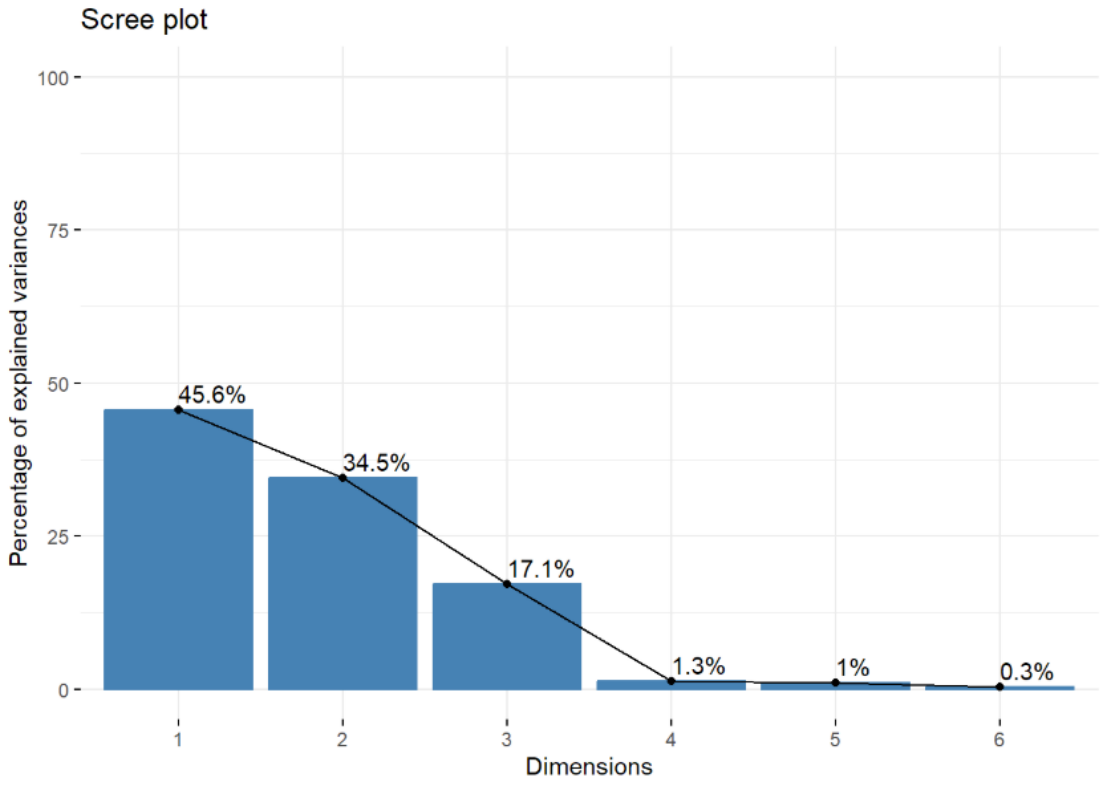

Figure 32: Dimension reduction by principal component analysis (PCA) referring to the 48h of incubation samples.

After that, the 2D plane graphic for all species from more than 48h of incubation was done, as shown in Figure 33, and it demonstrated a clear differentiation of *Penicillium sp.* in the first quadrant, and that, fungi of the same genus (*Aspergillus*) had the same volatile metabolite profile. *Alternaria sp.* showed the same profile as the controls.

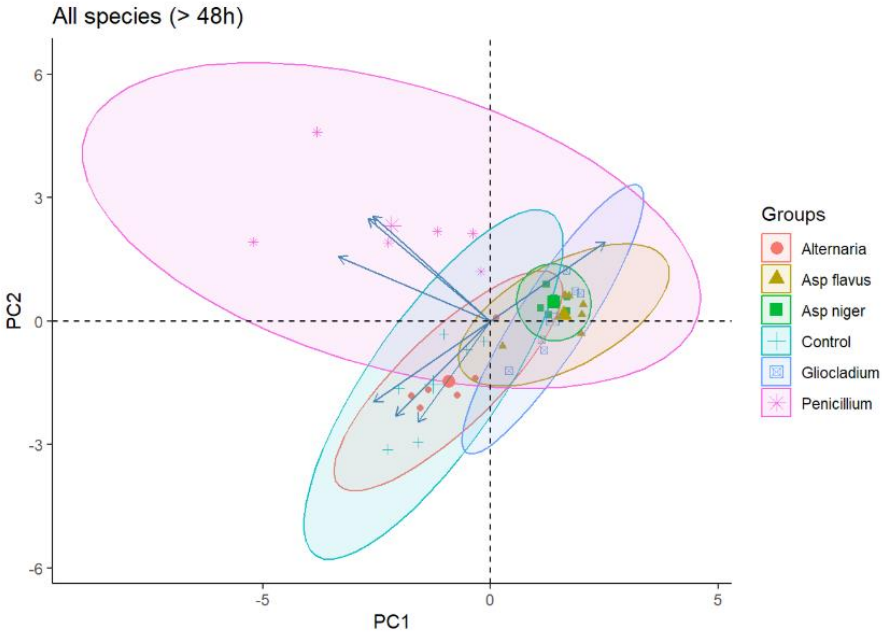

Figure 33: PCA – Differentiation by species at incubation period of > 48h.

Another PCA was performed (after 48h of incubation), presenting a difference between the fungi and controls groups, as it can be observed in Figure 34. The group 0 corresponding to the control samples showed to be biased to the left quadrant, although group 1, related to the fungi species, showed to be equally dispersed though all quadrants.

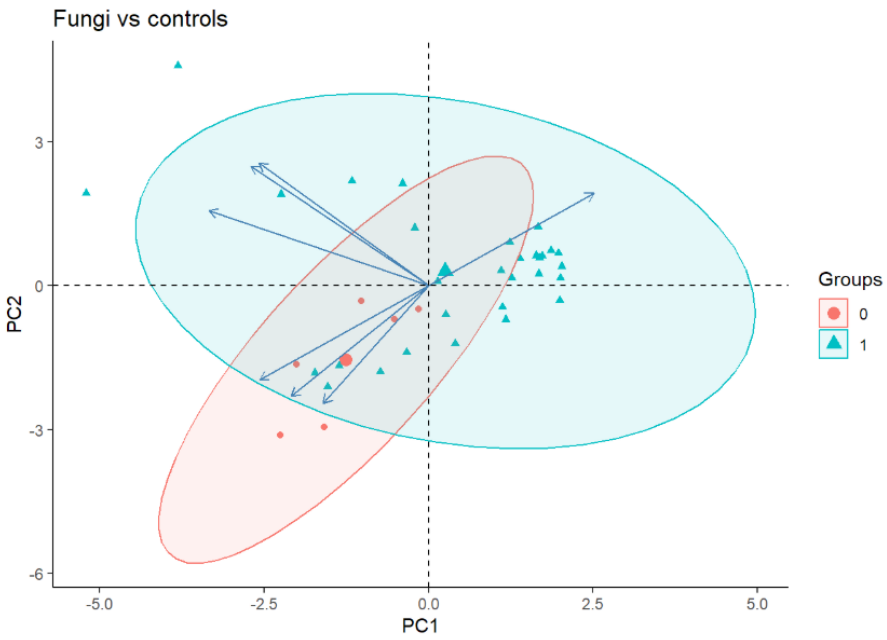

Figure 34: PCA – Differentiation by fungi species vs controls after 48h of incubation.

A different PCA demonstrated a difference between the *Penicillium sp.* fungus compared to the other species, as it can be observed in Figure 35, showing to be more present in the first left quadrant.

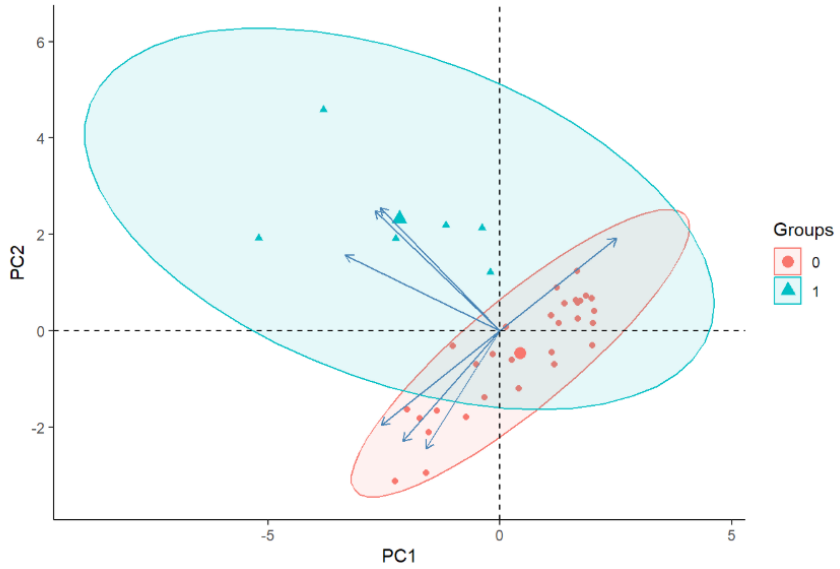

Figure 35: PCA – Differentiation by Penicillium sp. vs other species after 48h of incubation.

Next, models were performed for functional groups with all the times of incubation (0 to 72h) with different predictors as temperature, humidity and the functional groups such alkanes, ketones and others, associated to PC1 and PC2, and to a grouped test of fungi vs control. Pearson's correlation showed

a main differentiation by ketones and alkanes in the yy axis (Figure 36). It can also be observed that red circles and the blue ones had an inversible proportion, as the red meant it was less detected by a higher number and the blue one indicated that the variable was more detected, having a lower number associated. PC1 showed mainly indirect associations with parameters, whereas PC2 was directly related to a higher quantity of alkanes and ketones.

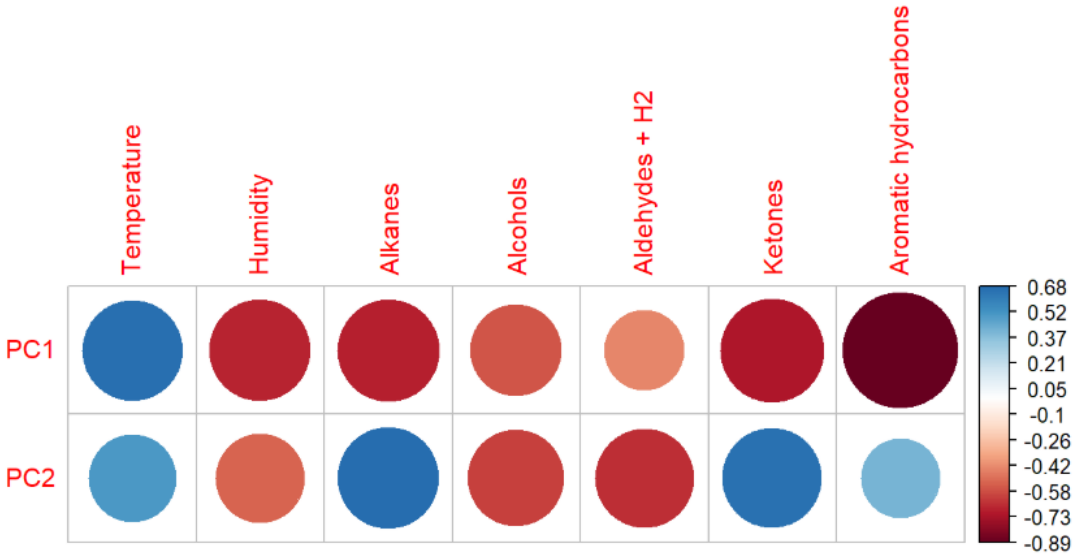

Figure 36: Correlation plot between PC1 and PC2 and different parameters such functional groups.

Other models related the predictors said before to the fungi vs control, by odds ratio, *CI* and *p*. The *p* value, shown in Table 14, was the lowest for alkanes (0,024) and ketones (0,028), showing more significance.

Table 14: Models by humidity and temperature parameters as well as functional groups with all incubation time periods (0 to 72h) differentiating fungi vs control. P value was also evaluated.

Predictors	Fungi vs control		
	Odds Ratios	*CI*	*p*
Temperature	1,05	0,70–1,59	0,793
Humidity	0,89	0,72–1,08	0,227
Alkanes	1,04	1,01–1,07	**0,024**
Alcohols	1,00	0,99–1,00	0,262
Aldehydes + H2	1,00	1,00–1,00	0,189
Ketones	0,99	0,99–1,00	**0,028**
Aromatic hydrocarbons	1,00	0,95–1,04	0,958

A ROC curve relating the sensitivity to specificity was performed, based on the previous information, differentiating fungi vs controls and having in account the functional groups, as seen in Figure 37. The area under the curve corresponded to 0,841 and the value of sensitivity was 0,767 (76,7%) and specificity was 0,833 (83,3%).

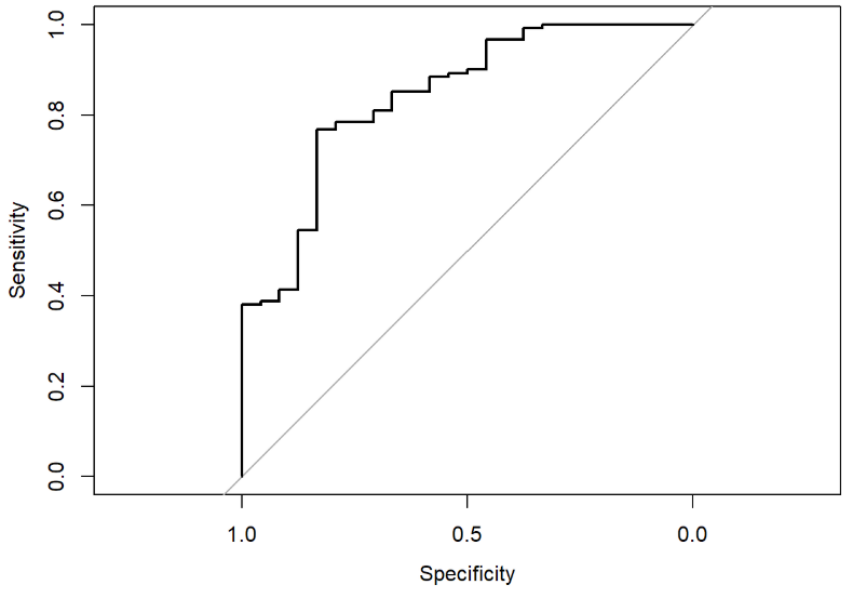

Figure 37: ROC curve differentiating fungi vs controls, based on the functional groups.

Then, shown in Table 15, there was a need to do an ordinary nonparametric bootstrap to verify stability, that simulates samples slightly lower and higher to see if the model is correct, which allowed a formation of a histogram.

Table 15: Bootstrap statistics, parameters for the verification of stability.

t	original	bias	std. error
t1	12,32	- 9,52	10,85
t2	0,053	- 0,080	0,22
t3	- 0,12	0,11	0,17
t4	0,035	- 0,034	0,0075
t5	- 0,0021	0,0021	0,0016
t6	0,0018	- 0,0018	0,0012
t7	- 0,0067	0,0066	0,0018
t8	- 0,0012	0,00079	0,025

A histogram and q-q plot were performed to verify stability as seen in Figure 38. The dashed line is far from the peak of the graphic, so the model appeared to not be stable. Although it was effective, the model's intercept showed a significant bias and alkanes remained prominent.

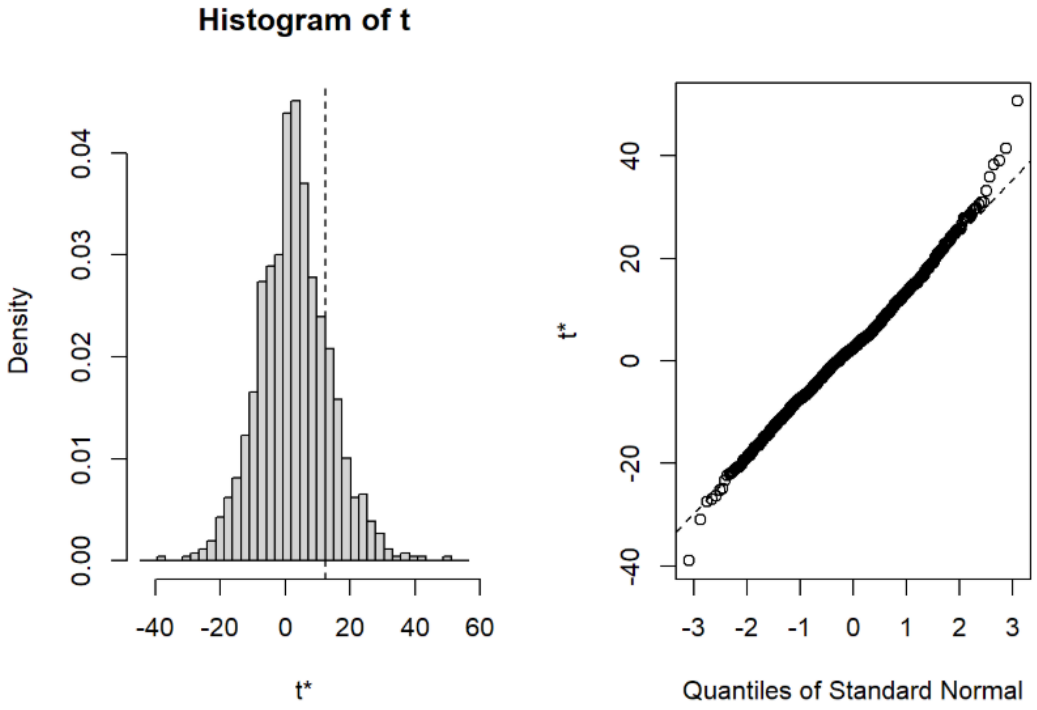

Figure 38: Bootstrap plot (histogram) and q-q plot.

Other models were done based on the two components of the most representative PCA model observed in Table 16, relating to odds ratio and *CI*. The *p* value was the lowest for PC2 showing more significance. A R^2 Tjur value was also determined being 0,311.

Table 16: Models by two main components of the most representative PCA model differentiating fungi vs control. P value was also evaluated.

Predictors	Fungi vs control		
	Odds Ratios	*CI*	*p*
PC1	1,69	0,74-3,59	0,139
PC2	2,35	1,22-6,75	**0,034**

Another ROC curve was done relating the sensitivity to specificity, differentiating fungi vs controls being based, in this case, on the two main components of the most representative model as seen in Figure 39. The area under the curve corresponded to 0,878 and the value of sensitivity was 0,767 (76,7%) and specificity was 1 (100%). A R^2 Tjur result, an important component in the analysis, was also presented being 0,311, which in this case indicated a good sign, despite that number usually being similar to the linear regression. In this repetition, the ROC curved presented a more promisor result having an area of approximately 88% which is above the previous one, indicating a better performance. Bias was reduced and more data was needed.

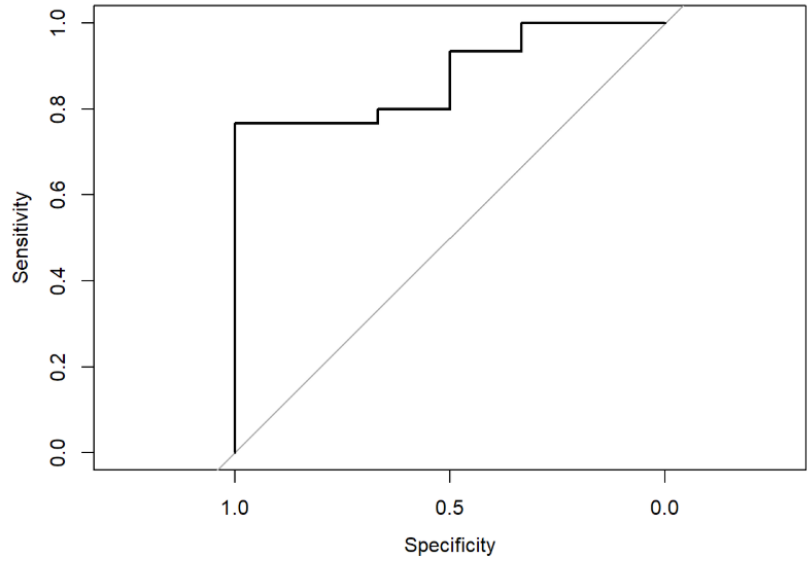

Figure 39: ROC curve differentiating fungi vs controls, based on the two main components of the most representative PCA model.

An ordinary nonparametric bootstrap was needed once again to verify stability, which allowed the formation of another histogram based on these results, seen in Table 17.

Table 17: Repetition of bootstrap statistics, parameters for the verification of stability.

t	original	bias	std. error
t1	2,36	0,39	11,12
t2	0,52	- 0,60	3,09
t3	0,85	- 0,61	2,20

Another histogram and q-q plot were performed to verify stability as seen in Figure 40. The dashed line was right at the peak of the graphic, which displayed a correct model to use, to know if it is fungal or not, although bias was reduced and more data was needed.

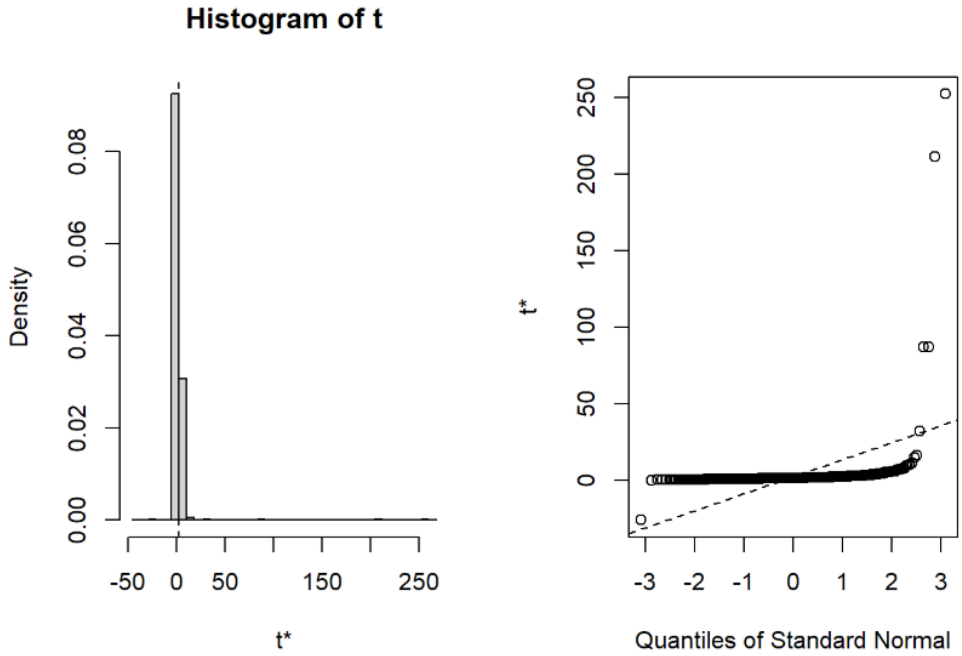

Figure 40: Bootstrap plot (histogram) and q-q plot performed to verify stability.

In order to continue the analysis of those results, a Hopkins test was performed to see how groupable the conditions were and analyse clusters, and the result obtained was approximately 0,853.

Then, the silhouette method was applied to verify the number of clusters, shown in Figure 41. The optimal number of clusters was k=5 per hierarchical cluster, as seen by the peak of the graphic.

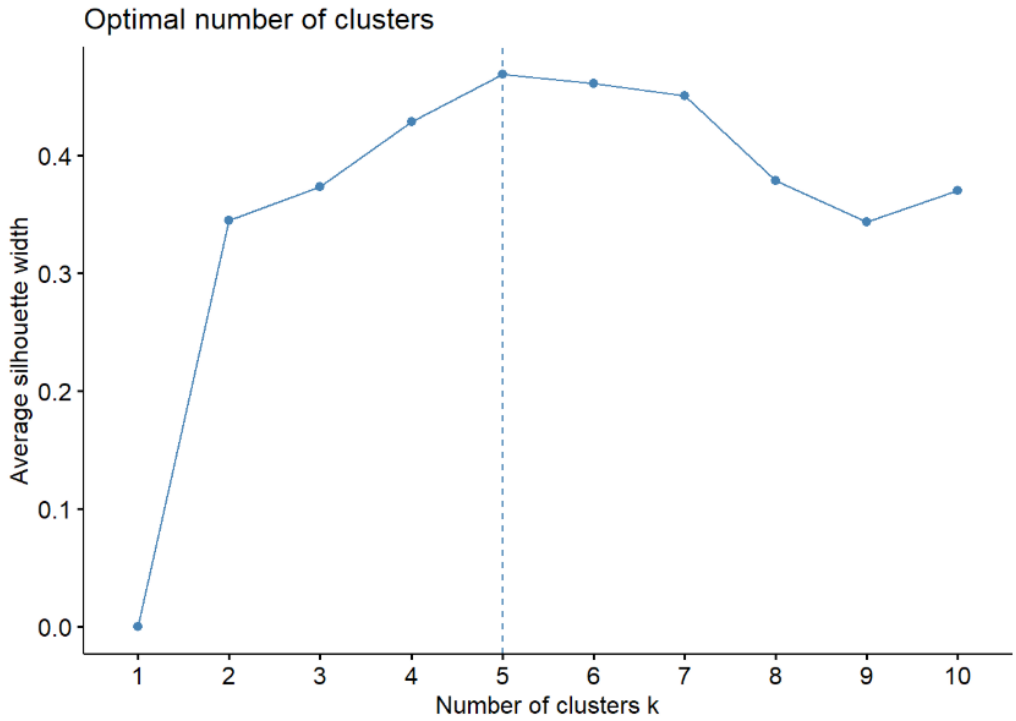

Figure 41: Silhouette plot. Optimal number of clusters was defined (k=5).

A heatmap (with K=5) of the hierarchical cluster analysis was performed by differentiation of species and relating to the parameters of functional groups, temperature and humidity as seen in Figure 42. A total of 5 clusters were defined, in which, *Penicillium sp.* samples were perfectly separated (even though by two different clusters) and *Alternaria sp.* showed the same profile as the controls. The remaining fungi from the *Ascomycota* phylum were all placed in the last cluster.

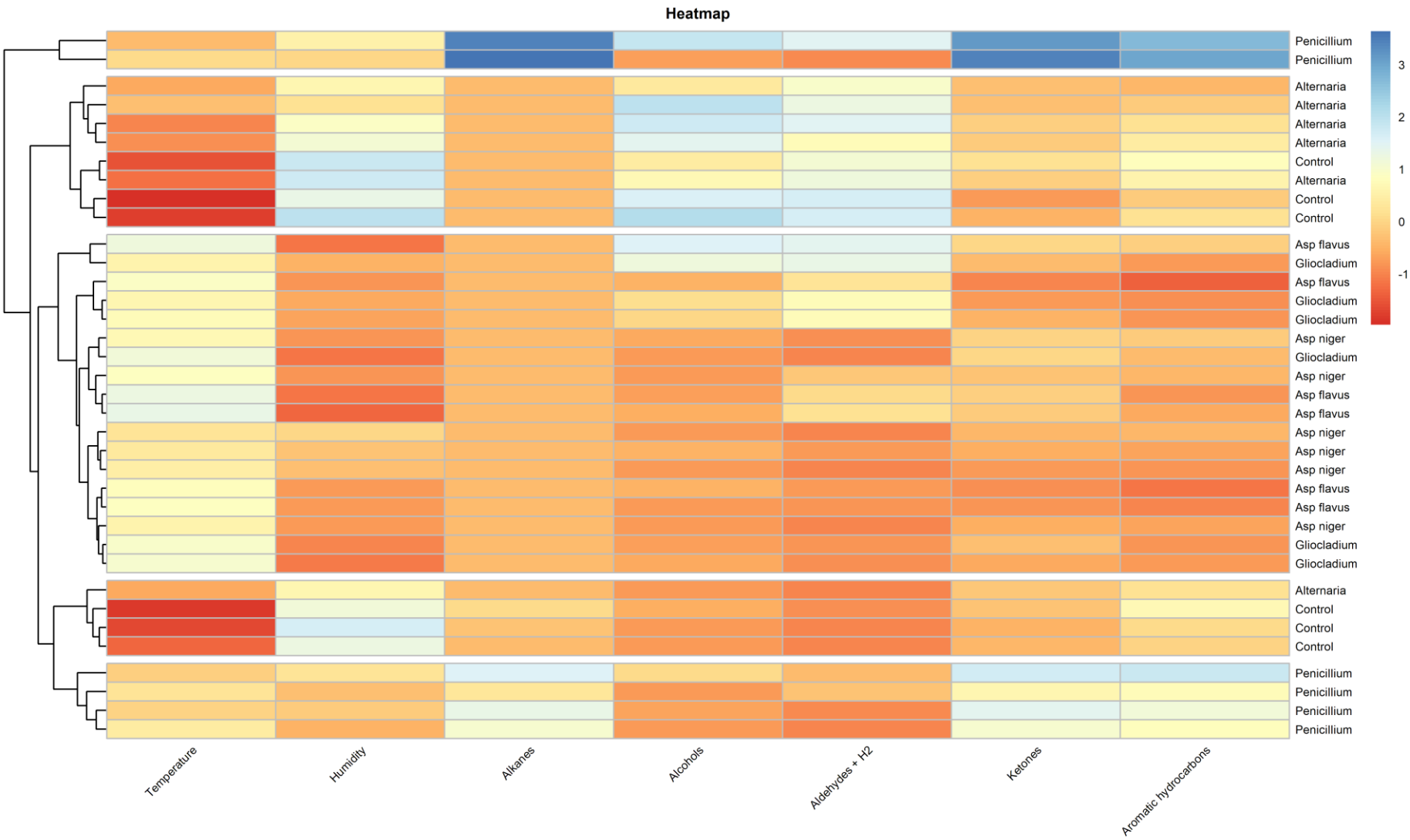

Figure 42: Heatmap (with K=5) of the hierarchical cluster analysis by species relating to the different parameters.

Table 18: Parameters of the silhouette method relating to all clusters (size and width).

cluster	size	Ave. sil. width
1	2	0,17
2	8	0,45
3	18	0,47
4	4	0,64
5	4	0,50

In relation to the q^2 tests to check whether there were differences in sample distribution across clusters, it was observed, seen in Table 19, the understanding of the comparing the fungi species to the control, in which, there was a higher percentage in cluster 2 and 4 related to control, and the cluster that had a higher percentage of fungi species was the cluster 3. The *p* value (0,002) showed significance.

Table 19: Parameters used to check whether there are differences in sample distribution across clusters for identification of inoculated samples comparing the control to the samples from fungi species. P value was also evaluated.

Cluster	Control (N = 6)	Fungi species (N = 30)	TOTAL (N = 36)	*p*
1	0 (0,0%)	2 (6,7%)	2 (5,6%)	0,002
2	3 (50,0%)	5 (16,7%)	8 (22,2%)	
3	0 (0,0%)	18 (60,0%)	18 (50,0%)	
4	3 (50,0%)	1 (3,3%)	4 (11,1%)	
5	0 (0,0%)	4 (13,3%)	4 (11,1%)	

Using the same method, it was observed, in Table 20, the comparison of the *Penicillium sp.* fungus to the other species and control, in which, there was a higher value of *Penicillium sp.* presence in cluster 5 (100%) corresponding to all samples being from that species, and the ones related to the presence of control and the other species of fungi were the cluster 2 and 3. The *p* value (< 0,001) showed significance as well.

Table 20: Parameters used to check whether there are differences in sample distribution across clusters for identification of Penicillium sp. P value was also evaluated.

	1 (N = 2)	2 (N = 8)	3 (N = 18)	4 (N = 4)	5 (N = 4)	TOTAL (N = 36)	*p*
Not *Penicillium sp.*	0	8	18	4	0	30	< 0,001
Penicillium sp.	2	0	0	0	4	6	

Another heatmap (with K=5) of the hierarchical cluster analysis was performed based on the CFUs count of all species, relating the CFUs count with the parameters previously used such temperature, humidity and functional groups as seen in Figure 43. It can be observed that, in general, the prevalent numbers of colonies were less than 70 CFUs and 70–100 CFUs in the five clusters but the 70–100 CFUs and more than 100 CFUs revealed to be present in the *Penicillium* genus and associated with the number 3 of the scale.

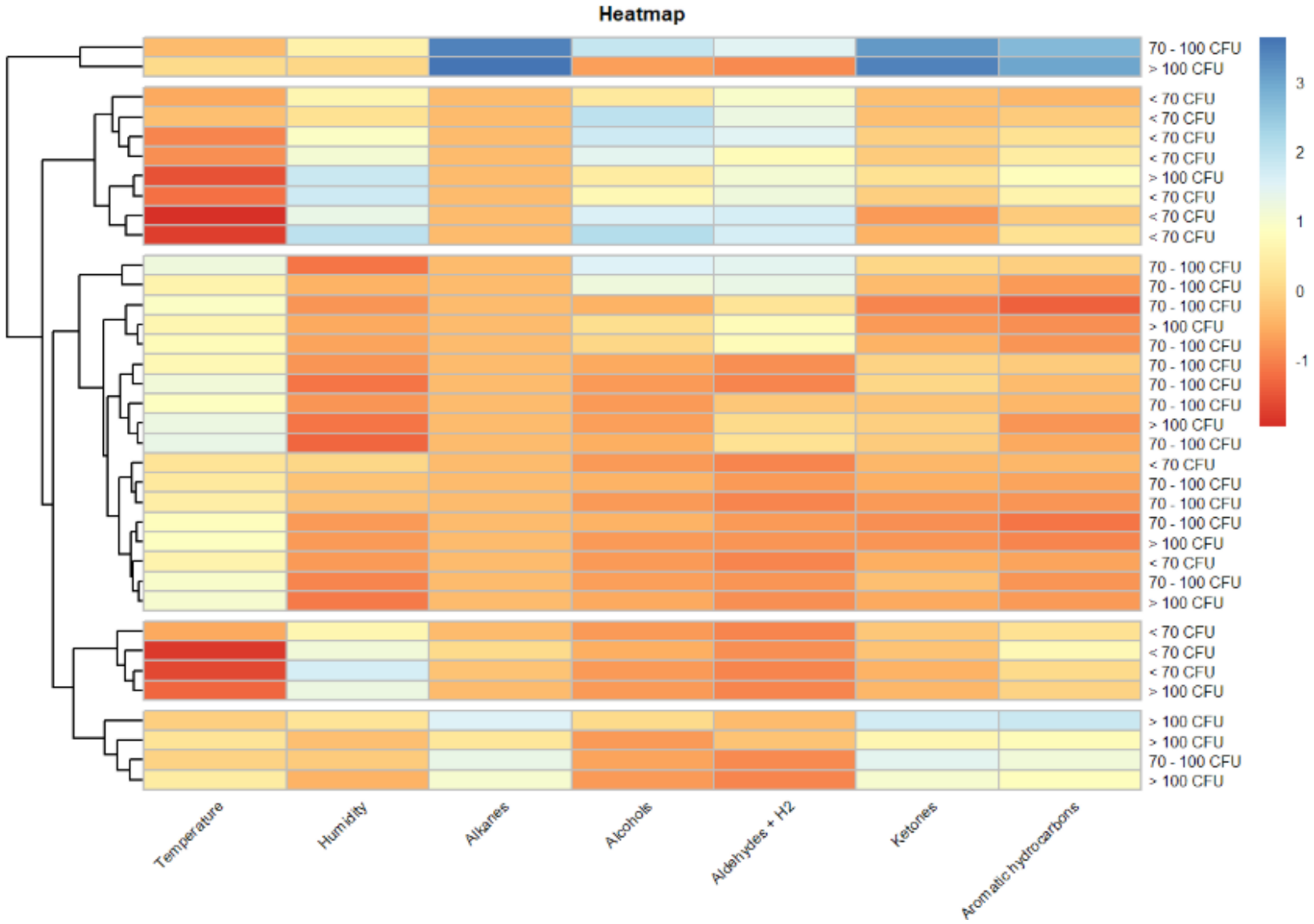

Figure 43: Heatmap (with K=5) of the hierarchical cluster analysis by CFUs count relating to the different parameters.

The CFUs were also analysed and corresponded to different clusters, being the three categories of number of colonies: less than 70 CFUs, 70 to 100 CFUs and more than 100 CFUs, as seen in Table 21. There was a higher percentage of colonies from 70–100 in cluster 3, the lower group of colonies (<70 colonies) verified to be associated to cluster 2 and the highest number (>100 colonies) corresponded to cluster 3. The *p* value (< 0,001) showed significance.

Table 21: Number of CFUs relating to the 5 clusters after 48h of incubation. P value was also evaluated.

After 48h of incubation	1 (N = 2)	2 (N = 8)	3 (N = 18)	4 (N = 4)	5 (N = 4)	TOTAL (N = 36)	*p*
< 70 CFUs	0	7	2	3	0	12	< 0,001
70 – 100 CFUs	1	0	12	0	1	14	
>100 CFUs	1	1	4	1	3	10	

3.2.2. Colony forming units after 72h of incubation

The CFUs of the different samples of fungi were counted after an incubation of 72h at room temperature, using the drop and spread methods for the samples with no dilution and with a dilution of 10^{-3}, having the results shown in Table 22.

The results revealed that for the controls (Figure 44), the plates corresponding to tubes 1 and 3 presented contamination contrary to the plate from tube 2, which didn't show colonies growth in any of the inoculation's methods. Talking about the *Alternaria sp.* plates (Figure 45), all plates showed growth, except for the one from tube 1 and tube 3 in the spread and the plate from tube 3 in the drop method, both being from the samples with a 10^{-3} dilution. The higher number of colonies was 10 which was seen in the plate from tube 2 for the three categories of inoculation. Referring to *Penicillium sp.* tubes (Figure 46), there was a notorious difference from the previous fungus. The only plates that didn't present growth were from tube 1 and 2 in the spread method. The highest number of colonies was visible for the drop method at the sample with no dilution, with a number per drop of approximately 200 colonies. *Aspergillus niger* plates (Figure 47) demonstrated growth in general, despite plates from tube 1 showing no growth in the spread method and for two drops in the sample with a 10^{-3} dilution. The highest number of colonies

was 100 colonies from the plate referring to tube 3, in the drops, for the sample with no dilution. Plates from tube 2 showed contamination in the drop method for the sample with a 10^{-3} dilution. In the case of *Gliocladium virens* (Figure 48), all plates showed colonies formed, being the highest number 150 colonies in the plate from tube 2 for the drop method with no dilution and the lowest number was 2 colonies observed in the plate coming from tube 1 for a drop with the sample with a 10^{-3} dilution. Finally, the plates from *Aspergillus flavus* (Figure 49) also showed growth in general, having one case of no sight of growth from the plate from tube 2 in the spread method. The highest number of colonies observed were 152 colonies for plate from tube 2 in the drop method for the sample with no solution. In general, the highest number of colonies counted (160 colonies) was for *Penicillium sp.* in the drop method and the lowest number was 0 colonies for some samples such the controls and *Alternaria sp.*

Table 22: CFUs count of the different samples of control and fungi species used by the drop and spread methods.

	CFUs count at 72h incubation						
	Drop 1 (10^0)	Drop 2 (10^0)	Drop 3 (10^0)	Spread method (10^{-3})	Drop 1 (10^{-3})	Drop 2 (10^{-3})	Drop 3 (10^{-3})
Control (1)	20	18	37	200	>400	>400	>400
Control (2)	0	0	0	0	0	0	0
Control (3)	>400	>400	>400	8	14	12	7
Alternaria sp. (1)	5	5	8	0	2	1	1
Alternaria sp. (2)	5	10	6	10	5	10	6
Alternaria sp. (3)	7	7	5	0	0	0	0
Penicillium sp. (1)	100	100	50	0	13	11	11
Penicillium sp. (2)	150	200	170	0	1	4	4
Penicillium sp. (3)	150	200	160	24	9	11	12
A. niger (1)	71	71	51	0	0	0	1
A. niger 2)	63	95	58	5	1	0	0

A. niger (3)	100	100	100	20	10	15	14
G. virens (1)	100	100	100	6	2	14	6
G. virens (2)	150	150	150	10	11	14	7
G. virens (3)	100	100	100	17	11	19	10
A. flavus (1)	105	84	53	46	32	38	30
A. flavus (2)	90	59	152	0	15	18	10
A. flavus (3)	56	87	89	1	2	2	3

The CFUs on the PDA plates were counted and are shown in the figures below. Each fungus has one representative photo from each method used.

Control

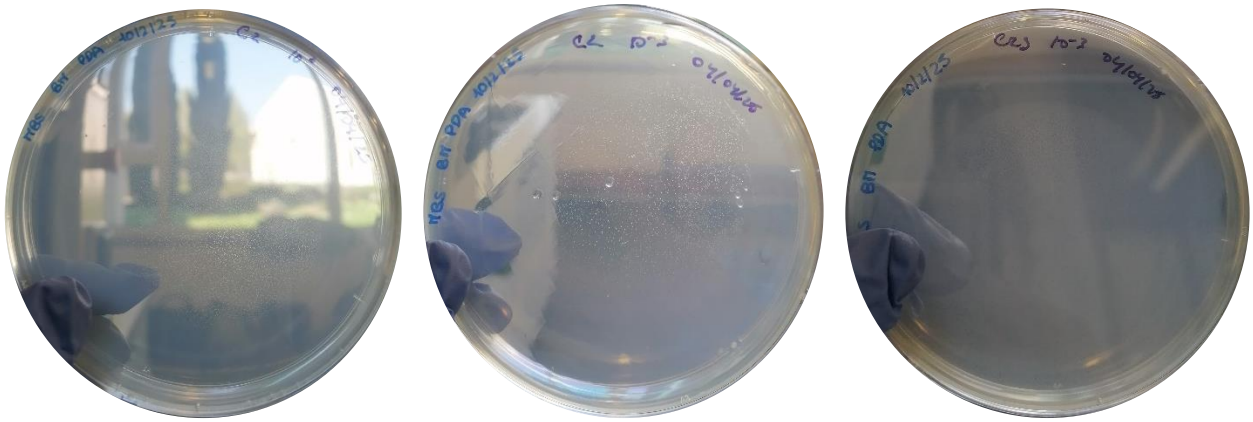

Figure 44: CFUs count of the control samples using drop (10^0), spread (10^{-3}) and drop (10^{-3}) methods respectively.

Alternaria sp.

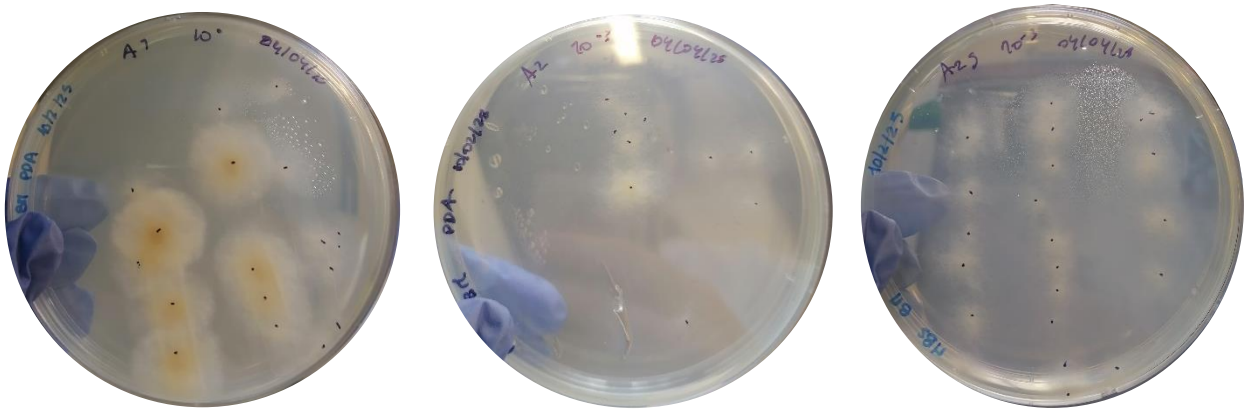

Figure 45: CFUs count of the Alternaria sp. samples using drop (10^0), spread (10^{-3}) and drop (10^{-3}) methods respectively.

Penicillium sp.

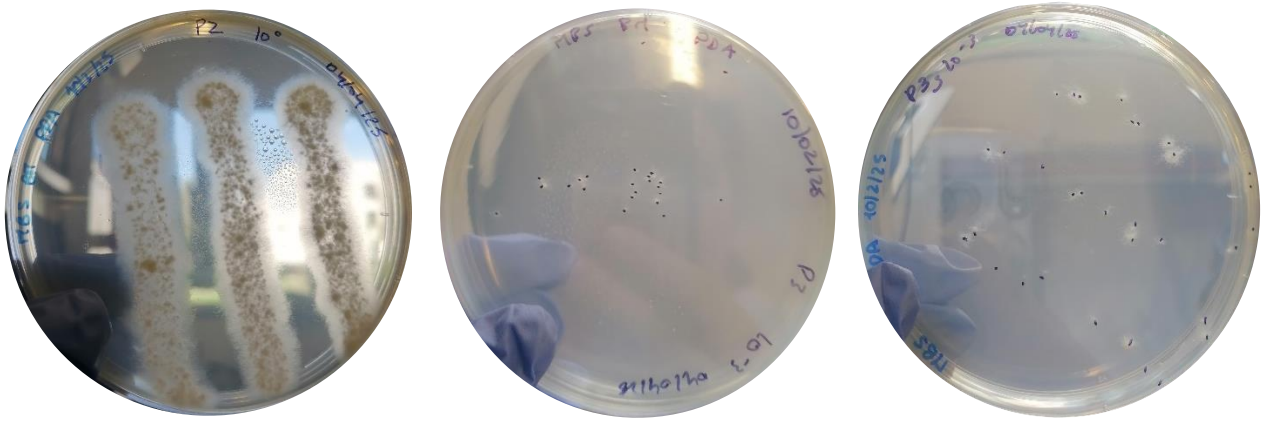

Figure 46: CFUs count of the Penicillium sp. samples using drop (10^0), spread (10^{-3}) and drop (10^{-3}) methods respectively.

Aspergillus niger

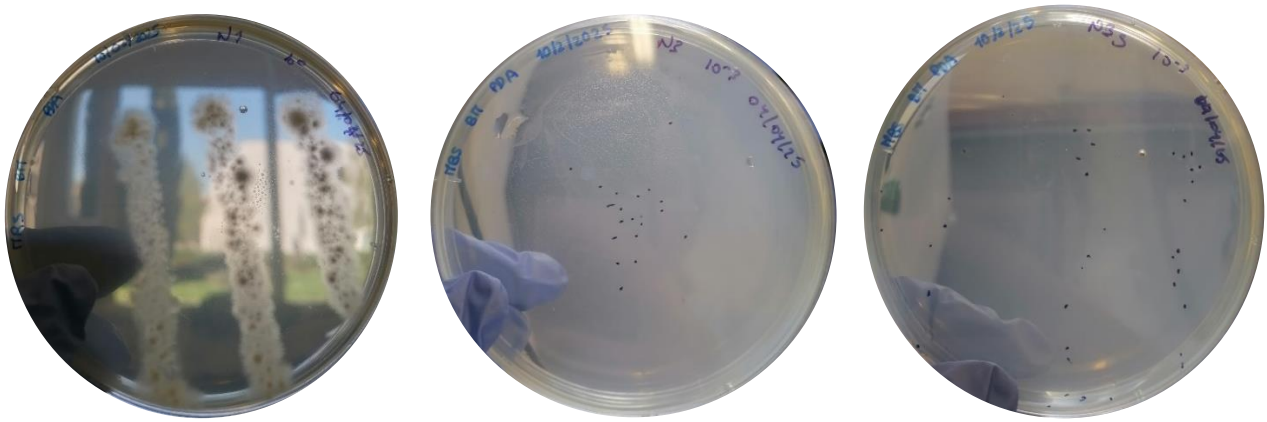

Figure 47: CFUs count of the Aspergillus niger samples using drop (10^0), spread (10^{-3}) and drop (10^{-3}) methods respectively.

Gliocladium virens

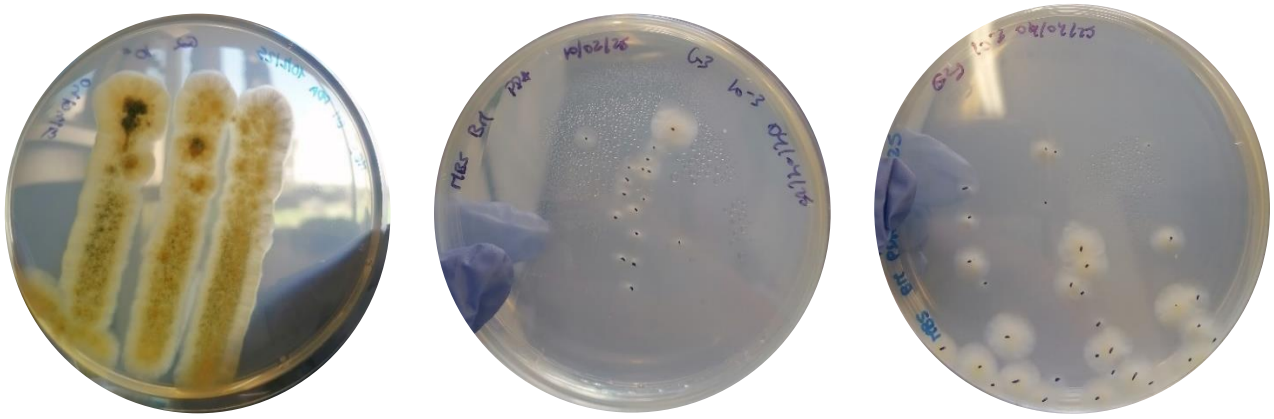

Figure 48: CFUs count of the Gliocladium virens samples using drop (10^0), spread (10^{-3}) and drop (10^{-3}) methods respectively.

Aspergillus flavus

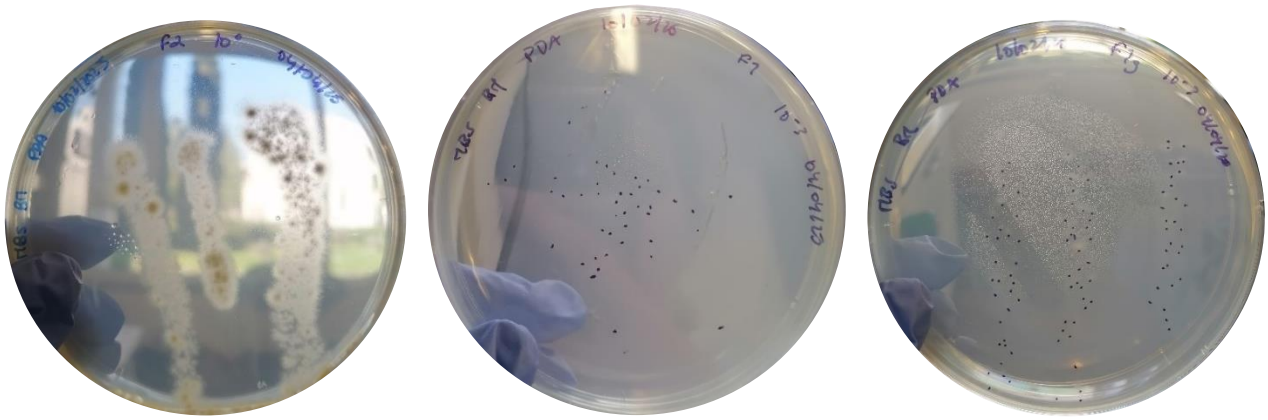

Figure 49: CFUs count of the Aspergillus flavus samples using drop (10^0), spread (10^{-3}) and drop (10^{-3}) methods respectively.

3.3. Phenotypical identification of fungi

The last part of the study was to confirm the fungi used through the phenotypical identification. In this step, the fungal colonies grown in PDA medium were visualised and identified at the macro and microscopic levels. The characteristic structures of the fungi were observed using a microscope, with various magnifications up to 400x, using slides prepared for this purpose.

Alternaria sp.

As it can be seen in Figure 50, the macroscopic characteristics emphasised were the colour of the surface and reverse of the plate, that presented initially a white colour leading to a brownish colour in the surface, having a light border and a velvet aspect, and the reverse showed to be similar.

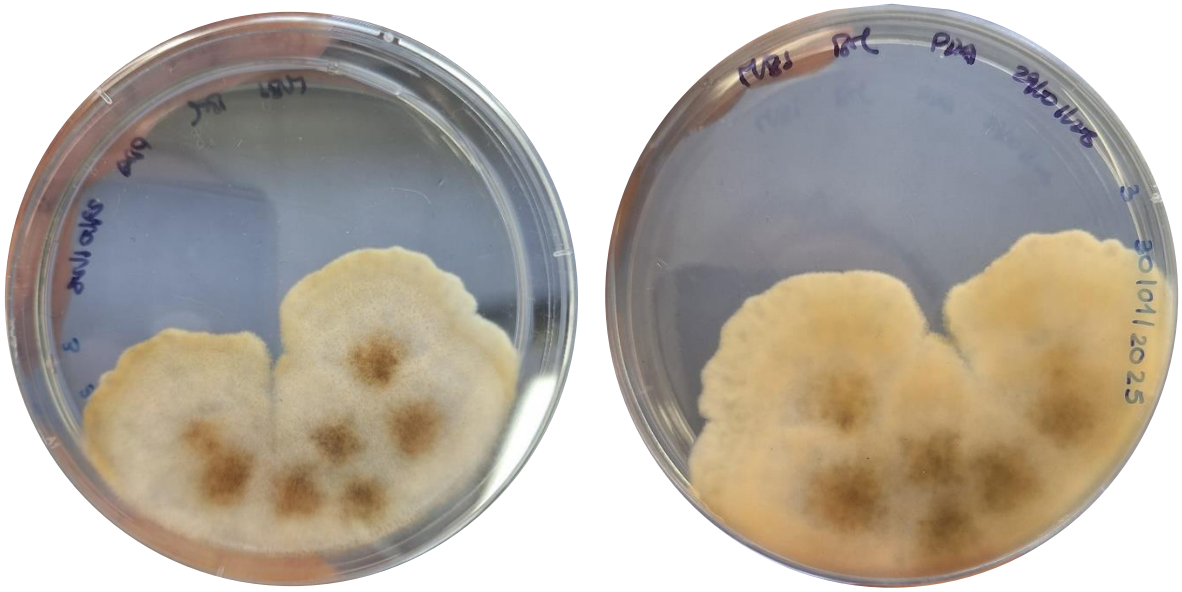

Figure 50: Fungal growth observed on the plate, on the front and back respectively, referring to the fungus Alternaria sp.

The microscopic features, seen in Figure 51, demonstrated the presence of septate hyphae and septate conidiophores, with large conidia contained transverse and longitudinal septations and in the form of inverted clubs.

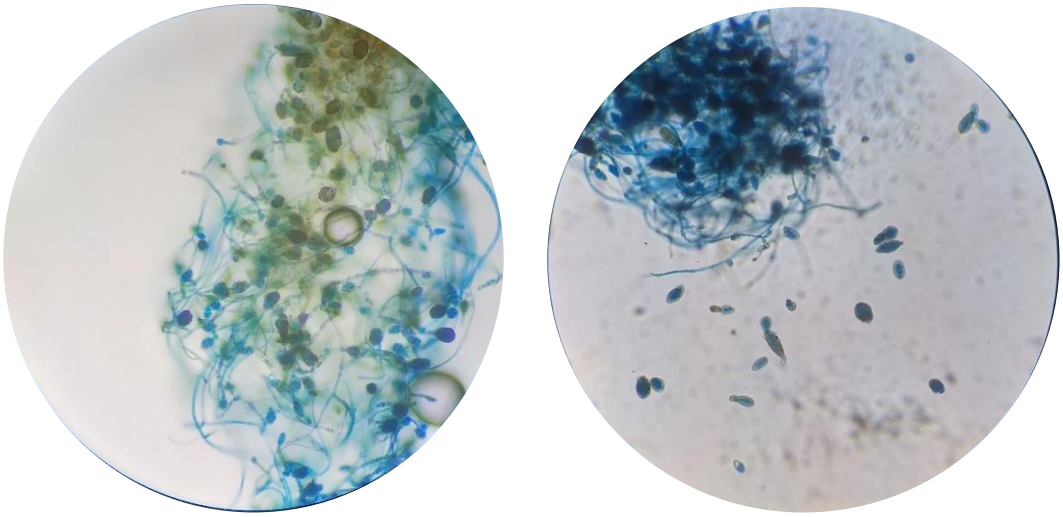

Figure 51: Microscopic view of fungal growth of fungus Alternaria sp. with a magnification of 400x.

Aspergillus flavus

The *Aspergillus flavus* fungus presented a surface with yellow green to olive colonies, with blackish borders and a velvety/cottony texture, and the reverse showed to be yellow to tanned as seen in Figure 52.

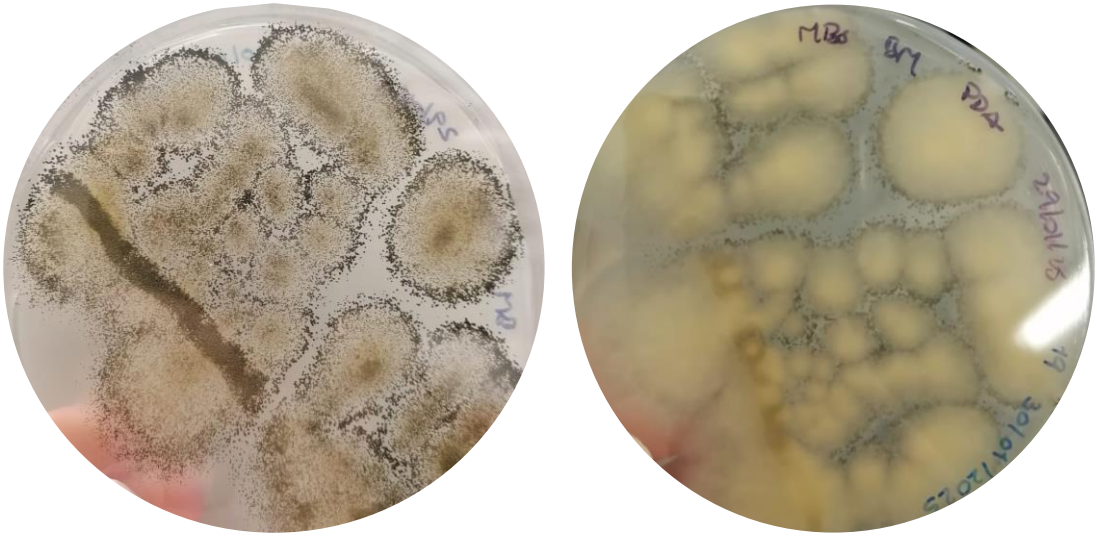

Figure 52: Fungal growth observed on the plate, on the front and back respectively, referring to the fungus Aspergillus flavus.

Figure 53 showed that microscopic morphology consisted in a rough, ending in a globular vesicle that is covered by single- or double-rowed phialides and the conidia is spherical, forming dense and radiated conidial heads.

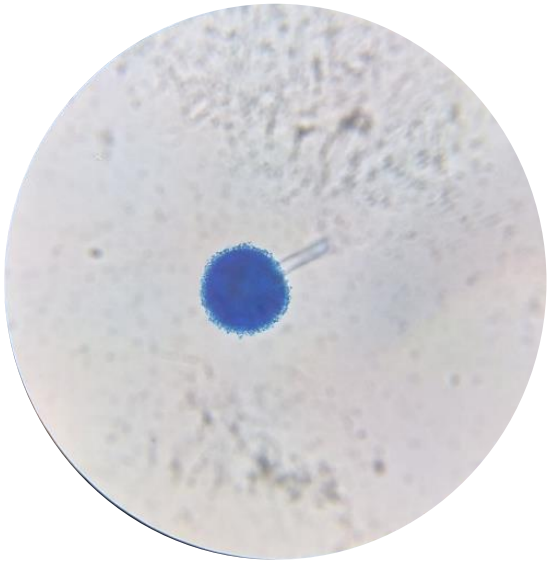

Figure 53: Microscopic view of fungal growth of fungus Aspergillus flavus with a magnification of 400x.

Aspergillus niger

Aspergillus niger, as seen in Figure 54, showed colonies composed of long, white to cream, erect hyphae with clusters of black conidia at the apices. Also, it can be observed the white border and the cottony texture.

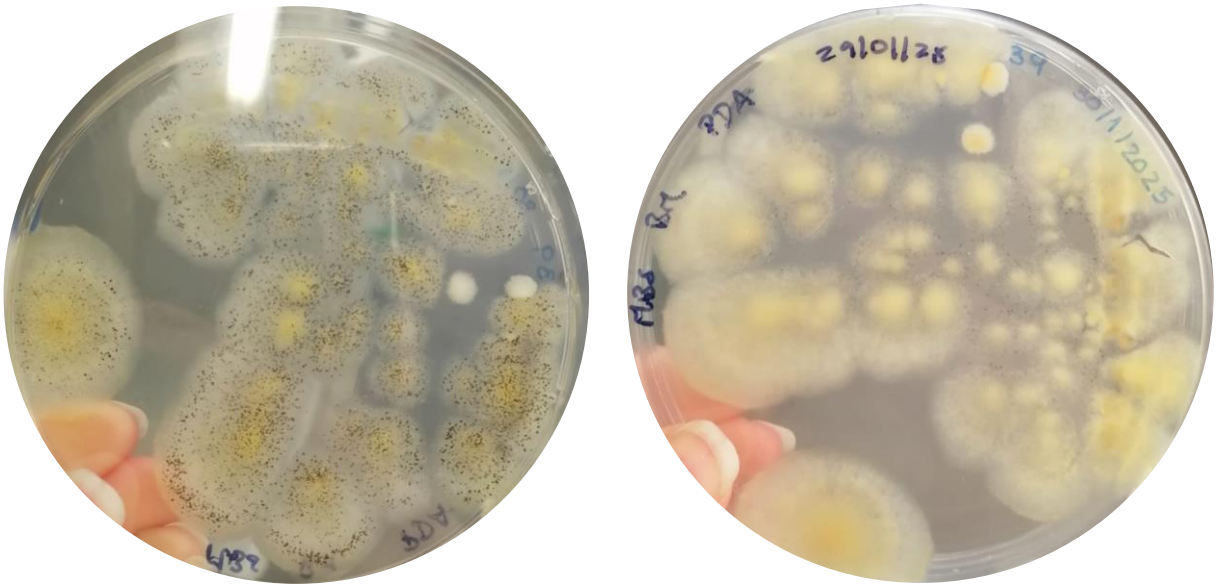

Figure 54: Fungal growth observed on the plate, on the front and back respectively, referring to the fungus Aspergillus niger.

The microscopic observation, shown in Figure 55, allowed to see the long and smooth conidiophore and the biseriate phialides that radiate around the entire vesicle, counting with a round and dark conidia.

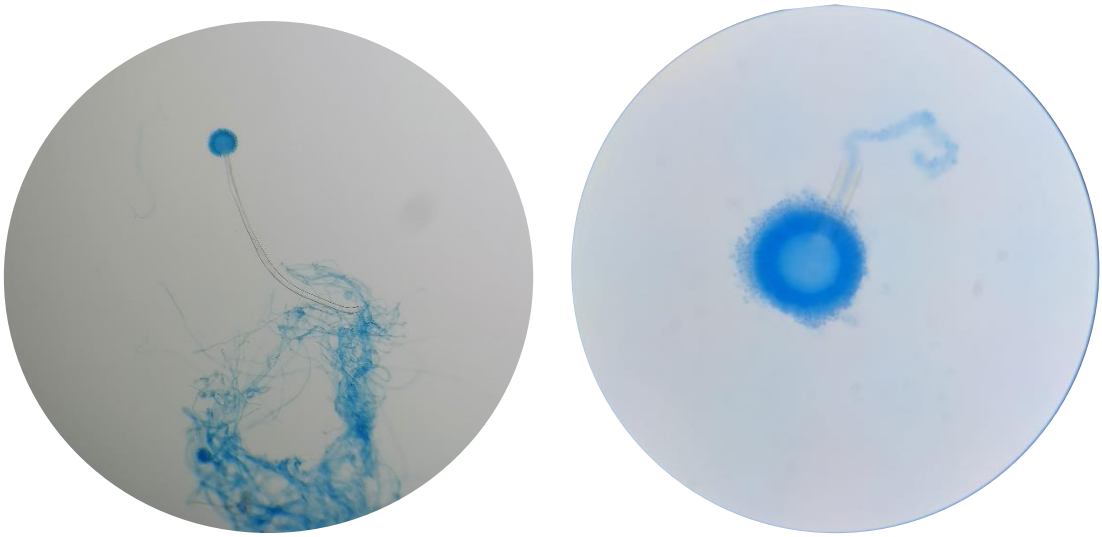

Figure 55: Microscopic view of fungal growth of fungus Aspergillus niger with a magnification of 100x and 400x respectively.

Penicillium sp.

The *Penicillium sp.* fungus, shown in Figure 56, didn't mature enough so the usual characteristics weren't so obvious, but it can be said that the plate showed a white surface at first, which then would have become very powdery and bluish green with a white border, and the reverse showed to be white.

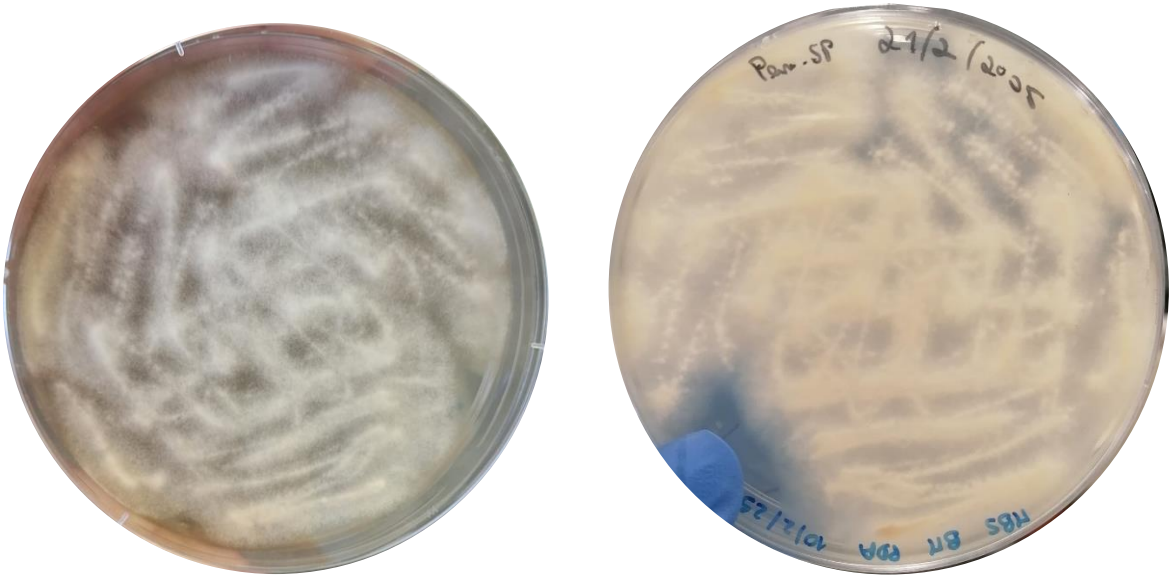

Figure 56: Fungal growth observed on the plate, on the front and back respectively, referring to the fungus Penicillium sp.

As seen in Figure 57, this fungus showed a structure that forms the characteristic "penicillus" or "brush" appearance, with the septate hyphae with branched conidiophores that have secondary branches known as metulae, that are arranged in whorls and have flask-shaped phialides that bear unbranched chains of smooth or rough, almost round conidia.

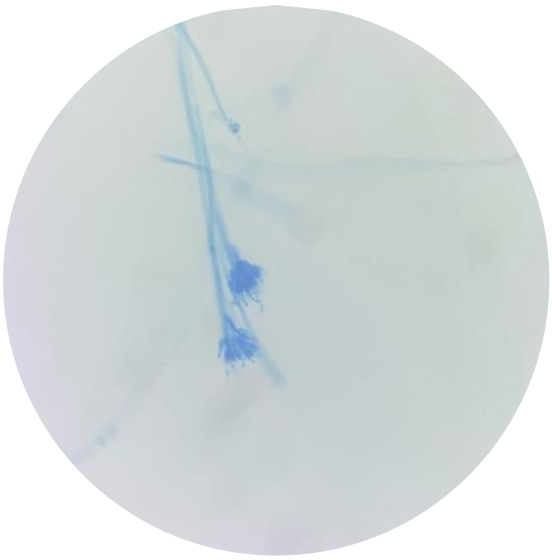

Figure 57: Microscopic view of fungal growth of fungus Penicillium sp. with a magnification of 400x.

Gliocladium virens

Lastly, the plate of *Gliocladium virens*, seen in Figure 58, demonstrated an initially white/yellow colour, turning to green due to formation of conidia that typically are at the margin of the colony. Reverse showed to be light orangey tan to yellow.

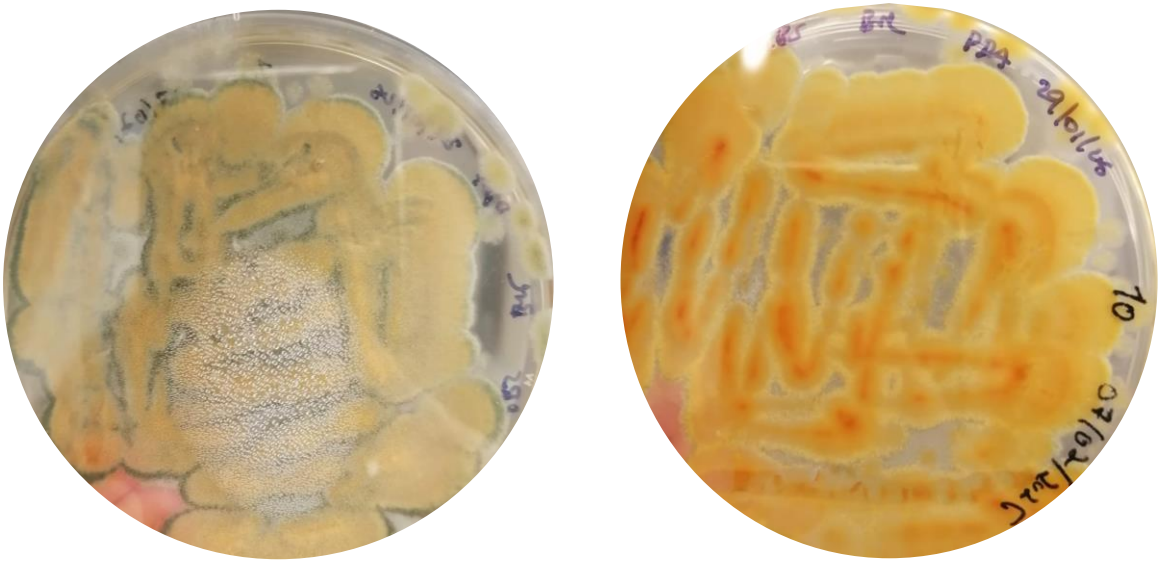

Figure 58: Fungal growth observed on the plate, on the front and back respectively, referring to the fungus Gliocladium virens.

The microscopic characteristics, shown in Figure 59, presented the hyphae, conidiophores, and phialides like the *Penicillium sp.* however, the conidia of *Gliocladium virens* didn't remain in chains and it can be seen as the beginning of the clump together with the conidia of adjacent phialides and the formation of clusters.

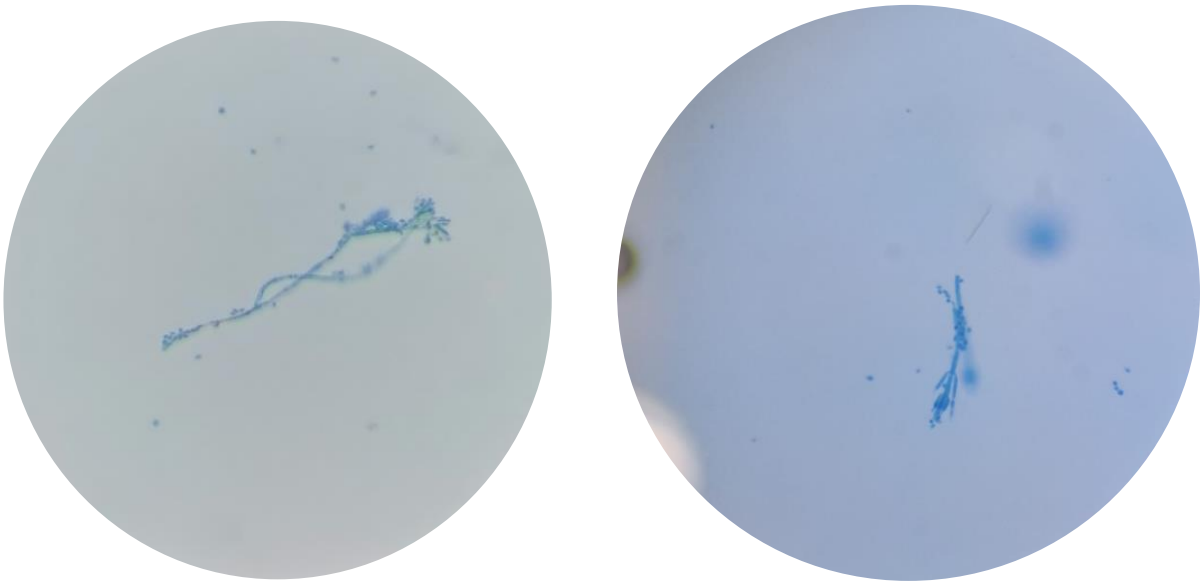

Figure 59: Microscopic view of fungal growth of fungus Glicocladium virens with a magnification of 400x.

4. Discussion

Although interest in volatile organic compounds and their relation to various diseases has been around for a few years, it is only recently that more in-depth research has begun, with more time and knowledge applied in the study of their relation and characterisation of those VOCs to see the potential for the goal of clinical application. In this work, five species of fungi were used and their volatilome was analysed followed by phenotypic characterisation to confirm their potential to be used in the identification of fungi potentially associated with hypersensitivity pneumonitis development.

During the optimisation process, different wavelengths were analysed for optical density measurement. A study by Morris *et. al* (49), demonstrated that wavelengths about 500-600 nm and greater, minimize the effects of variation in cell sizes and different spectrophotometers. Also, wavelengths above 700 nm can decrease the effects of absorption by virtue of pigments production from the spores. In this study, the wavelength that showed to be more coherent was 600 nm, which is in agreement with the findings by Langvad (50). Also, it is shown in other studies that multiple species respond to wavelengths between 600–850 nm, such as species from *Alternaria* and *Aspergillus* genus (51), corresponding to red light that mediated by phytochromes (52,53, 54).

The spectrophotometry results demonstrated that the optical density wasn't always increasing as the time of incubation passed, i.e., as the fungi was expected to growth. Turbidity is directly correlated with unit population size fungi proliferation alters the optical density (OD) of liquid cultures, which forms the basis of the conventional spectrophotometric examination of fungal development (55). However, the unexpected results in the first approach may be explained by agglomeration of mycelium in the media, compartmentalizing the conidia due to the hydrophobicity that usually characterises filamentous fungi (56).

For that reason, the process was adapted by using Tween 20 reagent, polyoxyethylene sorbitan monolaurate. It is a nonionic surfactant that has been used extensively as a dispersing agent to create conidial suspensions of hydrophobic fungus, especially *Aspergillus* species (44). It facilitates spore dispersion over water, resulting in a more dependable inoculum preparation process (57). It also has hydrophilic and lipophilic qualities and plays the role of emulsifying, dispersing and moisturizing (58). This solution facilitated the liberation of conidia and other fungal components, providing more consistent results.

The best optimisation method adopted used sterile distilled water samples containing the fungi species for the construction of concentration curves. However, although this method provided the best

optical density curves, it still showed some negative slopes and low R^2 values in the concentration curves. In relation to the CFUs count, the results demonstrated a more reliable count in the plates using a low dilution factor such as the 10^{-3}.

The next part of the study consisted in measuring the volatilome from the five species of fungus, using the electronic nose in order to detect the volatile organic compounds produced by those microbial species. The results were evaluated through statistical analysis.

The PCA based on the differentiation of the species demonstrated that the difference didn't appear to be explained by the two components due to the similarity of growth patterns among these fungi species.

However, there appeared to be a clear distinction between the profiles after 48 hours of incubation, suggesting that this may be the minimum time required to capture the distinguishable metabolic footprints for the fungi. This is supported by a case study from Nickles *et al.* (59) where they were able to extract secondary metabolites from *Aspergillus sp.* in liquid medium and grew a *A. fumigatus* culture at 25°C while shaking at 250 rpm for three days (72h). Other studies showed that for identification of VOCs released from headspace of fungi species, samples were normally collected at a mature stage of growth, in the case, from 48 h to 96 h (60).

The PCA including only data from after 48h of incubation showed a clear differentiation between *Penicillium sp.* and controls. On the other hand, *Alternaria sp.* had an indistinguishable profile when compared to controls. Fungi of the same genus, in this case, referring to the *Aspergillus* genus, shared similar volatile metabolite profiles, probably due to physiological similarities between the species. However, fungi from the same genus and, sometimes, species, can be associated with different VOC profiles, depending, for example on the fungus strain, environment conditions, growth and maturation process and genetics factors (36). *Penicillium sp.* was also clearly separated from the other fungi species, suggesting that it produces a clearly distinguishable metabolic profile from the other *Ascomycota*.

The ROC curves supported the high efficacy of the method, by showing large areas under the curve (AUC). The AUC values range from 0 to 1, in which, a value of 0 indicates an inaccurate test and a value of 1 demonstrates a perfectly accurate test. Also, a test is considered excellent with values above 0,8 (61, 62), which, in this case, the value obtained indicates a very good performance of the test used. This can also be supported by the study from Pouris *et. al* (63), that aimed to analyse different fungal species from *Aspergillus* genus and one from *Penicillium* genus, for identification based on chromogenic profiling of colony colour patterns. Their ROC curves demonstrated AUC values of 0,78 for *A. flavus* and 0,82 for *P. chrysogenum*, revealing similarities and that the model used in reliable. The results also

showed that it is close to an ideal model test, as it is known that a perfect diagnostic test would have the sensitivity and specificity of 100% (62).

However, the sensitivity analysis using bootstrapped simulated measures revealed that the applied model was not stable because the model estimate is far from the peak of the distribution, suggesting significant bias. For that reason, the model containing only sample from at least 48h of incubation showed a significantly lower bias in the sensitivity analysis.

The heatmap depicting the hierarchical clustering analysis revealed two clusters for *Penicillium sp.,* being the first more associated with alkanes and ketones. *Alternaria sp.* and controls were grouped together in two different clusters, being one of them more associated with alcohols and aldehydes, and the other more related to the other functional groups such aromatic hydrocarbons and, in less quantity, to alkanes, ketones. The other 3 fungi species were also allocated in one shared cluster likely due to their similarities with the type of compounds found. As expected, the two fungi from the *Aspergillus* genus were in the same group due to their shared characteristics. *Gliocladium virens*, as a part of the *Ascomycota* phylum, was related to these values as well.

In terms of colony counts, *Penicillium sp.* was highlighted, having the highest number of colonies, while *Alternaria sp.* showed low concentrations, not having a big difference from the control. This was an unexpected result, as *Alternaria sp.* usually grows quickly. A study from Blagojević *et. al* (64) aimed different types of analyses of 113 isolates collected from rapeseed-growing areas in Serbia that identified four pathogens: *Alternaria brassicae, A. brassicicola, A. japonica,* and *A. alternata*, causing leaf spot disease. This study showed that *A. alternata* had the fastest and highest growth rate (10.0 ± 1.12 mm/day), comparing to the others, which means that this species can develop its morphological characteristics quickly at optimal temperatures ranging from 20 to 30°C.

A hierarchical clustering analysis relating the different parameters with the colonies counted was performed and showed the same numbers of clusters, allowing the association of the different parameters and functional groups to the three levels of CFUs count.

The fungus of the genus *Penicillium* was completely differentiated from the other samples. However, considering all results obtained, it can be said that in the case of *Alternaria sp.*, it may take even longer to capture a distinct VOC profile, due to the similar results to controls. In the Weikl *et. al* study (65), the VOC measurement of the *Alternaria* species (*Alternaria alternata*) used was performed after a minimum time incubation of 48h, prolongating to days, indicating that this may be the needed time for the metabolic pathways to produce a distinguishable VOC profile, in the *Alternaria sp.*

Although *Alternaria sp.* profiles showed to be similar to controls, some samples showed different patterns in the production of compounds with the hydroxyl functional group (alcohols), which is also supported by the study of Weikl (65). This study analysed the divergence of VOCs, also determining their quantities in the headspace of cultures of *A. alternata* and *Fusarium oxysporum* subjected to different conditions. 26 distinct VOCs were emitted being 24 sesquiterpenes and two alcohols such Isobutanol and 2-Methyl-1-butanol where, at day 14, only traces of alcohols were detected.

Aspergillus genus demonstrated to be more associated with aldehydes and alcohols in the case of *A. flavus*, and this can be correlated to a study from Josselin *et. al* (66), that had the goal to analyse the VOCs emitted by non-toxigenic and toxigenic strains of *A. flavus*. They identified different VOCs, that were emitted in symbolic proportions, founding 4 aldehydes and 11 alcohols, such 3-methylbutan-1-ol (alcohol) and 2-methylbutanal (aldehyde), and they could be used to detect the presence of a fungal contamination.

A. niger produced a diverse array of compounds depending on the sample; however, no particular class of VOCs appeared to be predominant.

Gliocladium virens exhibited a compound emission profile comparable to the profiles observed in the other fungal species, namely the *Aspergillus* genus; nevertheless, in one sample, the profile was more strongly associated with alcohols and aldehydes.

Samples inoculated with *Penicillium sp.* were characterised by a higher concentration of ketones, alkanes and aromatic hydrocarbons. A study from Caron *et. al* (67), revealed that esters and methyl ketones (especially 2-pentanone and 2-heptanone) were observed at higher quantity in cheeses made with strains from *P. roqueforti*. In this fungus, this type of compound with different numbers of carbons are frequently produced by fatty-acid beta-oxidation and by the same pathway or autoxidation of fatty acids. It was verified that they played a key role on lipolysis in the usual blue cheese aroma. The higher concentration of ketones may also be associated with the production of polyketides as verified in the study of Hu *et. al* (68). This study aimed to investigate bioactive natural compounds derived from the endophytic fungus *Penicillium ochrochloron*, concentrated on secondary metabolites. It showed a presence of methyl ketones in some compounds composition and that polyketides have an important role in the secondary metabolites produced by *Penicillium* species.

These polyketides can be associated with the formation of penicillin precursors such as sorbicillin. The study from Salo *et. al* (69) had the objective to identify polyketides synthases-encoding genes (pks13) that are important for sorbicillinoid formation, using a strain of *P. chrysogenum*. In general, their results indicated that pks13 is essential for the production of the polyketide precursors for the

biosynthesis of sorbicillinoids and they reestablished the biosynthesis of sorbicillin-related metabolites within the genetic history of an enhanced penicillin-producing strain.

Other studies such as the one developed by Silva *et. al* (70), verified the production of a great quantity of alkanes (26% to 77% of the total abundance) from *Penicillium commune* in olives. Some VOCs emitted in plants that were inoculated with the endophyte can have antimicrobial features, such as dodecane and may play necessary roles in inhibiting pathogen growth.

It is known that most classical mycologists, primarily focus on the morphological characteristics of species grown under standardised cultural conditions, with odor considered only occasionally as a supplementary trait. Although odor itself is less reliable for species identification, it has been recognised that the analysis of specific volatile compounds or characteristic mixtures work as biomarkers for the indirect detection of fungal growth. In certain cases, species and even individual strains have been successfully described and differentiated based on their volatile profiles (36), which this study also corroborates.

This study provided a new methodology to not only identify HP-related fungi in homes, but also a potential tool to study the relationship between the composition of the compounds detected and the metabolism of fungi, as they come from the various metabolites produced that have different functions in their metabolic pathways.

There were limitations with this study, firstly related to the medium used for the fungi growth. The medium that should had been used for the growth of fungi in Petri plates is MEA, which translates to Malt Extract Agar, that is a solid growth medium rich in maltose and other carbohydrates, used to cultivate and isolate yeasts, molds, and other fungi. Its acidic pH inhibits most bacteria, making it ideal for germinating fungal spores (71). Furthermore, the measurement of optical density had possible errors leading to different values for the same sample and negative values as well. Those issues could have been, for example, the fact that the tubes were not vortexed enough to homogenize the solutions and the samples and the cuvettes for the measurement could had some residuals which can influence the absorption. Another limitation of the work consisted in the presence of contamination in some samples, verified by the CFUs count on plates. This could be associated with the insufficient sterilization of the work environment. Nevertheless, the multiple optimisation procedures, along with a robust analytical approach, helped to address these limitations, mitigating the potential bias.

5. Conclusion

The results obtained allowed the characterisation of the volatilome of each fungi species used related to the hypersensitivity pneumonitis. The *Penicillium sp.* demonstrated to be the fungus that had more distinguishable VOC patterns, identified through electronic nose.

A relevant consideration in this project is the temporal advantage conferred by VOC-based identification compared to conventional phenotypic approaches. While volatile metabolite profiling enables reliable discrimination of microbial species within 48 hours of incubation as verified by the results, phenotypic characterisation typically requires extended culture periods of at least one week before definitive results can be obtained. This substantial reduction in time not only enhances the usefulness of early and accurate identifications but also has potential implications for optimizing therapeutic interventions and improving laboratory workflows.

Beyond its clinical relevance, this study also contributes to fundamental science by enhancing the understanding of host–fungus interactions and the specific metabolic signatures that characterise fungal species. Consequently, the use of the e-nose, not only offers immediate prospects for environmental exposure assessment aimed at HP patients but also serves as an initial investigative tool, representing a starting point for further investigations into the pathophysiology of HP and other conditions in which VOCs play a decisive role, possibly understanding disease mechanisms.

However, this project has some work that can be continued in order to enrich the study. Saying that, the future perspectives may include the validation and confirmation of the compounds detected by the electronic nose using reference techniques such as gas chromatography coupled with mass spectrometry (GC-MS). This step will strengthen the robustness of the obtained profiles, increasing both their reliability and clinical utility.

In summary, the objectives for the study were accomplished and it highlighted the potential of the electronic nose as a bridge between fundamental research and clinical application.

Bibliographic References

1. Calaras D, David A, Vasarmidi E, Antoniou K, Corlateanu A. Hypersensitivity Pneumonitis: Challenges of a Complex Disease. Can Respir J. 2024;2024.
2. Gomes ML, Morais A, Cavaleiro Rufo J. The association between fungi exposure and hypersensitivity pneumonitis: a systematic review. Porto Biomed J. 2021;6(1):e117.
3. Dabiri M, Jehangir M, Khoshpouri P, Chalian H. Hypersensitivity Pneumonitis: A Pictorial Review Based on the New ATS/JRS/ALAT Clinical Practice Guideline for Radiologists and Pulmonologists. Diagnostics. 2022;12(11).
4. Barnes H, Troy L, Lee CT, Sperling A, Strek M, Glaspole I. Hypersensitivity pneumonitis: Current concepts in pathogenesis, diagnosis, and treatment. Allergy: European Journal of Allergy and Clinical Immunology. 2022;77(2):442–53.
5. Wawszczak M, Bielecka T, Szczukocki M. Hypersensitivity pneumonitis in children. Annals of Agricultural and Environmental Medicine. 2021;28(2):214–9.
6. Rivera-Ortega P, Molina-Molina M. Interstitial lung diseases in developing countries. Ann Glob Health. 2019;85(1):1–14.
7. Santos V, Martins N, Sousa C, Jacob M, Padrão E, Melo N, et al. Hypersensitivity pneumonitis: Main features characterization in a Portuguese cohort. Pulmonology. 2020;26(3):130–7.
8. Pereira JO, Fernandes V, Alfaro TM, Freitas S, Cordeiro CR. Diagnosis of Fibrotic Hypersensitivity Pneumonitis: Is There a Role for Biomarkers? Life. 2023;13(2).
9. Tomioka H, Miyazaki Y, Inoue Y, Egashira R, Kawamura T, Sano H, et al. Japanese clinical practice guide 2022 for hypersensitivity pneumonitis. Respir Investig. 2024;62(1):16–43.
10. Alberti ML, Rincon-Alvarez E, Buendia-Roldan I, Selman M. Hypersensitivity Pneumonitis: Diagnostic and Therapeutic Challenges. Front Med (Lausanne). 2021;8(September):1–10.
11. Churg A. Hypersensitivity pneumonitis: new concepts and classifications. Modern Pathology. 2022;35(September):15–27.
12. Mota I, Teixeira-Santos R, Cavaleiro Rufo J. Detection and identification of fungal species by electronic nose technology: A systematic review. Fungal Biol Rev. 2021;37:59–70.
13. Baxi SN, Portnoy JM, Larenas-Linnemann D, Phipatanakul W, Barnes C, Grimes C, et al. Exposure and Health Effects of Fungi on Humans. Journal of Allergy and Clinical Immunology: In Practice. 2016;4(3):396–404.

14. Vasakova M, Selman M, Morell F, Sterclova M, Molina-Molina M, Raghu G. Hypersensitivity pneumonitis: Current concepts of pathogenesis and potential targets for treatment. Am J Respir Crit Care Med. 2019;200(3):301–8.
15. Riario Sforza GG, Marinou A. Hypersensitivity pneumonitis: A complex lung disease. Clinical and Molecular Allergy. 2017;15(1):1–8.
16. Env S, Phwrgh U, Sulvshynd X, Rgsruqrvwl D, Hohphqwry N, Mhnohqlk LWD, et al. SLOVENSKI STANDARD iTeh STANDARD PREVIEW iTeh STANDARD PREVIEW. 2013;
17. David E, Niculescu VC. Volatile organic compounds (Vocs) as environmental pollutants: Occurrence and mitigation using nanomaterials. Int J Environ Res Public Health. 2021;18(24).
18. Mangotra A, Singh SK. Volatile organic compounds: A threat to the environment and health hazards to living organisms – A review. J Biotechnol [Internet]. 2024;382(December 2023):51–69. Available from: https://doi.org/10.1016/j.jbiotec.2023.12.013
19. Madureira J, Paciência I, Rufo J, Severo M, Ramos E, Barros H, et al. Source apportionment of CO2, PM10 and VOCs levels and health risk assessment in naturally ventilated primary schools in Porto, Portugal. Build Environ. 2016;96:198–205.
20. Li Y, Wang Z, Zhao T, Li H, Jiang J, Ye J. Electronic nose for the detection and discrimination of volatile organic compounds: Application, challenges, and perspectives. TrAC - Trends in Analytical Chemistry [Internet]. 2024;180(July):117958. Available from: https://doi.org/10.1016/j.trac.2024.117958
21. Haick H. Advances in volatile organic compounds detection: From fundamental research to real-world applications. Appl Phys Rev [Internet]. 2024;11(4). Available from: https://doi.org/10.1063/5.0230205
22. Cerimi K, Pöther DC, Klar S. A bibliometric analysis of fungal volatile organic compounds. Fungal Biol Biotechnol. 2025;12(1).
23. Loulier J, Lefort F, Stocki M, Asztemborska M, Szmigielski R, Siwek K, et al. Detection of fungi and oomycetes by volatiles using e-nose and spme-gc/ms platforms. Molecules. 2020;25(23):1–27.
24. Capuano R, Mansi A, Paba E, Marcelloni AM, Chiominto A, Proietto AR, et al. A Pilot Study for Legionella pneumophila Volatilome Characterization Using a Gas Sensor Array and GC/MS Techniques. Sensors. 2023;23(3):1–14.
25. Rios-Navarro A, Gonzalez M, Carazzone C, Celis Ramírez AM. Learning about microbial language: possible interactions mediated by microbial volatile organic compounds (VOCs) and relevance to

understanding Malassezia spp. metabolism. Metabolomics [Internet]. 2021;17(4):1–11. Available from: https://doi.org/10.1007/s11306-021-01786-3

26. Fitzgerald S, Holland L, Ahmed W, Piechulla B, Fowler SJ, Morrin A. Volatilomes of human infection. Anal Bioanal Chem. 2024;416(1):37–53.
27. Tan JY, Zhang Z, Izzah HJ, Fong YK, Lee D, Mutwil M, et al. Volatile-Based Diagnosis for Pathogenic Wood-Rot Fungus Fulvifomes siamensis by Electronic Nose (E-Nose) and Solid-Phase Microextraction/Gas Chromatography/Mass Spectrometry. Sensors. 2023;23(9).
28. Capuano R, Ciotti M, Catini A, Bernardini S, Di Natale C. Clinical applications of volatilomic assays. Crit Rev Clin Lab Sci [Internet]. 2025;62(1):45–64. Available from: https://doi.org/10.1080/10408363.2024.2387038
29. Micheluz A, Manente S, Rovea M, Slanzi D, Varese GC, Ravagnan G, et al. Detection of volatile metabolites of moulds isolated from a contaminated library. J Microbiol Methods [Internet]. 2016;128:34–41. Available from: http://dx.doi.org/10.1016/j.mimet.2016.07.004
30. Guo Y, Jud W, Weikl F, Ghirardo A, Junker RR, Polle A, et al. Volatile organic compound patterns predict fungal trophic mode and lifestyle. Commun Biol [Internet]. 2021;4(1). Available from: http://dx.doi.org/10.1038/s42003-021-02198-8
31. Razo-Belmán R, Ángeles-López YI, García-Ortega LF, León-Ramírez CG, Ortiz-Castellanos L, Yu H, et al. Fungal volatile organic compounds: mechanisms involved in their sensing and dynamic communication with plants. Front Plant Sci. 2023;14(September):1–8.
32. Li Y, Yang K, He Z, Liu Z, Lu J, Zhao D, et al. Can Electronic Nose Replace Human Nose?—An Investigation of E-Nose Sensor Responses to Volatile Compounds in Alcoholic Beverages. ACS Omega. 2023;8(18):16356–63.
33. Wang Q, Fang Y, Tan S, Li Z, Zheng R, Ren Y, et al. Diagnostic performance of volatile organic compounds analysis and electronic noses for detecting colorectal cancer: a systematic review and meta-analysis. Front Oncol. 2024;14(May).
34. Capuano R, Paba E, Mansi A, Marcelloni AM, Chiominto A, Proietto AR, et al. Aspergillus Species Discrimination Using a Gas Sensor Array. :1–12.
35. Gębicki J, Szulczyński B. Discrimination of selected fungi species based on their odour profile using prototypes of electronic nose instruments. Measurement (Lond). 2018;116(October 2017):307–13.
36. K.K. Pennerman, H.S. AL-Maliki SL and JWB. Fungal Volatile Organic Compounds (VOCs) and the Genus Aspergillus. 2016. p. 95–115.

37. Wilson AD. Applications of electronic-nose technologies for noninvasive early detection of plant, animal and human diseases. Chemosensors. 2018;6(4):1–36.
38. Wilson AD, Baietto M. Applications and advances in electronic-nose technologies. Sensors. 2009;9(7):5099–148.
39. Yang HY, Chen WC, Tsai RC. Accuracy of the electronic nose breath tests in clinical application: A systematic review and meta-analysis. Biosensors (Basel). 2021;11(11):1–14.
40. Gautam AK, Verma RK, Avasthi S, Bohra Y, Devadatha B, Niranjan, M. &, et al. Diversity Estimates. Journal of Fungi. 2022;8(3):226.
41. Alsohaili SA, Bani-Hasan BM. Morphological and molecular identification of fungi isolated from different environmental sources in the northern eastern Desert of Jordan. Jordan J Biol Sci. 2018;11(3):329–37.
42. Indunil Chinthani S, Achala R R, Diana S M, Mark S C, Eleni G, Hyang Burm L, et al. Morphological approaches in studying fungi: collection, examination, isolation, sporulation and preservation. Mycosphere. 2020;11(1):2678–754.
43. Morris AJ, Byrne TC, Madden JF, Barth Reller L. Duration of incubation of fungal cultures. J Clin Microbiol. 1996;34(6):1583–5.
44. Aberkane A, Cuenca-Estrella M, Gomez-Lopez A, Petrikkou E, Mellado E, Monzón A, et al. Comparative evaluation of two different methods of inoculum preparation for antifungal susceptibility testing of filamentous fungi. Journal of Antimicrobial Chemotherapy. 2002;50(5):719–22.
45. Martini KM, Boddu SS, Nemenman I, Vega NM. Maximum likelihood estimators for colony-forming units. Microbiol Spectr. 2024;12(9).
46. Pasrija R, Kumari D. Growth Curve Preparation for the Calculation of Fungal Cell Count Over Time. Protocols for Studying Pathogenic Fungi. 2025;63–71.
47. Azar MM. Larone's Medically Important Fungi: A Guide to Identification. Vol. 30, Emerging Infectious Diseases. 2024.
48. Das P, Roychowdhury A, Das S, Roychoudhury S, Tripathy S. sigFeature: Novel Significant Feature Selection Method for Classification of Gene Expression Data Using Support Vector Machine and t Statistic. Front Genet. 2020;11(April):1–12.
49. Morris SC. An Evaluation of Optical Density to Estimate Fungal Spore Concentrations in Water Suspensions. Phytopathology. 1978;68(8):1240.

50. Langvad F. A rapid and efficient method for growth measurement of filamentous fungi. J Microbiol Methods. 1999;37(1):97–100.
51. Fuller KK, Loros JJ, Dunlap JC. Fungal photobiology: visible light as a signal for stress, space and time. 2016;61(3):275–88.
52. Heitman AI and J. Photosensing Fungi: Phytochrome in the Spotlight. Current Biology. 2005;15(20):829–32.
53. Schaller GE, Shiu SH, Armitage JP. Two-component systems and their co-option for eukaryotic signal transduction. Current Biology [Internet]. 2011;21(9):R320–30. Available from: http://dx.doi.org/10.1016/j.cub.2011.02.045
54. Blumenstein A, Vienken K, Tasler R, Purschwitz J, Veith D, Frankenberg-Dinkel N, et al. The Aspergillus nidulans phytochrome FphA represses sexual development in red light. Current Biology. 2005;15(20):1833–8.
55. Slowik AR, Hesketh H, Sait SM, de Fine Licht HH. A Rapid Method for Measuring In Vitro Growth in Entomopathogenic Fungi. Insects. 2023;14(8).
56. Smits THM, Wick LY, Harms H, Keel C. Characterization of the surface hydrophobicity of filamentous fungi. Environ Microbiol. 2003;5(2):85–91.
57. Gomez-Lopez A, Aberkane A, Petrikkou E, Mellado E, Rodriguez-Tudela JL, Cuenca-Estrella M. Analysis of the influence of tween concentration, inoculum size, assay medium, and reading time on susceptibility testing of Aspergillus spp. J Clin Microbiol. 2005;43(3):1251–5.
58. Deng Y, Yang G, Lens PNL, He Y, Qie L, Shen X, et al. Enhanced removal of mixed VOCs with different hydrophobicities by Tween 20 in a biotrickling filter: Kinetic analysis and biofilm characteristics. J Hazard Mater [Internet]. 2023;450(October 2022):131063. Available from: https://doi.org/10.1016/j.jhazmat.2023.131063
59. Nickles G, Ludwikoski I, Keller NP. Comprehensive guide to extracting and expressing fungal secondary metabolites: Aspergillus fumigatus as a case study Grant. 2022;1(12):1–62.
60. Ahmed WM, Geranios P, White IR, Lawal O, Nijsen TM, Bromley MJ, et al. Development of an adaptable headspace sampling method for metabolic profiling of the fungal volatome. Analyst. 2018;143(17):4155–62.
61. Çorbacıoğlu ŞK, Aksel G. Receiver operating characteristic curve analysis in diagnostic accuracy studies: A guide to interpreting the area under the curve value. Turk J Emerg Med. 2023;23(4):195–8.

62. Mandrekar JN. Receiver operating characteristic curve in diagnostic test assessment. Journal of Thoracic Oncology [Internet]. 2010;5(9):1315–6. Available from: http://dx.doi.org/10.1097/JTO.0b013e3181ec173d

63. Pouris J, Konstantinidis K, Pyrri I, Papageorgiou EG, Voyiatzaki C. FungID: Innovative Fungi Identification Method with Chromogenic Profiling of Colony Color Patterns. Pathogens. 2025;14(3):1–14.

64. Blagojević JD, Vukojević JB, Ivanović ŽS. Occurrence and characterization of Alternaria species associated with leaf spot disease in rapeseed in Serbia. Plant Pathol. 2020;69(5):883–900.

65. Weikl F, Ghirardo A, Schnitzler JP, Pritsch K. Sesquiterpene emissions from Alternaria alternata and Fusarium oxysporum: Effects of age, nutrient availability, and co-cultivation. Sci Rep [Internet]. 2016;6(November 2015):1–12. Available from: http://dx.doi.org/10.1038/srep22152

66. Josselin L, De Clerck C, De Boevre M, Moretti A, Haïssam Jijakli M, Soyeurt H, et al. Volatile organic compounds emitted by Aspergillus flavus strains producing or not aflatoxin B1. Toxins (Basel). 2021;13(10).

67. Caron T, Piver M Le, Péron AC, Lieben P, Lavigne R, Brunel S, et al. Strong effect of Penicillium roqueforti populations on volatile and metabolic compounds responsible for aromas, flavor and texture in blue cheeses. Int J Food Microbiol. 2021;354(March).

68. Hu J, Qin D. Diversity and Biological Activity of Secondary Metabolites Produced by the Endophytic Fungus Penicillium ochrochlorae. Fermentation. 2025;11(7):1–14.

69. Salo O, Guzmán-Chávez F, Ries MI, Lankhorst PP, Bovenberg RAL, Vreeken RJ, et al. Identification of a polyketide synthase involved in sorbicillin biosynthesis by Penicillium chrysogenum. Appl Environ Microbiol. 2016;82(13):3971–8.

70. Silva S, da Costa H, Lopes T, Ramos V, Rodrigues N, Pereira JA, et al. Potential of the endophyte Penicillium commune in the control of olive anthracnose via induction of antifungal volatiles in host plant. Biological Control. 2023;187(August).

71. Merck KGaA. 70145 Malt Extract Agar Composition : Directions : Principle and Interpretation : 2018;70145.

Work presented at Scientific Events

I TBIO Annual Meeting – 18th October 2024, E2S - **Poster Presentation**

Relvas, S., Vieira, M., Rufo, J.C., Characterisation of volatilomics in fungal samples extracted from the homes of patients with hypersensitivity pneumonitis

7th Meeting on Medicinal Biotechnology & 3rd Iberian Congress on Medicinal Biotechnology – 30th May 2025, E2S - **Poster Presentation**

Relvas, S., Vieira, M., Rufo, J.C., Rapid identification of environmental fungi by volatile compound profiles

II TBIO Annual Meeting – 24th October 2025, E2S – **Poster Presentation**

Relvas, S., Vieira, M., Rufo, J.C., Electronic nose profiling of fungal VOCs reveals ketone-enriched signature of Penicillium species

RISE DAY – 29th October 2025, University of Aveiro – **Poster Presentation**

Relvas, S., Vieira, M., Rufo, J.C., Volatile Organic Profiles as Phenotypic Markers in Environmental Fungal Screening

Annex I

Table 23: Parameters of the measurement of VOCs using the electronic nose (MIDAS Breathprinter). Each sensor corresponded to a certain functional group (M2 – Alkanes, M3 – Alcohols , M4 – Methanes, M8 – Aldehydes + H_2, M9 – Ketones, M135 – Aromatic hydrocarbons).

Sample_ID	Sample	Tube	Sampling points	Time	Temperature	Humidity	M2	M3	M4	M8	M9	M135
C00	Control	1	0	09:46:01	33.5	36	225.000	0.000	0.000	80.000	2160.000	131.000
C00	Control	2	0	09:49:39	33.7	33	214.000	0.000	0.000	0.000	2125.000	134.000
C00	Control	3	0	09:52:39	34.1	31	192.000	29.000	0.000	0.000	2076.000	133.000
A00	*Alternaria sp.*	1	0	09:55:28	34.4	31	193.000	204.000	0.000	818.000	2125.000	139.000
A00	*Alternaria sp.*	2	0	09:58:02	34.7	30	214.000	903.000	0.000	1385.000	2176.000	144.000
A00	*Alternaria sp.*	3	0	10:00:45	35.0	30	192.000	136.000	0.000	120.000	2077.000	129.000
P00	*Penicillium sp.*	1	0	10:03:30	35.2	30	186.000	0.000	0.000	0.000	2072.000	133.000
P00	*Penicillium sp.*	2	0	10:06:08	35.5	30	159.000	1052.000	0.000	1453.000	1936.000	122.000

P00	*Penicillium sp.*	3	0	10:08:54	35.6	29	165.000	1163.000	0.000	1419.000	2000.000	128.000
N00	*A. niger*	1	0	10:11:59	35.8	29	160.000	459.000	0.000	1076.000	1981.000	122.000
N00	*A. niger*	2	0	10:15:07	35.9	29	153.000	0.000	0.000	0.000	1974.000	121.000
N00	*A. niger*	3	0	10:17:51	35.9	28	208.000	0.000	0.000	0.000	2239.000	143.000
G00	*G. virens*	1	0	10:21:14	36.1	28	179.000	1003.000	0.000	982.000	2094.000	131.000
G00	*G. virens*	2	0	10:23:45	36.1	28	164.000	606.000	0.000	1168.000	2035.000	117.000
G00	*G. virens*	3	0	10:26:47	36.2	28	153.000	0.000	0.000	0.000	2017.000	117.000
F00	*A. flavus*	1	0	10:29:31	36.3	27	151.000	183.000	0.000	208.000	2002.000	118.000
F00	*A. flavus*	2	0	10:31:58	36.5	27	147.000	16.000	0.000	574.000	1997.000	113.000
F00	*A. flavus*	3	0	10:34:28	36.6	27	150.000	0.000	0.000	0.000	2035.000	114.000
C01	Control	1	1	10:46:03	36.8	27	166.000	747.000	0.000	1273.000	2236.000	125.000
C01	Control	2	1	10:48:31	36.4	29	158.000	5.000	0.000	0.000	2209.000	135.000
C01	Control	3	1	10:50:46	36.6	28	144.000	59.000	0.000	53.000	2117.000	130.000
A01	*Alternaria sp.*	1	1	10:53:19	36.8	28	137.000	0.000	0.000	0.000	2066.000	123.000
A01	*Alternaria sp.*	2	1	10:55:42	37.0	27	134.000	0.000	0.000	0.000	2071.000	128.000
A01	*Alternaria sp.*	3	1	10:57:54	37.1	27	131.000	0.000	0.000	284.000	2066.000	125.000
P01	*Penicillium sp.*	1	1	11:00:32	37.2	27	128.000	138.000	0.000	144.000	2102.000	120.000

P01	*Penicillium sp.*	2	1	11:02:43	37.3	27	123.000	0.000	0.000	419.000	2063.000	122.000
P01	*Penicillium sp.*	3	1	11:05:06	37.4	27	119.000	688.000	0.000	742.000	2064.000	114.000
N01	*A. niger*	1	1	11:07:38	37.5	27	112.000	590.000	0.000	1171.000	2003.000	114.000
N01	*A. niger*	2	1	11:10:03	37.5	27	112.000	0.000	0.000	0.000	1991.000	112.000
N01	*A. niger*	3	1	11:12:15	37.6	27	587.000	0.000	0.000	0.000	4095.000	322.000
G01	*G. virens*	1	1	11:15:05	37.7	26	161.000	961.000	0.000	1409.000	2055.000	119.000
G01	*G. virens*	2	1	11:17:28	37.7	26	147.000	1083.000	0.000	1403.000	2075.000	112.000
G01	*G. virens*	3	1	11:19:54	37.7	26	111.000	996.000	0.000	1392.000	1910.000	106.000
F01	*A. flavus*	1	1	11:22:13	37.7	26	105.000	0.000	0.000	0.000	1906.000	106.000
F01	*A. flavus*	2	1	11:24:26	37.8	26	112.000	0.000	0.000	0.000	1936.000	102.000
F01	*A. flavus*	3	1	11:26:39	37.8	25	106.000	1081.000	0.000	1437.000	1925.000	107.000
C02	Control	1	2	11:45:50	37.9	26	164.000	0.000	0.000	0.000	2281.000	125.000
C02	Control	2	2	11:48:00	36.2	29	138.000	1232.000	0.000	1424.000	2181.000	116.000
C02	Control	3	2	11:50:19	36.5	28	129.000	0.000	0.000	0.000	2132.000	117.000
A02	*Alternaria sp.*	1	2	11:52:48	36.7	27	100.000	44.000	0.000	21.000	1945.000	96.000
A02	*Alternaria sp.*	2	2	11:55:17	37.0	26	80.000	0.000	0.000	0.000	1841.000	91.000
A02	*Alternaria sp.*	3	2	11:57:29	37.1	25	75.000	130.000	0.000	128.000	1799.000	82.000

P02	*Penicillium sp.*	1	2	11:59:57	37.3	25	158.000	625.000	0.000	1178.000	2117.000	114.000
P02	*Penicillium sp.*	2	2	12:02:14	37.4	25	176.000	20.000	0.000	0.000	2258.000	118.000
P02	*Penicillium sp.*	3	2	12:04:39	37.4	25	128.000	0.000	0.000	0.000	2043.000	111.000
N02	*A. niger*	1	2	12:07:27	37.4	25	320.000	0.000	0.000	0.000	3155.000	186.000
N02	*A. niger*	2	2	12:09:40	37.3	25	157.000	911.000	0.000	1333.000	2183.000	119.000
N02	*A. niger*	3	2	12:11:59	37.3	25	130.000	755.000	0.000	1200.000	2086.000	117.000
G02	*G. virens*	1	2	12:14:35	37.4	25	112.000	0.000	0.000	0.000	2055.000	114.000
G02	*G. virens*	2	2	12:17:53	37.3	25	99.000	368.000	0.000	919.000	1993.000	107.000
G02	*G. virens*	3	2	12:20:23	37.2	25	176.000	0.000	0.000	0.000	2287.000	126.000
F02	*A. flavus*	1	2	12:22:41	37.3	25	79.000	0.000	0.000	0.000	1776.000	96.000
F02	*A. flavus*	2	2	12:25:02	37.3	25	50.000	0.000	0.000	0.000	1728.000	80.000
F02	*A. flavus*	3	2	12:27:19	37.4	25	69.000	0.000	0.000	0.000	1757.000	99.000
C03	Control	1	3	12:45:59	37.3	24	147.000	0.000	0.000	0.000	2255.000	114.000
C03	Control	2	3	12:48:25	36.1	27	137.000	927.000	0.000	1353.000	2191.000	112.000
C03	Control	3	3	12:50:38	36.3	26	162.000	1206.000	0.000	1376.000	2271.000	123.000
A03	*Alternaria sp.*	1	3	12:54:43	36.6	26	774.000	1101.000	0.000	1216.000	4095.000	387.000
A03	*Alternaria sp.*	2	3	12:57:21	36.5	27	355.000	459.000	0.000	1055.000	2038.000	128.000

A03	*Alternaria sp.*	3	3	12:59:44	36.6	26	245.000	0.000	0.000	137.000	1613.000	99.000
P03	*Penicillium sp.*	1	3	13:02:28	36.7	26	208.000	101.000	0.000	85.000	1499.000	86.000
P03	*Penicillium sp.*	2	3	13:04:44	36.8	25	176.000	849.000	0.000	912.000	1394.000	80.000
P03	*Penicillium sp.*	3	3	13:07:05	36.9	25	154.000	1115.000	0.000	1351.000	1354.000	79.000
N03	*A. niger*	1	3	13:10:08	37.0	25	175.000	209.000	0.000	815.000	1510.000	84.000
N03	*A. niger*	2	3	13:12:24	37.0	26	159.000	109.000	0.000	106.000	1488.000	84.000
N03	*A. niger*	3	3	13:14:59	37.1	26	142.000	0.000	0.000	133.000	1461.000	79.000
G03	*G. virens*	1	3	13:17:36	37.1	26	129.000	0.000	0.000	0.000	1411.000	79.000
G03	*G. virens*	2	3	13:19:50	37.2	26	180.000	863.000	0.000	1376.000	1427.000	80.000
G03	*G. virens*	3	3	13:22:35	37.3	26	106.000	1136.000	0.000	1281.000	1456.000	77.000
F03	*A. flavus*	1	3	13:26:07	37.3	26	111.000	13.000	0.000	9.000	1454.000	72.000
F03	*A. flavus*	2	3	13:28:31	37.1	27	99.000	201.000	0.000	794.000	1425.000	69.000
F03	*A. flavus*	3	3	13:31:08	37.3	26	108.000	0.000	0.000	0.000	1466.000	75.000
C06	Control	1	6	15:47:35	22.3	47	181.000	919.000	0.000	971.000	2155.000	154.000
C06	Control	2	6	15:50:22	23.8	56	195.000	1155.000	0.000	1579.000	2256.000	163.000
C06	Control	3	6	15:52:56	25.4	52	183.000	135.000	0.000	122.000	2155.000	160.000
A06	*Alternaria sp.*	1	6	15:55:59	26.9	48	179.000	1335.000	0.000	1535.000	2162.000	151.000

A06	*Alternaria sp.*	2	6	15:58:23	28.5	43	181.000	537.000	0.000	1175.000	2153.000	150.000
A06	*Alternaria sp.*	3	6	16:01:50	29.7	40	176.000	1083.000	0.000	1471.000	2167.000	155.000
P06	*Penicillium sp.*	1	6	16:06:58	31.0	38	172.000	0.000	0.000	134.000	2102.000	144.000
P06	*Penicillium sp.*	2	6	16:10:01	32.4	36	158.000	0.000	0.000	0.000	2032.000	139.000
P06	*Penicillium sp.*	3	6	16:13:42	33.3	33	161.000	0.000	0.000	0.000	2066.000	144.000
N06	*A. niger*	1	6	16:16:43	34.0	32	177.000	70.000	0.000	59.000	2172.000	146.000
N06	*A. niger*	2	6	16:19:50	34.6	31	158.000	487.000	0.000	1057.000	2057.000	140.000
N06	*A. niger*	3	6	16:22:25	35.0	30	146.000	0.000	0.000	0.000	2021.000	133.000
G06	*G. virens*	1	6	16:26:05	35.4	30	187.000	0.000	0.000	7.000	2251.000	144.000
G06	*G. virens*	2	6	16:28:42	35.8	29	147.000	0.000	0.000	0.000	2000.000	129.000
G06	*G. virens*	3	6	16:31:18	36.1	28	144.000	640.000	0.000	1150.000	2034.000	134.000
F06	*A. flavus*	1	6	16:36:48	36.5	26	250.000	0.000	0.000	0.000	2255.000	170.000
F06	*A. flavus*	2	6	16:39:24	36.7	27	158.000	871.000	0.000	1287.000	1869.000	128.000
F06	*A. flavus*	3	6	16:42:05	36.9	26	143.000	0.000	0.000	0.000	1789.000	114.000
C24	Control	1	24	09:46:05	20.2	57	463.000	0.000	0.000	0.000	4095.000	275.000
C24	Control	2	24	09:48:33	22.3	61	249.000	67.000	0.000	41.000	2432.000	154.000
C24	Control	3	24	09:51:31	23.9	56	221.000	0.000	0.000	86.000	2256.000	133.000

A24	*Alternaria sp.*	1	24	09:54:22	25.6	52	193.000	0.000	0.000	0.000	2140.000	125.000
A24	*Alternaria sp.*	2	24	09:56:58	27.1	47	186.000	4.000	0.000	0.000	2094.000	122.000
A24	*Alternaria sp.*	3	24	09:59:24	28.4	43	176.000	1195.000	0.000	1296.000	2053.000	115.000
P24	*Penicillium sp.*	1	24	10:02:36	29.4	40	290.000	0.000	0.000	0.000	2732.000	167.000
P24	*Penicillium sp.*	2	24	10:05:16	30.5	38	194.000	0.000	0.000	28.000	2173.000	122.000
P24	*Penicillium sp.*	3	24	10:08:08	31.3	36	153.000	320.000	0.000	1051.000	1907.000	103.000
N24	*A. niger*	1	24	10:11:37	32.0	34	254.000	0.000	0.000	0.000	2502.000	144.000
N24	*A. niger*	2	24	10:14:27	32.6	32	179.000	0.000	0.000	0.000	2046.000	112.000
N24	*A. niger*	3	24	10:17:25	33.1	32	197.000	428.000	0.000	1111.000	2192.000	117.000
G24	*G. virens*	1	24	10:20:29	33.6	31	310.000	0.000	0.000	0.000	2813.000	170.000
G24	*G. virens*	2	24	10:23:08	33.9	30	210.000	1232.000	0.000	1580.000	2175.000	118.000
G24	*G. virens*	3	24	10:26:01	34.2	29	165.000	0.000	0.000	0.000	1943.000	103.000
F24	*A. flavus*	1	24	10:29:03	34.5	29	206.000	153.000	0.000	140.000	2192.000	121.000
F24	*A. flavus*	2	24	10:31:50	34.7	29	198.000	0.000	0.000	0.000	2160.000	113.000
F24	*A. flavus*	3	24	10:34:31	34.9	29	527.000	570.000	0.000	625.000	4095.000	282.000
C48	Control	1	48	10:41:43	17.8	53	13.000	110.000	0.000	76.000	1049.000	41.000
C48	Control	2	48	10:45:03	18.8	59	3.000	0.000	0.000	0.000	1007.000	31.000

C48	Control	3	48	10:47:42	20.6	54	0.000	0.000	0.000	0.000	1021.000	29.000
A48	*Alternaria sp.*	1	48	10:50:43	22.4	50	0.000	1187.000	0.000	1613.000	1089.000	33.000
A48	*Alternaria sp.*	2	48	10:53:51	24.3	47	0.000	528.000	0.000	1264.000	1039.000	23.000
A48	*Alternaria sp.*	3	48	10:56:50	26.0	41	0.000	1295.000	0.000	1448.000	1046.000	27.000
P48	*Penicillium sp.*	1	48	11:00:04	27.4	37	48.000	62.000	0.000	42.000	1404.000	48.000
P48	*Penicillium sp.*	2	48	11:02:47	28.7	35	19.000	0.000	0.000	454.000	1236.000	42.000
P48	*Penicillium sp.*	3	48	11:05:28	29.7	33	40.000	0.000	0.000	0.000	1318.000	43.000
N48	*A. niger*	1	48	11:08:28	30.6	30	0.000	0.000	0.000	0.000	996.000	19.000
N48	*A. niger*	2	48	11:11:13	31.3	29	0.000	92.000	0.000	50.000	1104.000	27.000
N48	*A. niger*	3	48	11:13:39	32.0	29	0.000	0.000	0.000	500.000	1055.000	23.000
G48	*G. virens*	1	48	11:16:33	32.6	27	0.000	44.000	0.000	106.000	1041.000	16.000
G48	*G. virens*	2	48	11:19:14	33.1	26	0.000	93.000	0.000	80.000	988.000	17.000
G48	*G. virens*	3	48	11:21:52	33.5	25	0.000	0.000	0.000	0.000	1115.000	24.000
F48	*A. flavus*	1	48	11:24:57	33.9	25	0.000	1098.000	0.000	1562.000	1118.000	28.000
F48	*A. flavus*	2	48	11:27:47	34.2	25	0.000	30.000	0.000	697.000	1093.000	16.000
F48	*A. flavus*	3	48	11:30:34	34.4	23	0.000	116.000	0.000	739.000	1079.000	20.000
C72	Control	1	72	08:48:20	17.1	55	0.000	1106.000	0.000	1697.000	947.000	27.000

C72	Control	2	72	08:51:01	18.0	63	0.000	1359.000	0.000	1714.000	1008.000	33.000
C72	Control	3	72	08:53:56	19.4	61	0.000	574.000	0.000	1353.000	1143.000	43.000
A72	*Alternaria sp.*	1	72	08:56:39	21.2	60	0.000	695.000	0.000	1423.000	1093.000	39.000
A72	*Alternaria sp.*	2	72	08:59:10	22.9	52	0.000	1043.000	0.000	1129.000	1079.000	36.000
A72	*Alternaria sp.*	3	72	09:01:31	24.3	47	0.000	0.000	0.000	0.000	1062.000	33.000
P72	*Penicillium sp.*	1	72	09:05:32	25.5	45	107.000	1237.000	0.000	1610.000	1766.000	73.000
P72	*Penicillium sp.*	2	72	09:08:14	27.0	42	54.000	406.000	0.000	375.000	1461.000	59.000
P72	*Penicillium sp.*	3	72	09:10:38	27.9	39	112.000	35.000	0.000	11.000	1835.000	78.000
N72	*A. niger*	1	72	09:13:19	28.7	39	0.000	0.000	0.000	0.000	1013.000	23.000
N72	*A. niger*	2	72	09:15:47	29.4	36	0.000	135.000	0.000	118.000	997.000	19.000
N72	*A. niger*	3	72	09:18:16	30.0	35	0.000	0.000	0.000	0.000	944.000	16.000
G72	*G. virens*	1	72	09:20:55	30.5	33	0.000	931.000	0.000	1484.000	1034.000	17.000
G72	*G. virens*	2	72	09:23:27	31.0	32	0.000	417.000	0.000	1136.000	943.000	15.000
G72	*G. virens*	3	72	09:25:55	31.4	31	0.000	377.000	0.000	1105.000	1008.000	16.000
F72	*A. flavus*	1	72	09:28:40	31.8	30	0.000	150.000	0.000	145.000	922.000	11.000
F72	*A. flavus*	2	72	09:31:20	32.1	30	0.000	0.000	0.000	96.000	933.000	14.000
F72	*A. flavus*	3	72	09:33:57	32.4	29	0.000	147.000	0.000	806.000	905.000	7.000

P.PORTO

ESCOLA SUPERIOR DE SAÚDE

M

MESTRADO

BIOQUÍMICA EM SAÚDE